DESIGN CONSIDERATIONS FOR MORTISE AND TENON CONNECTIONS

Richard J. Schmidt
Christopher E. Daniels

Department of Civil and
Architectural Engineering
University of Wyoming
Laramie, WY 82071

A Report on Research Sponsored by the

USDA NRI/CGP
Washington, DC

and

Timber Frame Business Council
Hanover, NH

April 1999

UNIVERSITY OF
WYOMING

REPORT DOCUMENTATION PAGE	1. REPORT NO.	2.	3. Recipient's Accession No.

4. Title and Subtitle
Design Considerations for Mortise and Tenon Connections

5. Report Date
April 1999

6.

7. Author(s)
Richard J. Schmidt & Christopher E. Daniels

8. Performing Organization Report No.

9. Performing Organization Name and Address

Department of Civil and Architectural Engineering
University of Wyoming
Laramie, WY 82071

10. Project/Task/Work Unit No.

11. Contract(C) or Grant(G) No.
(C)
(G)

12. Sponsoring Organization Name and Address

USDA NRI/CGP
CSREES
Washington, DC 20250

Timber Frame Business Council
PO Box B1161
Hanover, NH 03755

13. Type of Report & Period Covered
interim

14.

15. Supplementary Notes

USDA NRI/CGP Contract No. 9702896

16. Abstract (Limit: 200 words)

The objective of this research is to determine the strength and stiffness characteristics of timber-frame connections in tension. Timber-frame connections use wood pegs to secure the tenon within the mortise. The design of these connections is currently beyond the scope of building codes, including the National Design Specification for Wood Construction (NDS). Full-size joints were tested to determine failure modes and to establish minimum edge and end distances that ensure peg failure. These end and edge distances were used to verify a design procedure for satisfying NDS spacing requirements. Peg failure was identified as the preferred failure mode because of the ductility exhibited prior to ultimate failure. Mechanical properties, which included peg bending strength, shear strength, and dowel bearing strength were also established. An efficient method for establishing dowel bearing capacities for combinations of base material (mortise/tenon) and pegs utilizing springs in series was also developed.

17. Document

a. Descriptors

traditional timber framing, heavy timber construction, structural analysis, wood peg fasteners, mortise and tenon connections, European yield model, joint testing, design standards.

b. Identifiers/Open-Ended

c. COSATI Field/Group

18. Availability Statement	19. Security Class (This Report)	21. No. of Pages
Release unlimited.	Unclassified.	98
	20. Security Class (This Page)	**22. Price**
	Unclassified.	

(See ANSI-Z39.18)

OPTIONAL FORM 272 (4-77)
Department of Commerce

Acknowledgments

This report is based on the research conducted by Mr. Christopher E. Daniels, under the direction of Dr. Richard J. Schmidt, in partial fulfillment of the requirements for a Masters of Science Degree in Civil Engineering at the University of Wyoming. Primary funding for this research was provided by the USDA-NRI/CGP under contract #9702896. Additional funding was provided by the Timber Frame Business Council. Joint specimens were donated by Red Suspenders Timber Frames, Big Timberworks, Benson Woodworking, and Sunset Structures. Scott Northcott supplied the pegs.

Table of Contents

Page

List of Figures Page

List of Tables Page

List of Appendices Page

1. Introduction

1.1 General Overview

In some form or another, timber framed mortise and tenon connections have been used for centuries throughout the world. The connections are constructed entirely of wood, utilizing wood pegs to secure the joint. Timber framed structures have demonstrated their longevity throughout the world with structures that have survived hundreds of years of service. The durability of the structures coupled with their beauty and convenient use with holistic building schemes has led to a revival in the timber framing industry.

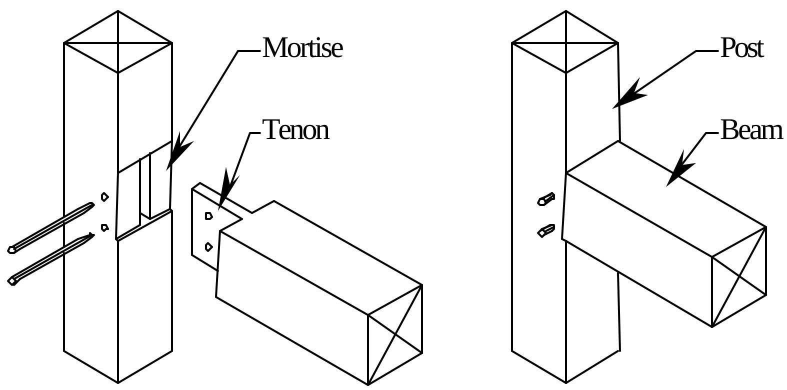

Figure 1-1 Typical Post to Beam Connection

Timber-frame connections use wood pegs to secure the tenon within the mortise. Figure 1-1 is a typical timber frame connection. The design of these connections is currently beyond the scope of building codes, including the National Design Specification for Wood Construction (NDS) (AFPA 1997). Full size joint tests were performed to determine failure modes and to establish minimum edge and end distances that ensure peg failure. These end and edge distances were used to verify a design procedure based on the current NDS spacing requirements. Peg failure was identified as the preferred failure mode because of the ductility exhibited prior to ultimate failure. Mechanical properties, which included peg bending strength, peg shear strength, and base material dowel bearing strength were also established. A mathematical model is proposed to establish dowel-bearing capacities for combinations of base material (mortise/tenon) and pegs.

1.2 Current Practice of Timber Framing

The current practice of timber framing has evolved through the study of past structures. Today's timber framers make decisions based on experience, whether it is obtained through personal endeavors or historic research.

Since the revival of timber framed construction in the United States in the 1970's, timber framing has remained a relatively small industry. The skilled labor required to produce a frame places the initial costs of a timber frame above that of typical light-frame construction. The development of automated machines to produce finished timbers could increase the availability of timber framed structures by increasing productivity. This advancement in technology will no doubt make the cost of timber frame structures more competitive with modern light-frame construction.

The availability of natural resources could play a roll in the marketability of timber framed structures. Timber frames lend themselves well to a number of advanced insulating systems, which perform better than present methods of construction. The use of any number of thermal barriers, such as structural insulated panels, polystyrene sheets with stud framed supports, and straw bales, to enclose a frame cut energy costs relative to typical stud construction with fiberglass insulation. While the majority of today's frames are constructed with new growth timbers, the use of glued laminated members and recycled timbers from obsolete structures is expected to become more prevalent.

Current design practice for timber framed joinery is much different than that of other construction methods. The sizing of members that comprise a timber frame is accomplished using traditional mechanics of materials and structural analysis methods, with material strengths governed by the design specifications for wood. However, detailing of the joinery, which connects these members is beyond the scope of current specifications and, more often than not, requires the designer to depend on engineering judgement coupled with the experience of the builder.

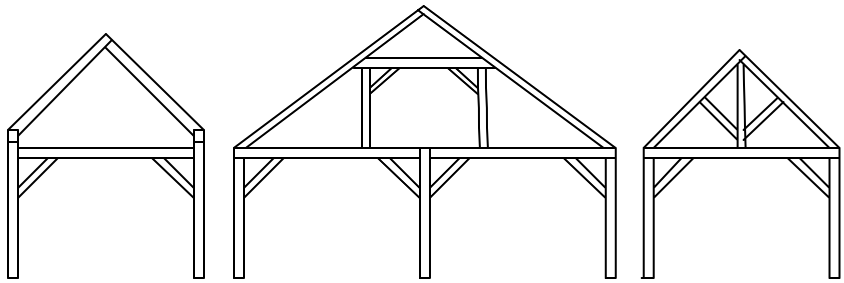

Figure 1-2 Common Timber Framed Bents

Figure 1-2 shows some common timber framed bents. Typical timber frame construction relies on the knee braces shown in Figure 1-2 to resist lateral forces imposed on the frame. The knee braces create a moment resisting frame that allows tension to develop in many connections. This tensile force is a critical consideration in the design of a frame, and often results in the over-sizing of members to accommodate the joinery necessary to prevent abrupt tensile failures at the connection.

1.3 Objectives and Scope

The focus of this research was to determine design guidelines for pegged mortise and tenon connections in tension. The three topics of primary concern are joint detailing, joint strength and joint stiffness. The first task was to establish a viable method of determining joint details that will develop the full design strength of any given mortise and tenon tension connection. The second task was to develop procedures for the design of traditional joinery.

Development of design guidelines for timber frame connections requires joint tests as well as supplemental material tests. The development of design procedures for timber framed connections requires the establishment of mechanical properties for the materials that comprise a joint. The required material properties include peg bending strength, peg shear strength, peg bearing strength and base material dowel bearing strength. The mechanical properties relevant to the joints tested in this research were established in an attempt to better understand the connection behavior. Additionally, preliminary tests were performed to determine the feasibility of a mathematical model for the development of dowel bearing strengths for timber framed connections.

An outline of the objectives for both the joint tests and the material tests is shown below.

1. Joint Tests

- Perform strength and stiffness data for southern yellow pine, recycled Douglas fir, and red oak joints.
- Develop design procedure for joints under short duration loading.

2. Material Tests

- Establish strength data for correlation to joint tests including peg bending, peg shear, and dowel bearing strengths.
- Develop an efficient method for determining dowel bearing strengths.

1.4 Literature Review

Little experimental research on timber framed joinery exists in the United States or abroad. The first known research was by Brungraber (Brungraber 1985). This work included full-scale frame tests and a limited number of individual joint tests. Brungraber also used the finite element method to create 2D models for frame and joint behavior based on a three spring joint model. The computer models were used for comparison to strength and stiffness data from the full-size frame tests. Available European research is limited to 120 joint tests conducted by M. H. Kessel (Kessel and Augustin 1996). The German test reports contain information on 80 traditional mortise and tenon joints. The joints were constructed with green oak and dry spruce timbers, connected with octagonal oak pegs. The work produced design recommendations for reconstruction of an eight story timber frame (Kessel *et al* 1988).

Researchers at the Michigan Technological University have studied various aspects of timber framed construction. Experimental tests were performed on frame subassemblies using simulated gravity loads to determine joint and peg behavior (Sandberg *et al* 1996). These tests were conducted on post and beam connections with and without knee braces to determine connection behavior. The study revealed that the joints had a significant load capacity and resistance to catastrophic failure. The tensile capacity of the knee braces was found to be the weak link in the frame system, which poses a potential problem in the design for lateral loads. The results of the tests were used to develop computer modeling procedures based on the strength and stiffness characteristics of the joints (Bulliet *et al* 1996). The frame models created in this work demonstrated that the joints can be modeled as pin connected members and that modeling of knee braces should be based on the stiffness of their connecting pegs.

Additional experimental work included tests of simplified mortise and tenon joints with a single peg to isolate peg behavior in timber framed connections (Reid 1997). Reid tested simplified mortise and tenon connections using 2x6 and 1x6 full sawn lumber. The test results were compared to the European Yield Model (EYM) equations for double shear connections, which is currently used by the NDS for the design of timber connections with steel fasteners. The work demonstrated that the EYM equations did not accurately predict capacities of timber framed connections, but the simplified tests did accurately represent the peg failure modes exhibited in full size timber framed connections.

Researchers at the University of Idaho investigated the dowel bearing strengths of white oak pegs combined with various base materials (Church and Tew 1997; Church 1995). Two important conclusions resulted from this work. The first was that the diameter of the peg had little effect on bearing strength, and second, that the effect of over-sizing the hole diameter by dimensions of 1/16, 3/32 and 1/8 had little effect on bearing strength.

Research at the University of Wyoming contains material property tests and joint tests pertinent to the development of timber frame design values (Schmidt and MacKay 1997). This work included peg and base material tests for several different wood species. The material tests included base material dowel bearing, peg bending, and peg shear strengths. The joints were constructed from dimensional lumber and fastened with two red oak pegs. The joints were tested in direct tension and the results were compared to the EYM double shear equations. Schmidt and MacKay concluded that two of the existing EYM equations (mode III_s and IV) from the NDS do not accurately represent the strength of wooden dowel fasteners. One of the joint tests had a failure mode similar to the mode III_s failure, but with a single hinge directly under the point of loading. This mode was denoted III'_s and is important to the design of timber connections because it would likely form at a lower load than the fastener bending modes (III_s and IV) currently recognized by the NDS. Two of the six joints tested in Schmidt and MacKay's work failed due to a combined shear and bending failure of the pegs. This peg failure was simulated with a shear test procedure using individual pegs in an attempt to model peg behavior within a joint. A characteristic shear strength equation was found for a particular peg species by varying the shear span to diameter ratio (*a/D*) in the peg tests. A characteristic *a/D* ratio was determined for the joints using the yield load from the two joint tests with a peg shear/bending failure. This characteristic *a/D* ratio was the basis for establishing peg shear strengths for the present research.

Research on wood products with steel fasteners could be applied to the development timber frame design specifications. The work by T. L. Wilkinson (1991) to develop dowel bearing strengths of wood with steel fasteners could be used as a guide to develop similar properties for timber framing. The data published by Wilkinson for the Forests Products Lab is now used in the NDS for dowel bearing strengths. The data itself may not be directly applicable to timber framing, but the report is a good reference for determining future reliability requirements for researchers developing timber frame mechanical properties. The EYM has been studied and adapted from various reports for use in the United States with bolted connections (Soltis *et al*. 1986; Soltis and Wilkinson 1987; Wilkinson 1993; McLain and Thangjitham 1983).

Timber frame construction incorporates steel fasteners in certain design situations. The use of internal fasteners is particularly appealing in timber frame construction because it does not affect the aesthetics of the frame (Brungraber 1992; Duff *et al.* 1996). The experimental work done by Duff revealed that internal timber fasteners demonstrated predictable behavior and may even be economical.

Table 1-1 Required NDS End and Edge Distance

Direction of Loading	Minimum End Distance for Reduced Design Value	Minimum End Distance for Full Design Value
Parallel to Grain, Tension: (bolt bearing toward member end)		
for softwoods	3.5D	7D
for hardwoods	2.5D	5D

Direction of Loading	Minimum Edge Distance
Perpendicular To Grain:	
loaded edge	4D
unloaded edge	1.5D

The current values used for end distance, in bolted timber connections, were reviewed experimentally by M. Patton-Mallory and J. D. Snodgrass (Patton-Mallory 1988; Snodgrass and Gleaves 1960). Table 1-1 contains the values required by the NDS for end distance parallel to grain and edge distance perpendicular to grain. Patton-Mallory concluded that the current end distances based on research by G. W. Trayer (1932) might need to be revised based on a more comprehensive testing program. Her report concluded that connections with one-half the specified end distances had a much higher factor of safety than connections with full end distance. The report by J. D. Snodgrass had similar findings. Snodgrass' work included tests on 800 connections (400 seasoned and 400 unseasoned) made from Douglas fir lumber with a single steel bolt fastener. The report recommended a minimum end distance of four fastener diameters. Based on a statistical analysis of variance, no significant difference was found for end distances that ranged from five to seven diameters. The margins of safety between the minimum loads at ultimate and the proportional limits were reported to be substantial in most cases. The report also made a comparison of the test values for seasoned and unseasoned wood, and concluded that the present 60% reduction in connection strength for unseasoned wood was conservative. The research did not include a study of connections that season in-place while under load, and the conclusions were based on the assumption that no strength reducing defects, such as checks or warping, would occur during the seasoning process.

2. Material Tests

2.1 General Procedures

This research was conducted using a population of 700 1-inch diameter x 12 inch long white oak pegs selected from a single stand of trees in the North Eastern United States. To identify and make predictions of failure modes for the full-size joint tests, several mechanical properties had to be established for the peg population. The properties included bending, dowel bearing and shear strengths. The tests were identical to those performed in previous research at the University of Wyoming (Schmidt and MacKay 1997), with the exception of the dowel bearing tests and a minor change in the bending test fixture.

The pegs had moisture contents (MC) that ranged from 20-40% upon arrival and were conditioned to about 12% prior to testing. The pegs were stacked on stickers and allowed to air dry to approximately 12% MC. Upon reaching 12% MC the pegs were vacuum bagged to prevent any further moisture losses (local equilibrium MC is approximately 6.5%). The average MC for all pegs was 13.4%.

A typical test procedure was as follows. Pegs were randomly selected from the population and inspected for defects. Defects included knots in critical locations relative to a given test, severe checks, and signs of decay. Slope of grain was not regarded as a defect. Defective pegs were discarded.

At the start of an individual test, a single peg was removed from the environmental chamber/vacuum bag and labeled. The peg was sanded if needed to insure proper fit into the test fixture. Diameter of the peg was measured at critical locations for the specific test in both the tangential and radial directions. The peg was then placed in the test fixture and positioned with a jig. The testing machine, a servo-hydraulic Instron model 1332, was adjusted until the loading platen was lightly resting on the test fixture. The load and displacement outputs were checked for zero readings. The data acquisition program and the testing machine were started simultaneously. Upon reaching ultimate load, the data acquisition program and the loading were stopped. The characteristics of the failure were noted and a 2" long sample was cut from the peg, weighed, measured and placed in an oven for a minimum of 24 hours at 212^{o} F. The oven-dry specimen was removed and weighed again to determine oven dry specific gravity and moisture content. The oven dry specific gravity was adjusted to specific gravity at 12% MC. This is a common practice in wood science literature. Several tests were conducted on pegs that had moisture contents above the fiber saturation point. The specific gravity of the specimens used in these tests could not be adjusted to 12% MC and are presented as oven-dry values.

All the pegs used in this research were loaded tangent to the grain of the specimen (see Figure 2-1). Prior research has shown that grain orientation does have a small effect on the capacity of pegs (Schmidt and MacKay 1997, Reid 1997). It was desirable to eliminate the effects of grain orientation to reduce the number of variables in the research.

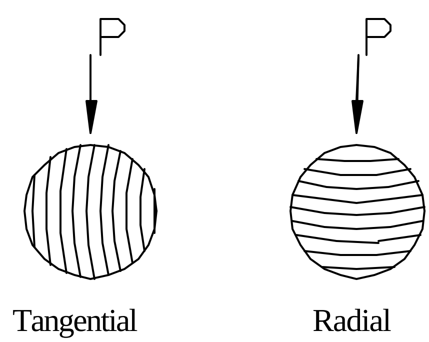

Figure 2-1 Peg Grain Orientations

The 5% offset method as per ASTM D5652 was used in all tests to determine the yield load (ASTM 1995a). The method is applied by offsetting the initial linear portion of the load versus deflection curve by 5% of the peg diameter, which for the tests in this research was always 0.05". The point at which this offset line intersects the load deflection curve is defined as the yield point (see Figure 2-2a). The method also defines the yield value as the ultimate load, if ultimate loads is reached prior to the intersection of the offset line and the load deflection curve (see Figure 2-2b).

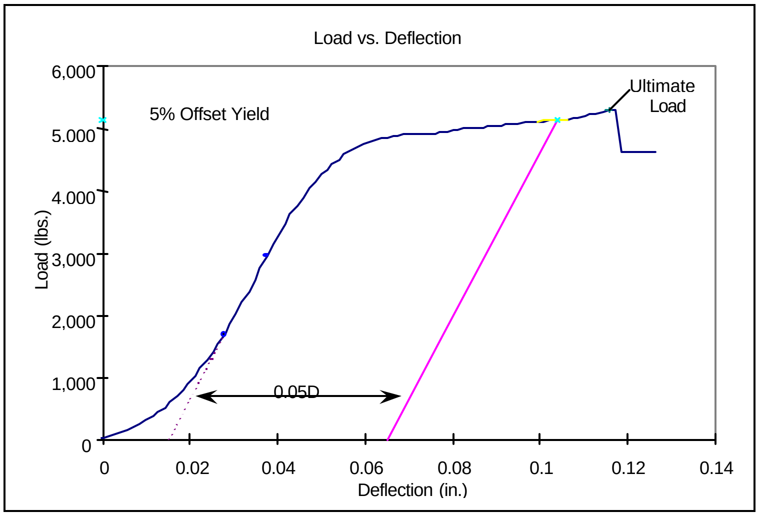

Figure 2-2a 5% Offset Method

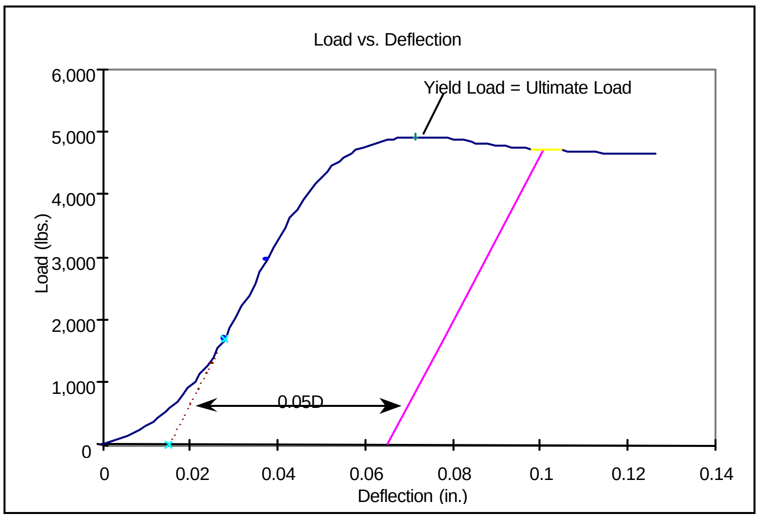

Figure 2-2b 5% Offset Method

2.2 Peg Bending

2.2.1 Peg Bending Procedure

Bending tests were performed to determine the flexural strength of the white oak peg population selected for the full-size joint tests. The tests were similar to that performed in previous research (Schmidt and MacKay 1997). The tests were limited to 1" diameter pegs that were randomly selected from the population and inspected for defects.

The testing was performed using an Instron model 1332 testing machine and Labview data acquisition software. All pegs were tested with a 9" span and loaded through two saddles spaced at 2.75" apart, centered on the peg (see Figure 2-3). The pegs were tested according to ASTM 4761-93 at a load rate of 0.15 in/min to reach failure in approximately two minutes (ASTM 1995a).

A load versus deflection curve was created using the test output file. The yield load was then determined using the 5% offset method and the yield stress was calculated using the average diameter of the peg.

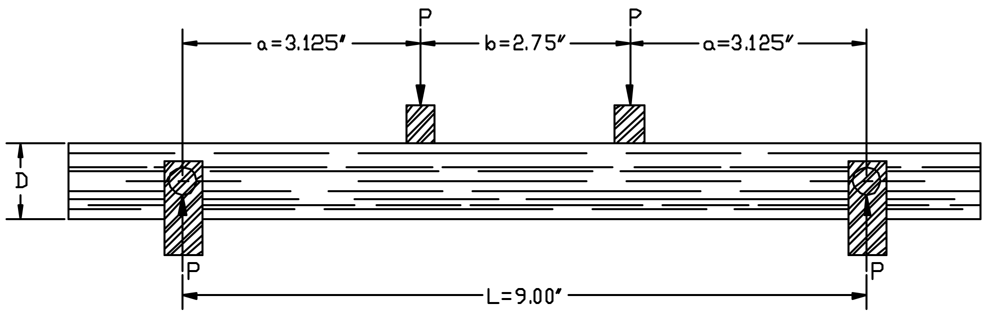

Figure 2-3 Bending Test Fixture

2.2.2 Peg Bending Results

A total of 41 bending tests was performed with 1" diameter pegs from the white oak peg population. The tests included 30 pegs that were near 12% MC and 11 pegs that were at the fiber saturation point (FSP). The averaged results of these tests can be seen in Table 2-1. The pegs with higher moisture content had a lower yield stress and stiffness compared to the dry pegs. The 11 pegs at FSP did have a lower average specific gravity, which may also influence the results.

Table 2-1 Average White Oak Bending Test Results

	Yield Stress (psi)	Stiffness (lb/in)	MC (%)	G_{12}
Mean	13,440	4,790	14.3	0.68
Std. Dev.	2,880			
5% Exclusion	7,990			
COV	0.214			

Dry Pegs

	Yield Stress (psi)	Stiffness (lb/in)	MC (%)	G
Mean	10,580	4,510	35.9	0.63
Std. Dev.	2,520			
5% Exclusion	5,370			
COV	0.238			

Green Pegs

The major factors contributing to the bending strength of the pegs were specific gravity (*G*) and moisture content. The relationship between the *G* and yield stress can be expressed with a regression function. A definite relationship between *G* and yield stress for the seasoned pegs can be seen in Figure 2-4. As *G* increases, the yield stress increases. The variability present in the test data prevents any relationship to be drawn between *MC* and yield stress. The higher *MC* affected the consistency of the results and a relationship between *G* and yield stress is not evident for the 11-peg group. Data for individual tests can be found in Appendix E.

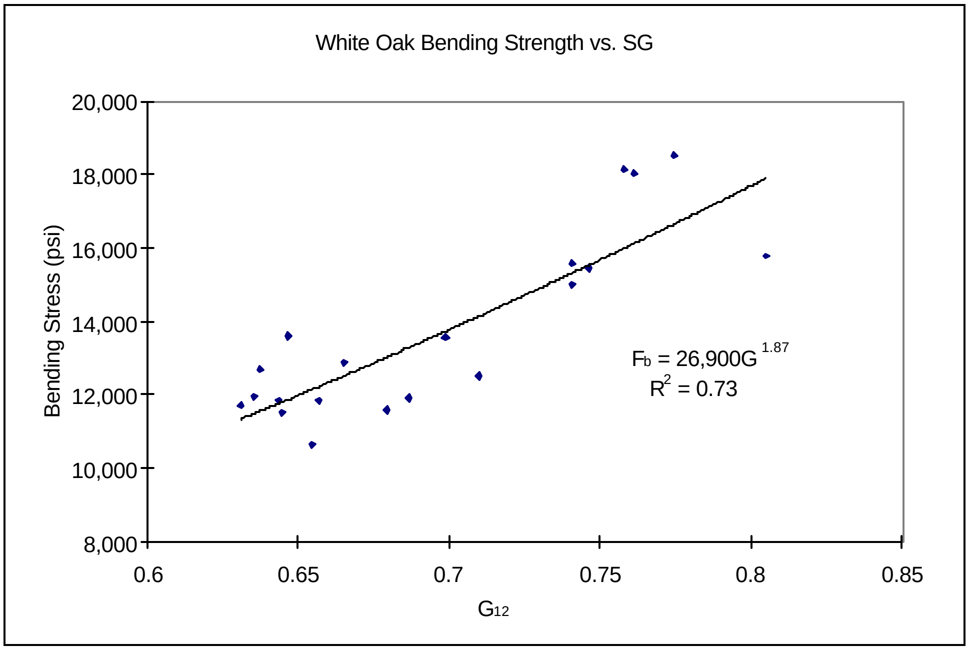

Figure 2-4 White Oak 1" Diameter Peg Bending Tests

2.3 Peg Shear

2.3.1 Peg Shear Procedure

Shear tests were performed to determine the combined shear and bending strength of the peg population selected for the full-size joint tests. The test method was the same as that used in previous research (Schmidt and MacKay 1997).

The test fixture (see Figure 2-5) was designed in previous work to model the behavior of a peg in a mortise and tenon connection. In the full-size tests the mortise and tenon members provide some degree of flexural restraint to the peg. However, the tenon-mortise interfaces also exhibited some local crushing at the edge of the peg holes in a few instances. This factor contributed to the reduction in restraint provided by the mortise and tenon peg holes. This reduction in restraint lead to the theory that instead of a true cross-grain shear condition relative to the peg, a combined shear/bending failure must be occurring. In other words, the pegs are allowed to deform across some finite-width shear span. Over this span, the material fails in shear or combined shear and bending.

The test fixture permitted variation of the shear span. Shear span *a* is defined as the distance from the face of the restraining block to the face of the loading block. Shear spans were measured on pegs removed from full-size tests. These shear span values ranged from 0.375" to 0.75" depending mainly on the species of the base material. Unlike the full size tests, the shear test fixture gripped the pegs tightly and prevented any horizontal movement of the peg during testing. The test fixture also had a 0.080" bevel at the edges to relieve the sharp edges of the test fixture that might otherwise cut the peg.

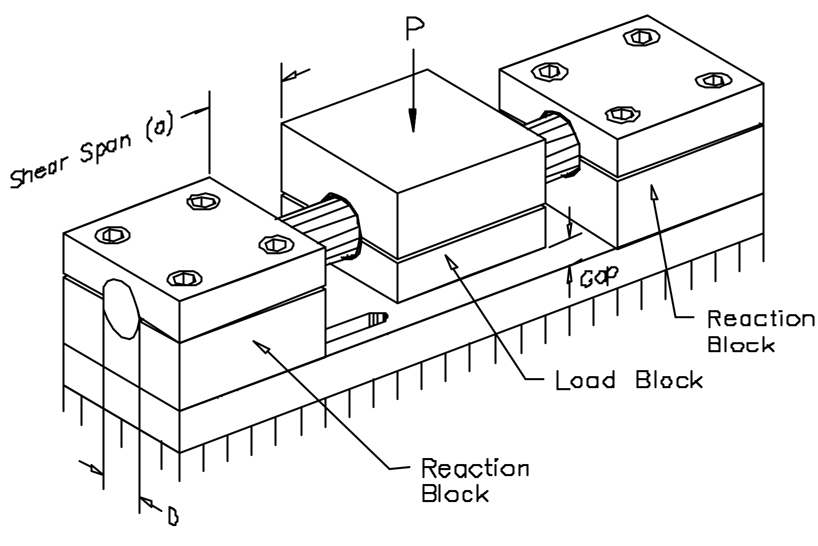

Figure 2-5 Shear Test Fixture, from Schmidt and MacKay (1997)

The shear tests were performed at shear spans of 1/8D, 1/4D, 1/2D, and 1D. The pegs were tested according to ASTM 4761-93 at a load rate of 0.048 in/min to reach failure in approximately five minutes

(ASTM 1995a). Again, the yield load was determined by the 5% offset method, and the corresponding yield stress was calculated based on the average diameter of the peg.

From these shear tests a linear regression equation was developed to relate shear span and yield stress for shear span ranges of 0.125” to 1”. The yield values from the full-size tests were then used to determine if there was a characteristic shear span for a particular mortise and tenon species and joint configuration. The characteristic *a/D* ratio for a group of joints was used to determine the shear stress on the pegs, and predictions of connection strength can be made using Equation 2-1.

$$P = \frac{\pi D^2 \tau_c}{4} \qquad (2\text{-}1)$$

P = total force exerted per peg
D = diameter of peg
τ_c = average shear strength of peg based on characteristic *a/D* ratio for joint species

2.3.2 Peg Shear Results

Thirty-six shear tests were performed with 1” diameter pegs from the white oak peg population. Nine tests were performed at each of the following shear spans: 1D, 1/2D, 1/4D and 1/8D. Table 2-2 shows the summary results of the 36 tests. As expected the yield stress decreased as the shear span increased. The coefficient of variability (COV) for the four test groups was between 7% and 13% and the average *MC* of all the pegs tested in shear was 12.6%. The specific gravity of the pegs ranged from 0.64 to 0.83 with an average of 0.70.

Table 2-2 Shear Test Results

Shear Span	Avg. Yield Stress (psi)	Std. Dev. (psi)	5% Exclusion (psi)	COV	No. of Tests
1/8 D	2,360	317	1,680	0.134	9
1/4 D	2,130	204	1,690	0.096	9
1/2D	1,880	182	1,490	0.097	9
1 D	1,560	141	1,330	0.068	9

This data was used to develop an equation for determining yield stress based on the shear span to diameter ratio (*a/D*) for the white oak peg population. This equation was used to relate yield loads from the full-size joints to an equivalent shear span for a given material. Figure 2-6 shows the average yield stress versus the shear span to diameter ratio for the four test groups. Also, Figure 2-6 contains the power series regression used to correlate the average shear stress for each group of pegs to the full size joint tests. The R-squared value for the population regression is 0.70, which is a reasonable representation of the shear behavior for the pegs. The R-squared value represents the correlation of the function to the test data with a value of 1.0 being exact and 0.0 having no correlation. A similar regression was performed on the average shear stress from each test group versus specific gravity and the equation was identical to the one shown in Figure 2-6 for the entire population, but the average shear stress regression had an R-squared value of 0.98. Figure 2-6 contains a power series regression for the 5% exclusion values from each group of pegs tested at the various shear spans.

The specific gravity of the pegs affected the strength of the pegs in shear. As with the previous peg tests, shear strength increased with G, but the rate of increase is much less than that demonstrated in the peg bending test results. Figure 2-7 shows the yield stress versus G plot. The graph shows very little increase in the strength of the pegs with an increase in G, but the trend is consistent with the previous mechanical properties of the white oak pegs.

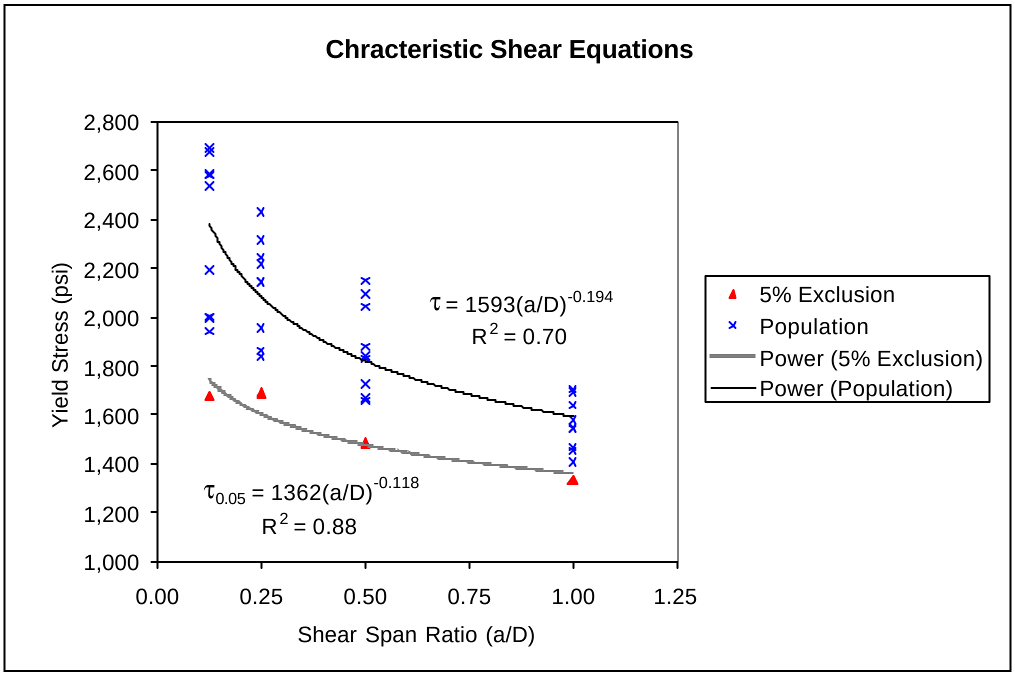

Figure 2-6 Characteristic Shear Stress Equation and 5% Exclusion Values

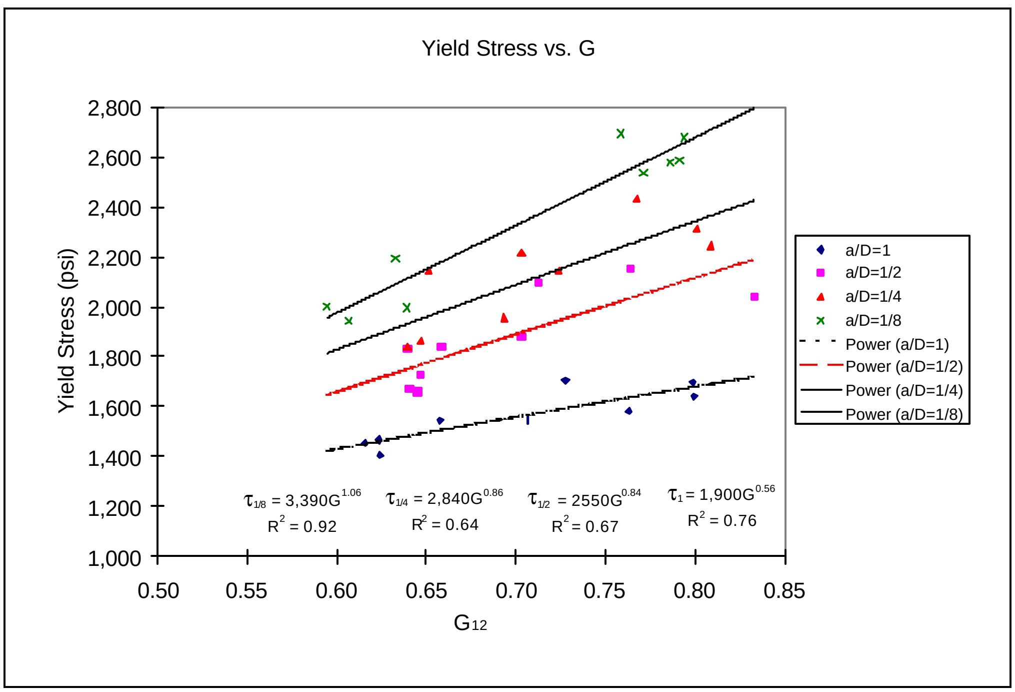

Figure 2-7 Shear Yield Stress vs. G

2.4 Bearing Concept

2.4.1 Combined Tests

The design of timber connections requires that several material properties be known. Bearing failures of the materials that comprise a timber joint are basic failure modes that are present in both timber frame joints and conventional connections with steel bolts. Assigning bearing strength capacities to the base material (mortise/tenon) and fastener (wood peg) in a timber frame connection is more difficult than a connection that uses steel fasteners. The bearing strength of the timber in a connection with steel fasteners governs the design. The bearing capacity of a typical steel bolt can be as much as 20 times the capacity of the wood that it connects. Therefore, bearing capacity of the joint is governed entirely by the strength of the wood. Timber frame joinery requires that the bearing strength of the fastener and base material be defined in combination.

Past research has defined the bearing strengths of several materials in combination. Schmidt and MacKay (1997) tested red oak pegs in combination with recycled Douglas fir and eastern white pine. Likewise, the work conducted by Church and Tew defined the dowel bearing strengths of white oak pegs combined with red oak and Douglas fir base materials (Church and Tew 1997; Church 1995).

This previous work has led to the investigation of alternative methods of defining dowel bearing strengths for timber frame connections. If the bearing behavior of various wood materials could be defined independently and combined mathematically to obtain the necessary bearing strengths for the design of timber frame connections, the use of existing data for individual species' dowel bearing strengths with steel fasteners could prove to be valuable.

The tests conducted for this work were performed under the assumption that materials could be tested separately and mathematically combined. Base material dowel bearing strengths were obtained using a smooth steel dowel, and the bearing strength of the pegs from the characteristic white oak population were found using a steel loading saddle. Mathematical models were developed for various material combinations. These models were based on a springs-in-series theory. It is hypothesized that the stiffness of an individual peg test can be added to the stiffness of a given base material, eliminating the need to perform testing on a vast number of peg and base material combinations. The springs-in-series theory is discussed in Chapter 4.

2.4.2 Base Material Dowel Bearing Procedure

Tests were performed to determine the dowel bearing strength of the base material used in the full-size joints. Previous research (Schmidt and MacKay 1997) contained tests with pegs and base materials in combination. Tests conducted for this research were performed using a 1-in. diameter steel bar (see Figure 2-8), instead of a wood peg as in previous research. Testing was performed using an Instron model 1332 testing machine and Labview data acquisition software. The specimens were tested according to ASTM 4761-93 at a load rate of 0.024 in/min to reach failure in approximately four to seven minutes (ASTM 1995a).

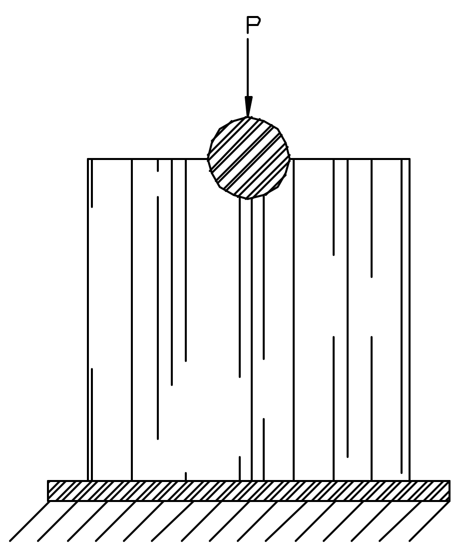

Figure 2-8 Base Material Dowel Bearing Test

Typically specimens for these tests were taken from the mortise and tenon members used in the full-size joint tests. Samples (4D x 4D x 1.5D) were cut from the vicinity of the mortise and tenon. An attempt was made to orient the samples as they would have been loaded during the full-size tests, however no designation was given to the orientation other than parallel or perpendicular to grain loading. The samples were also kept at the same moisture content as the full-size joints by storing the specimens in plastic bags.

A typical test procedure was as follows. Two specimens were removed from the environmental chamber/plastic bag and labeled. The specimens were clamped together end to end and drilled at the interface of the specimens using a 1" diameter spade bit and drill press. The resulting specimens had a half-cylindrical hole (trough) at the edge to be loaded; the length of the trough (1.5D) was then measured with calipers in two locations and averaged. The sample was placed in the test machine and a 1" diameter steel bar was placed in the trough. The Instron load head was adjusted until the loading platen was lightly resting on the test fixture. The load and displacement outputs were checked for zero readings. The data acquisition program and the Instron testing machine were started simultaneously. Upon reaching ultimate load, the data acquisition program and the loading was stopped. The characteristics of the failure were noted and a 2"x2"x1" sample from the specimen was measured, weighed, and placed in an oven for a minimum of 24 hours at 212^{o} F. The oven-dry specimen was removed, measured, and weighed again to determine specific gravity and moisture content.

A load verses deflection curve was created using the test output file. The yield load was found using the 5% offset method and the yield stress was calculated based on the projected area of the steel bar in the trough.

2.4.3 Base Material Dowel Bearing Results

Thirty-five tests were performed on samples of southern yellow pine (SYP). All the samples were cut from the mortise members of the full-size tests. For each SYP joint specimen, the two pieces of the specimen were cut from the same timber. Blocks approximately 6” long were removed from the timbers near the mortise. Dowel bearing samples were then cut from these blocks. Seven of the 35 tests were conducted parallel to grain. The remaining specimens were loaded perpendicular to grain.

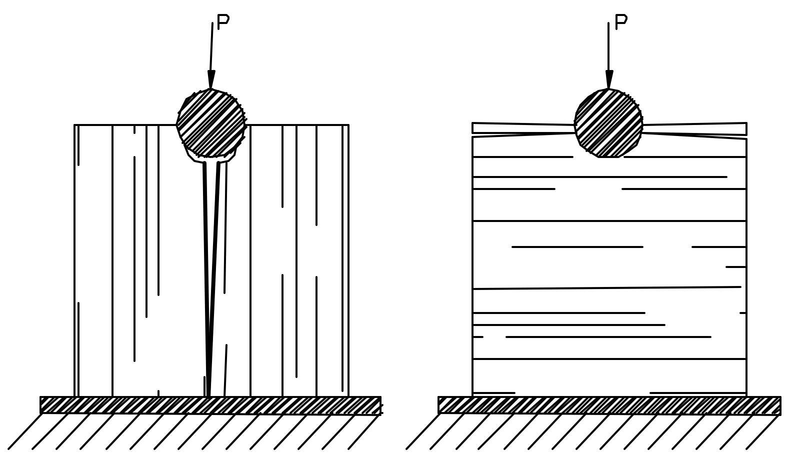

Figure 2-9 Base Material Bearing Failure Types

The characteristic failure modes were consistent with previous research (Schmidt and MacKay 1997, Church and Tew 1997). The parallel to grain specimens split longitudinally at ultimate while the perpendicular to grain specimens developed a horizontal shear failure (see Figure 2-9). The summary test results for the perpendicular to grain tests can be seen in Table 2-3. The parallel to grain results are not presented due to the limited data. A complete list of test data can be found in Appendix G.

A correlation between bearing strength and *G* could not be made for the SYP material. A plot was made with the results from the bearing tests, but a mathematical regression to obtain the bearing characteristics could not be made.

Table 2-3 SYP Bearing Perpendicular to Grain Results

	Yield Stress (psi)	Stiffness (lb/in)	MC (%)	G_{12}
Mean	1,870	42,200	16.5	0.52
Std. Dev.	407			
5% Exclusion	1,100			
COV	0.218			

Tests were conducted on 48 Recycled Douglas fir (RDF) samples. Samples were taken from both the mortise and tenon members of the full-size joint specimens. The specimens were cut so the bearing tests could be conducted in the same orientation as the peg exerted load on the members during the full size test procedure. Twenty-four tests were performed in each direction.

Obtaining quality samples from the mortise and tenon members was difficult. The recycled Douglas fir contained many checks that were not visible before cutting. Samples that could not be oriented in the same direction as the full-size joints are noted in the test data contained in Appendix G.

The characteristic failure modes for the specimens were consistent with previous research. The specimens loaded parallel to grain failed primarily by longitudinal splitting. The specimens loaded perpendicular to grain all failed with local crushing of the material below the loading bar. The test results for both sets of tests are summarized in Tables 2-4 and 2-5. A complete list of test data is in Appendix G.

Table 2-4 RDF Perp. to Grain Bearing Results

	Yield Stress (psi)	Stiffness (lb/in)	MC (%)	G_{12}
Mean	2,130	46,100	10.3	0.51
Std. Dev.	335			
5% Exclusion	1,480			
COV	0.158			

Table 2-5 RDF Parallel to Grain Bearing Results

	Yield Stress (psi)	Stiffness (lb/in)	MC (%)	G_{12}
Mean	6,560	324,000	9.2	0.46
Std. Dev.	1,040			
5% Exclusion	4,580			
COV	0.159			

The RDF tests parallel to grain did allow for a mathematical representation of the data. Figure 2-10 shows the 5% offset yield stress verse G. A regression was done using a power series equation similar to those found in prior research. As mentioned earlier, the R-squared value represents the correlation of the function to the test data with a value of 1.0 being exact and 0.0 having no correlation. Current dowel bearing strengths in the NDS are computed based on tests done with R-squared values ranging from 0.35 to 0.71 (Wilkinson 1991). These values were used as a guide in this research for determining the validity of any bearing test regressions. The correlation factor for the RDF parallel to grain dowel bearing tests was 0.63. The perpendicular to grain tests did not fall into the 0.35 to 0.71 correlation range. The specimens were noted if defects were unavoidable, but the majority of the specimens had no apparent defects. No conclusions are offerec as to why a correlation could not be made for the perpendicular to grain tests.

Forty-two tests were conducted with red oak (RO) samples. Samples were taken from both the mortise and tenon members of the full-size joint specimens. The specimens were cut so the bearing tests could be conducted in the same orientation as the peg exerted load on the members during the full size test procedure. Twenty-two tests were performed parallel to grain and 20 tests were performed perpendicular to grain.

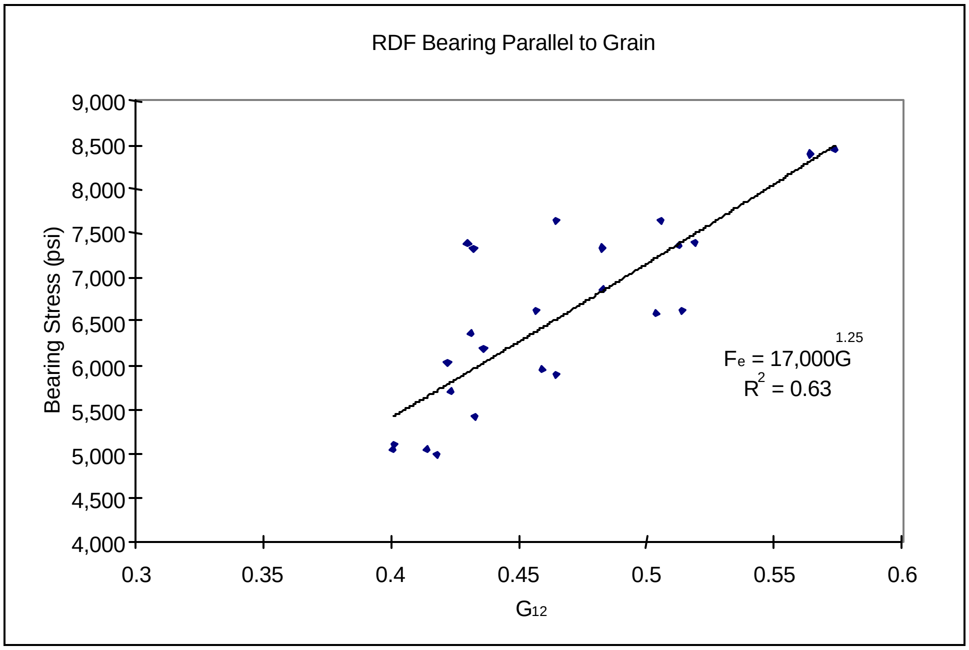

Figure 2-10 RDF Bearing Strength vs. G

Similar to the recycled Douglas fir tests, obtaining samples from the red oak timbers proved to be difficult. The exterior checks, coupled with internal honeycombing in the timbers, made it difficult to produce defect free samples. Samples were noted if they were not obtained in the same orientation as mentioned earlier and defects were noted when they were unavoidable.

Again, the RO bearing tests had failure modes consistent with tests in previous research. Half of the test specimens loaded parallel to grain failed by longitudinal splitting and the remainder failed due to local crushing of the material below the loading bar. The specimens loaded perpendicular to grain also had two modes of failure. In tests with specimens that had an annual ring tangent at approximately 45 degrees to the axis of loading, a rolling shear between annual rings was dominant. The cell walls of the material crushed due to the shear stress present in the specimen and this allowed movement between annual rings. A rolling shear failure occurred prior to any significant deformation at the trough due to local crushing. The remainder of the tests produced horizontal splitting failures similar to the southern yellow pine tests. The results from both sets of tests are summarized in Tables 2-6 and 2-7.

Table 2-6 RO Bearing Strengths Perp. to Grain

	Yield Stress (psi)	Stiffness (lb/in)	MC (%)	G_{12}
Mean	4,910	110,000	9.0	0.66
Std. Dev.	446			
5% Exclusion	4,040			
COV	0.091			

Table 2-7 RO Bearing Strengths Parallel to Grain

	Yield Stress (psi)	Stiffness (lb/in)	MC (%)	G_{12}
Mean	11,400	438,000	7.4	0.68
Std. Dev.	1,850			
5% Exclusion	7,840			
COV	0.163			

The results of the red oak tests were similar to that of the RDF. The specimens loaded parallel to grain did fall within the specified correlation range (R^2=0.35 to 0.71) with a correlation factor of 0.62. The perpendicular to grain tests were consistent with the previous two species in that they did not produce a viable regression. Figure 2-11 shows the RO bearing strength parallel to grain versus specific gravity.

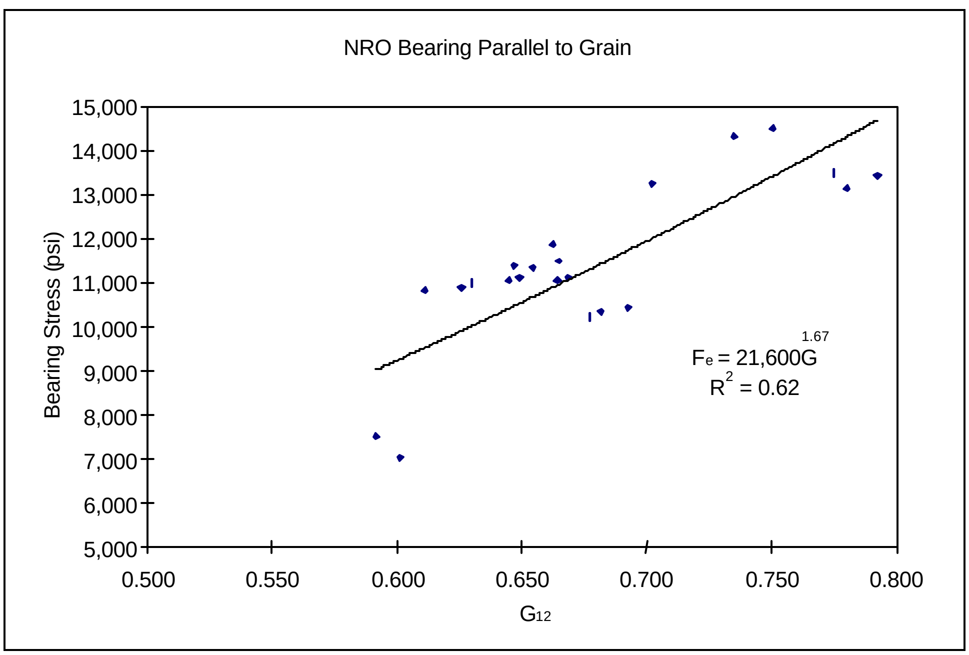

Figure 2-11 RO Bearing Strength vs. *G*

The dowel bearing tests parallel to grain had a better correlation to specific gravity than the perpendicular to grain tests. The results of all of the parallel to grain tests were plotted versus *G* at 12%

MC and compared to the NDS equation for dowel bearing strength (see Figure 2-12). The plot shows that all of the test specimens had higher strengths than that computed with the NDS bearing equation shown in the plot. Figure 2-13 shows all of the parallel to grain tests with a best-fit equation correlation coefficient of 0.9, which exceeds that for the material tests used to develop the NDS values.

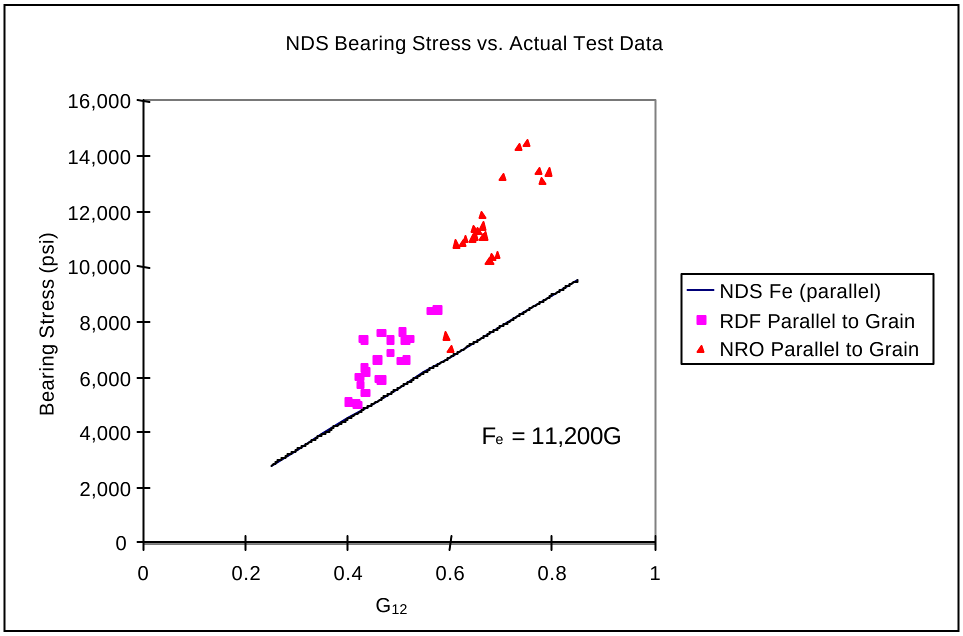

Figure 2-12 Comparision of Data to NDS Dowel Bearing Equation Parallel to Grain Loading

The test values for the perpendicular to grain tests were also compared to the NDS design equation in Figure 2-14. As shown in the plot, all of the RO tests exceed the values used by the NDS and the SYP, as well as the RDF, data fell on or below the NDS values. The results of the perpendicular to grain tests were combined to establish a best-fit equation in Figure 2-15. The correlation coefficient (R^2=0.60) for the test data again fell within the range (R^2=0.35 to 0.71) for data used to develop the NDS design equations.

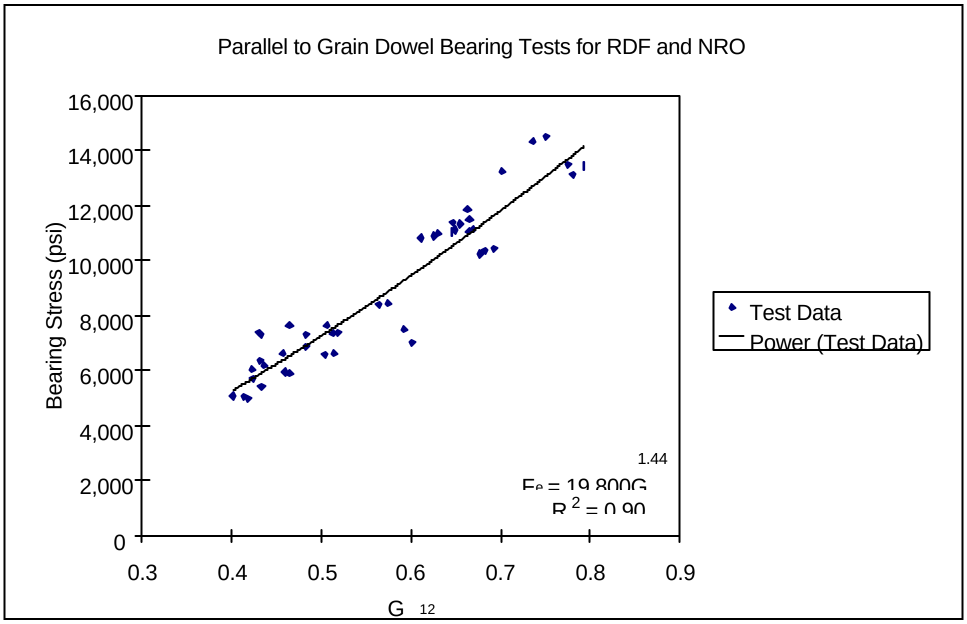

Figure 2-13 Best Fit Equation for Parallel to Grain Bearing Tests

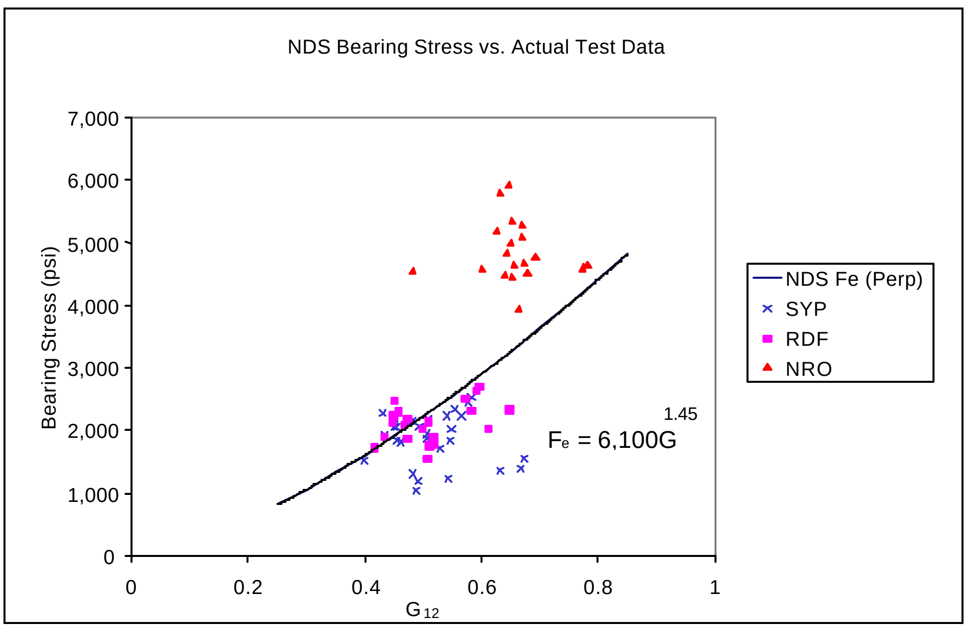

Figure 2-14 Comparision of the Test Data to NDS Dowel Bearing Equation Perp. to Grain Loading

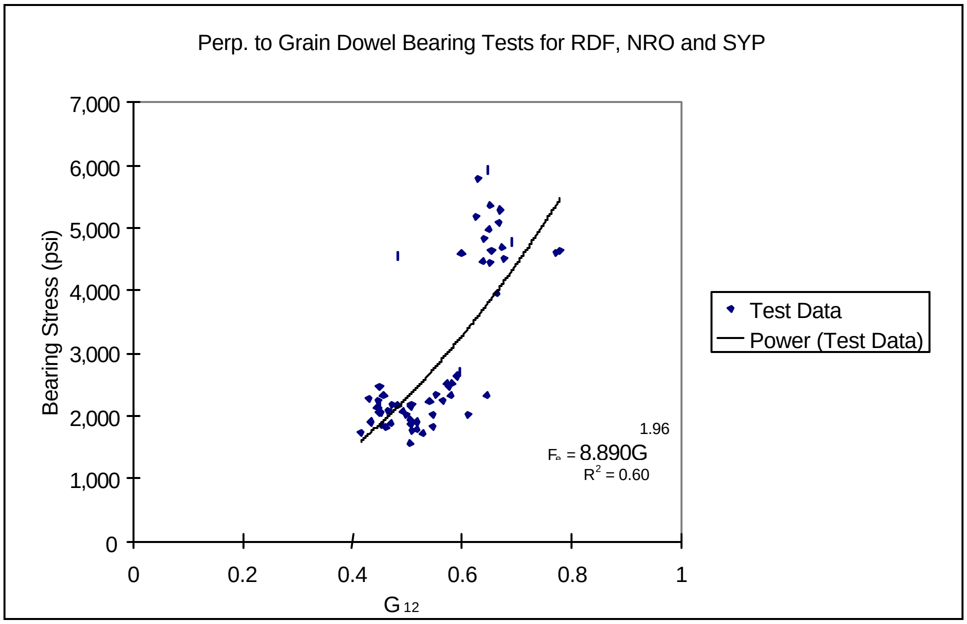

Figure 2-15 Best Fit Equation for the Perp. To Grain Tests

2.4.4 Peg Bearing Procedure

Peg bearing tests were performed to determine the bearing strength for the peg population selected for the full-size joint tests. Previous research contained tests with pegs and base materials in several combinations (Schmidt and MacKay 1997). Tests for this research were performed using a 1.5" wide steel saddle (see Figure 2-16), which replaced the wood base material in previous tests. The testing was performed using an Instron model 1332 testing machine and Labview data acquisition software. The pegs were tested according to ASTM 4761-93 at a load rate of 0.024 in/min (ASTM 1995a).

A load versus deflection curve was created using the test output file. The yield load was then determined using the 5% offset method and the yield stress was calculated using the average diameter of the peg.

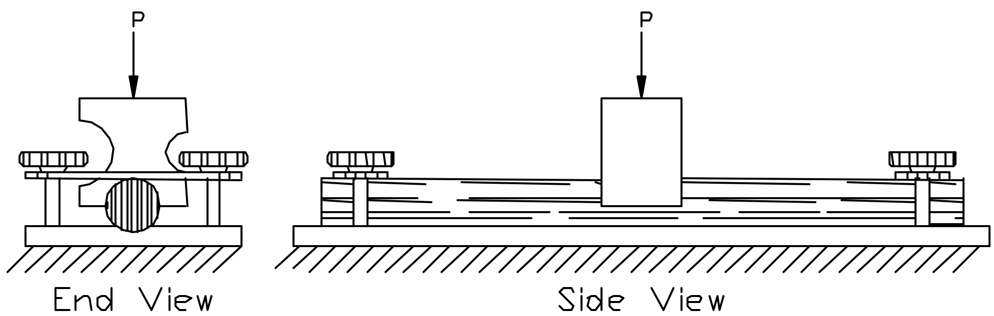

Figure 2-16 Peg Bearing Test Fixture

2.4.5 Peg Bearing Results

Fifty bearing tests were conducted with 1" diameter pegs from the white oak peg population. The tests included 30 pegs at approximately 12% *MC*. The remaining 20 pegs were tested green, with a *MC* of approximately 31%. The summary results of these tests are listed in Table 2-8. The green pegs had a 37.4% lower yield stress than the dry pegs. Likewise, the green peg stiffness was 38.7% lower than the dry peg stiffness. The average *G* of the dry pegs and green pegs was 0.71 and 0.62, respectively.

Table 2-8 White Oak Peg Bearing Results

Dry Pegs

	Yield Stress	Stiffness (lb/in)	MC (%)	G_{12}
Mean	2,690	110,000	13.7	0.71
Std. Dev.	580			
5% Exclusion	1,600			
COV	0.216			

Wet Pegs

	Yield Stress (psi)	Stiffness (lb/in)	MC (%)	G
Mean	1,720	67,600	31.1	0.62
Std. Dev.	212			
5% Exclusion	1,310			
COV	0.123			

The major factor contributing to the bearing strength of the pegs was specific gravity. The variability in the MC and yield stress prevents any mathematical regression to establish a relationship for the data. A definite relationship between *G* and yield stress for the dry pegs can be seen in Figure 2-13. A trend line with a correlation factor (R^2) of 0.75 is shown in Figure 2-17 for all of the dry peg tests. Similar to the previous base material bearing tests, the pegs exceed the correlation range (R^2 = 0.35 to 0.71) that resulted from the development of dowel bearing strengths for the current NDS (Wilkinson 1991). The dry pegs actually had a greater COV, based on a lower 5% exclusion value, than the green pegs. The green and dry pegs exhibited no change in yield stress when compared with MC within each test group.

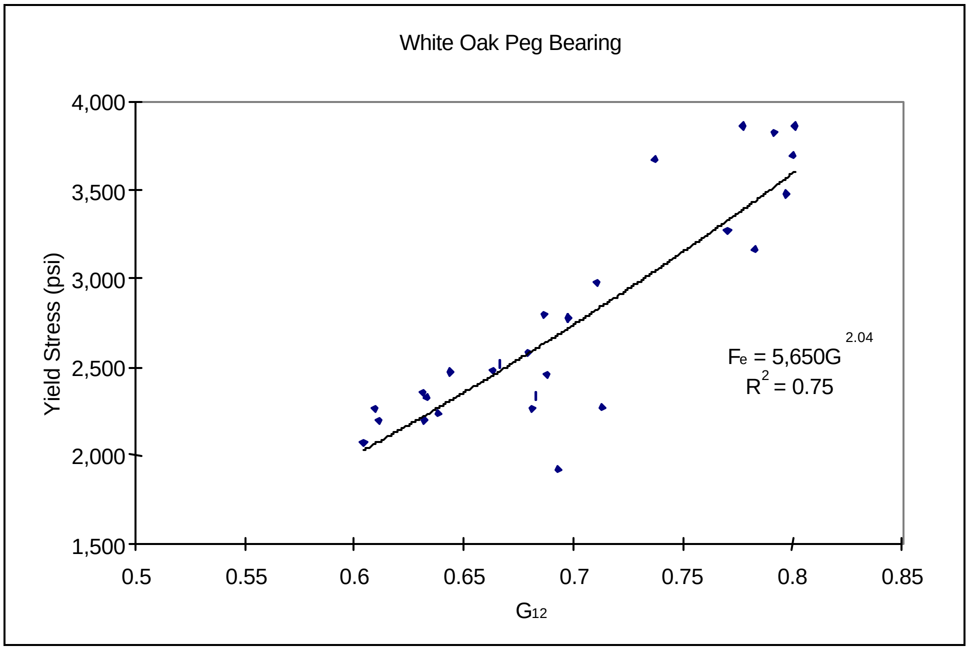

Figure 2-17 White Oak Peg Bearing Stress vs. G

3. Joint Tests

3.1 Introduction

The intent of the full-size joint tests was to establish detailing requirements to assure peg failure within the joint and to determine the strength and stiffness of the joints. The tests included monotonic loading of specimens to failure, as well as a small number of cyclically loaded specimens to study toughness.

3.2 General Procedure

Full-size joints were tested using a steel load frame and an Enerpac RCH 123 hydraulic ram operated by a hand pump. Figure 3-1 shows the test apparatus and a typical joint specimen. Labview data acquisition software was used to record data from a pressure transducer and two linear potentiometers. The potentiometers measured displacement between the mortised and tenoned members; the two measurements were averaged to obtain a displacement for the joint.

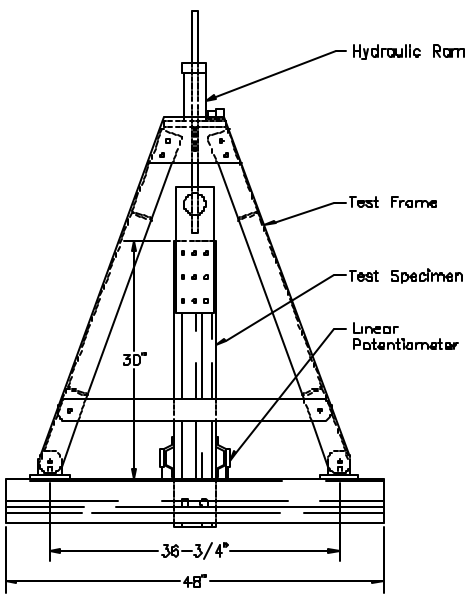

Figure 3-1 Joint Test Apparatus from Schmidt and MacKay (1997)

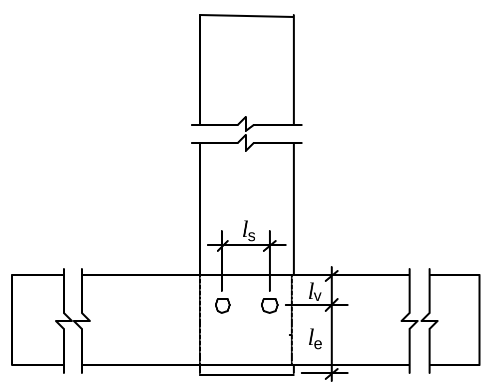

Figure 3-2 Typical Joint Detailing

The objectives of the tests were to determine appropriate end distance, edge distance and spacing requirements, and to determine strength, stiffness, and the mode of failure for mortise and tenon joints. The joints were tested in tension to simulate frame and joint behavior subjected to lateral loads such as a wind loading. Joints were initially tested with large end and edge distances so that failure would likely occur in the pegs. The detailing values were reduced until minimum values that still produced peg failure at yield were found. The optimum joint configuration for a given species was found using the smallest values for edge distance (l_v), end distance (l_e) and fastener spacing (l_s) that produced failure in the pegs (see Figure 3-2). A minimum of three joints was tested with this optimum configuration. During and following each test, the joints were inspected to determine the mode of failure. All monotonically loaded specimens were tested in an attempt to reach yield in approximately 10 minutes with load rates load between 0.0002 in/sec and 0.0005 in/sec.

Several joints were also cyclically loaded to obtain hysteresis characteristics and to demonstrate toughness. The joints were successively loaded and released in 0.05" displacement increments until failure. Seven joints were cyclically loaded to failure.

All joints were fabricated using the same techniques and tolerances that could be expected in a commercial shop. All joints were assembled with 1" diameter white oak pegs from the characteristic population and from dry timbers for the mortise and tenon members (see Figure 3-1). Softwood joints were constructed with 2" thick tenons and hardwood joints were constructed with 1 1/2" tenons. If possible, obvious defects such as large knots, severe checking, and decay were avoided in the construction and assembly of the joints. The mortise members were constructed with a through mortise. The through mortise allowed for examination of the tenon during testing, which enabled the researcher to determine the exact point during the test if a tenon failure occurred. A total of 56 tests were conducted on 42 joints: 20 southern yellow pine, 12 recycled coastal Douglas fir, and 10 red oak.

3.2.1 Southern Yellow Pine

Twenty-four tests were conducted on 20 southern yellow pine joints. The first 16 joints were constructed and tested at a Timber Framer's Guild of North America workshop in Nacodoges, TX in

March 1998. Students attending the workshop constructed the joints as practice joints. Students cut the mortise and tenon members as shown in Figure 3-3, and the peg holes were located and drilled by the researcher. Twelve of the joints were loaded monotonically to failure. Two joints were loaded monotonically with an 1/8" drawbore (see Figure 3-4). The final two joints were cyclically loaded to determine hysteresis characteristics.

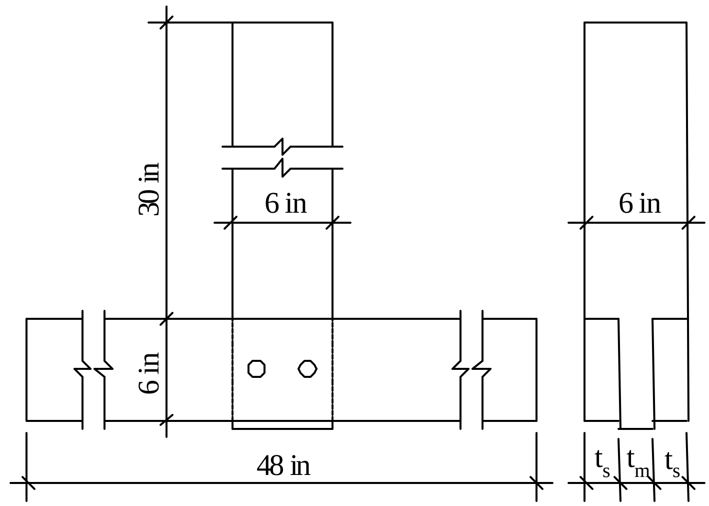

Figure 3-3 Typical Joint Specimen

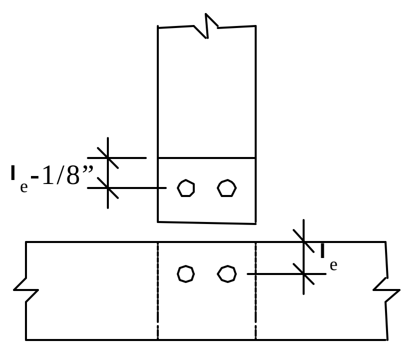

Figure 3-4 Typical Draw Bored Joint

Eight additional tests were performed on four joints shipped from Red Suspenders Timber Frames, Nacodoges, TX. The specimens were fabricated by Red Suspenders Timber Frames and the peg holes were located and drilled by the researcher. The tests were performed using white oak 0.75" diameter round pegs and 1.25" diameter octagonal pegs. These tests were performed to verify the detailing dimensions determined from the initial 16 tests. Also, two joints were tested three times each to simulate the replacement of damaged pegs in a structure that has been exposed to excessive loads.

3.2.2 Recycled Douglas Fir

Twelve recycled coastal Douglas fir joints were used in this work. The joints were fabricated and tested at Big Timberworks in Gallatin Gateway, MT in May 1998. The joints were fabricated and assembled by the researchers. Ten of the twelve joints were loaded monotonically to failure. The remaining two joints were cyclically loaded to determine hysteresis characteristics.

3.2.3 Red Oak

Twenty tests were conducted in August 1998 on ten red oak joints shipped to the University of Wyoming by Sunset Structures, Ltd. Elkview, WV. The timbers were kiln dried by a radio frequency vacuum process. Sunset Structures, Ltd. cut the mortise and tenons; the peg holes were located and drilled by the researcher. Ten tests on six joints were performed with monotonic loading and 1” diameter pegs from the white oak population to determine optimum spacing requirements. The remaining four joints and ten tests were conducted with 0.75”, 1” and 1.25” octagonal white oak pegs with cyclic loadings and the repair procedure mention earlier.

3.3 Failure Modes

Two categories of failures were present in the 56 tests conducted. The first category of failure was a brittle failure. A brittle failure is defined as cross grain tension splitting of the mortise member or a splitting failure of the tenon member. The second category of failure was a ductile failure of the peg. The peg failure was a shear/bending failure and it was the most common failure mode. Figure 3-5 shows the three failure modes.

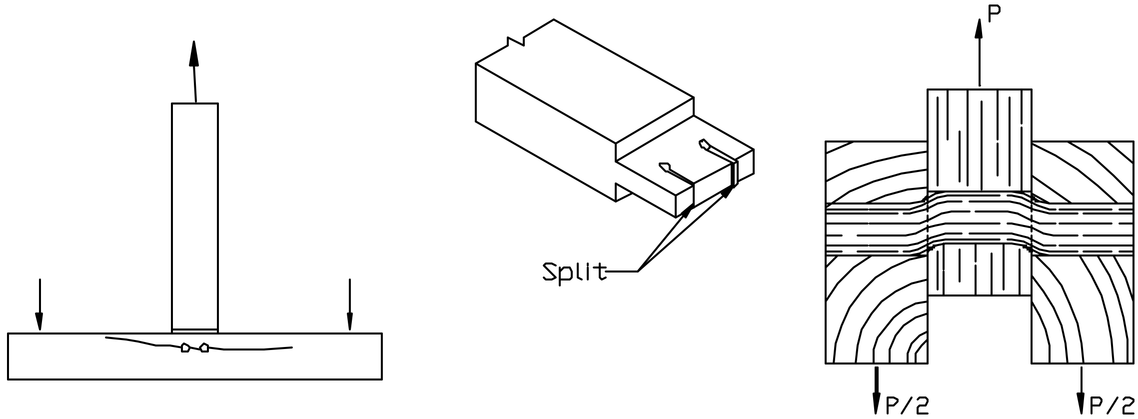

Mortise Split Tenon Split Peg Shear

Figure 3-5 Typical Test Specimen Failure Modes

The peg shear/bending failure mode was the characteristic failure mode for all of the tests. The southern yellow pine failures were exclusively peg shear/bending failures, regardless of peg location. The recycled Douglas Fir tests were more sensitive to peg location. However, upon establishment of minimum spacing requirements the peg shear/bending failure mode was again exclusive, barring failures caused by defects. Inspection of the joints after testing showed that both the mortise and tendon members had minor localized crushing at the peg holes. The crushing of this material lengthens the shear span discussed in earlier sections.

The red oak tests had similar failures. The monotonically loaded joints with 1” diameter pegs had shear/bending failures of the peg at yield. The high material stiffness of the red oak created a shear failure with a much lower shear span to diameter ratio than the previous tests with softwoods. Inspection of the 1” peg joints after testing showed no signs of damage to either the mortise or tenon members. Inspection of the pegs showed signs of the same failure evident in the softwood tests. However, the pegs did exhibit more signs of bearing failure at the tenon member than they did in the softwood tests.

3.4 Southern Yellow Pine Results

Twenty-four tests were conducted on 20 shortleaf southern yellow pine joints. The timbers were graded as dense select structural with an average moisture content of 17%.

Peg shear/bending failure was the most common failure mode. All joints had this failure mode at yield regardless of end and edge distance. At ultimate, 17 of the 24 tests displayed the same peg shear/bending failure. The remainder of the tests also had a failure of the tenon or mortise at ultimate. Typically, the mortise and tenon failures occurred at extreme displacements, on the order of 40% of the peg diameter for the joints with 1” pegs.

Overall, the strength values for the southern pine joints were consistent. The average yield strength for the 12 monotonically loaded joints with 1” diameter pegs was 4906 lbs. The COV was 13.7% and the 95% exclusion value for load was 3634 lbs. Table 3-1 shows the results for the 12 tests and the geometry of the connections. The calculated average shear span for the joints is 1.14”. This number is relatively high when compared to the other species tested and can possibly be explained by the fact that the pegs were at FSP. It was not possible to condition the pegs to 12% MC prior to testing the initial group of southern pine joints. Figure 3-6 shows a typical load deflection plot for the southern yellow pine joints.

The joint geometry necessary to ensure peg failure was established for the southern pine. As shown in Table 3-1, the end and edge distances were reduced to 1.5D with no additional failure modes (i.e. mortise splitting or tenon relish failures). These values were considered to be extreme for actual practice and unpleasant visually. The recommended minimum detailing dimensions for SYP based on the 12 monotonically loaded joints is 2D edge and end distance with a 3D peg spacing.

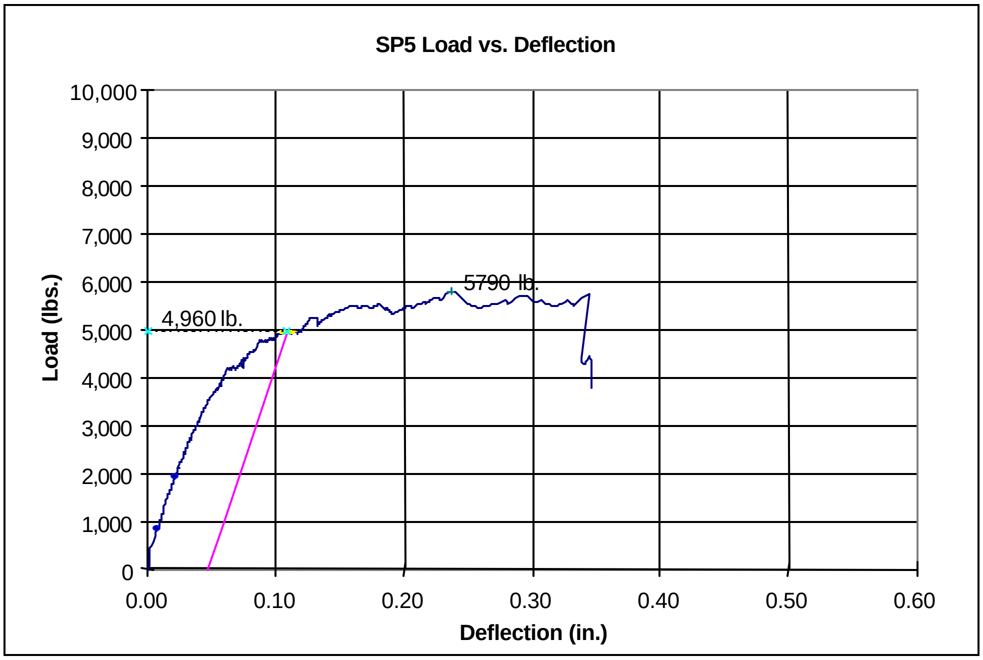

Figure 3-6 Typical SYP Load Deflection Plot

A second set of southern pine joints was tested at a later date to verify the recommended geometry. Four joints were tested a total of eight times. The four joints were tested with 0.75” round and 1.25” octagonal pegs with the recommended geometry. The 0.75” pegs were from the same peg population as the 1” diameter pegs used in the initial tests, while the 1.25” were from a different source. Unlike the initial joint tests with 1” diameter pegs, the 0.75” and 1.25” pegs were at approximately 12% MC. All of the tests had a peg failure with the exception of one joint, which had a large knot adjacent to the peg locations. The joint developed a mortise split due to the severe slope of grain caused by the knot. The ultimate load for this joint was 6444 lbs. Tables 3-2 and 3-3 show the summary results for the eight tests.

The second set of SYP joints was used to verify the desired failure mode discussed in Chapter 4. Two of the four joints were loaded beyond yield a total of three times each. The joints were loaded to failure and the damaged pegs were replaced with new pegs. This retrofit procedure was used to model the behavior of a joint that has been overloaded and repaired. The joints behaved as would be expected. There was a small loss in initial stiffness due to the localized damage to the mortise and tenon members, which led to larger shear spans and slightly lower yield strengths. The load versus deflection plot for one of the retrofitted joints can be seen in Figure 3-7. The tests with 1.25” pegs did not reach the 5% offset point on the load deflection plot. The pegs failed due to a single flexural hinge directly under the tenon member and did not display the same ductility as the joints tested with 1” diameter pegs.

Test	Peg Diameter (in)	End Dist. (l_v)	Edge Dist. (l_e)	Spacing Dist. (l_s)	Yield Disp. (in)	Yield Load (lbs)	Yield Stress (psi)	Stiffness (lbs/in)	Ultimate Disp. (in)	Ultimate Load (lbs)	Ave. Peg G	Failure Type @ Yield	Failure Type @ Ultimate
SP1	1.0	2D	4D	3D	0.16	6,700	2,060	41,100	0.42	8,880	0.76	Peg Shear/Bending	Peg Bending/Shear
SP2	1.0	2D	4D	3D	0.11	5,450	1,720	74,300	0.55	9,400	0.76	Peg Shear/Bending	Mortise Split
SP3	1.0	1.5D	3D	3D	0.16	4,420	1,370	33,900	0.42	6,310	0.58	Peg Shear/Bending	Peg Bending/Shear
SP4	1.0	1.5D	3D	3D	0.13	5,010	1,550	57,900	0.35	6,160	0.63	Peg Shear/Bending	Peg Bending/Shear
SP5	1.0	1.5D	2D	2D	0.11	4,960	1,580	80,200	0.24	5,790	0.64	Peg Shear/Bending	Mortise Split
SP6	1.0	1.5D	2D	2D	0.08	4,470	1,400	466,000	0.27	5,530	0.62	Peg Shear/Bending	Mortise Split
SP7	1.0	1.5D	2D	2.5D	0.08	4,470	1,400	114,000	0.31	6,020	0.62	Peg Shear/Bending	Tenon Split
SP8	1.0	1.5D	2D	2.5D	0.16	5,300	1,650	48,700	0.22	5,530	0.59	Peg Shear/Bending	Peg Bending/Shear
SP9	1.0	2D	2D	2.5D	0.11	4,970	1,550	73,200	0.38	5,520	0.63	Peg Shear/Bending	Mortise Split
SP10	1.0	2D	2D	2.5D	0.11	4,720	1,470	101,000	0.58	6,640	0.62	Peg Shear/Bending	Mortise Split
SP11	1.0	2D	2D	3D	0.12	4,360	1,410	51,200	0.50	6,600	0.60	Peg Shear/Bending	Tenon Split
SP12	1.0	2D	2D	3D	0.10	4,720	1,470	89,500	0.59	8,220	0.62	Peg Shear/Bending	Tenon Split
					Mean=	4,960	1,550						
					Std. Dev.=	649	193						
					5% Exclusion=	3,630	1,160						
					COV=	0.131	0.124						

Table 3-1 SYP Monotonic Test Results

Test	Peg Diameter (in)	End Dist. (l_v)	Edge Dist. (l_e)	Spacing Dist. (l_s)	Yield Disp. (in)	Yield Load (lbs)	Yield Stress (psi)	Stiffness (lbs/in)	Ultimate Disp. (in)	Ultimate Load (lbs)	Ave. Peg G	Failure Type @ Yield	Failure Type @ Ultimate
50	0.75	2D	2D	3D	0.07	2,390	1,370	60,000	0.44	4,060	0.62	Peg Shear/Bending	Peg Shear/Bending
51a	0.75	2D	2D	3D	0.13	3,020	1,770	29,500	0.39	4,430	0.64	Peg Shear/Bending	Peg Shear/Bending
51b	0.75	2D	2D	3D	0.12	2,520	1,480	23,700	0.34	3,580	0.67	Peg Shear/Bending	Peg Shear/Bending
51c	0.75	2D	2D	3D	0.12	2,610	1,530	23,100	0.41	4,540	0.65	Peg Shear/Bending	Peg Shear/Bending
					Mean=	2,640	1,540						
					Std. Dev.=	272	169						
					5% Exclusion=	1,900	1,080						
					COV=	0.103	0.110						

Table 3-2 SYP ¾” Diameter Joint Test Results

Test	Peg Diameter (in)	End Dist. (l_v)	Edge Dist. (l_e)	Spacing Dist. (l_s)	Yield Disp. (in)	Yield Load (lbs)	Yield Stress (psi)	Stiffness (lbs/in)	Ultimate Disp. (in)	Ultimate Load (lbs)	Ave. Peg G	Failure Type @ Yield	Failure Type @ Ultimate
52	1.25	2D	2D	2.5D				42,000	0.18	6,440	N/A		Mortise split at knot
53a	1.25	2D	2D	3D	0.17	8,000	1,790	65,200	0.18	8,190	0.65	Peg Shear/Bending	Peg Shear/Bending
53b	1.25	2D	2D	3D				39,800	0.16	7,130	0.64		Peg Shear/Bending
53c	1.25	2D	2D	3D				39,300	0.14	6,340	0.57		Peg Shear/Bending

Table 3-3 SYP 1 ¼” Diameter Joint Test Results

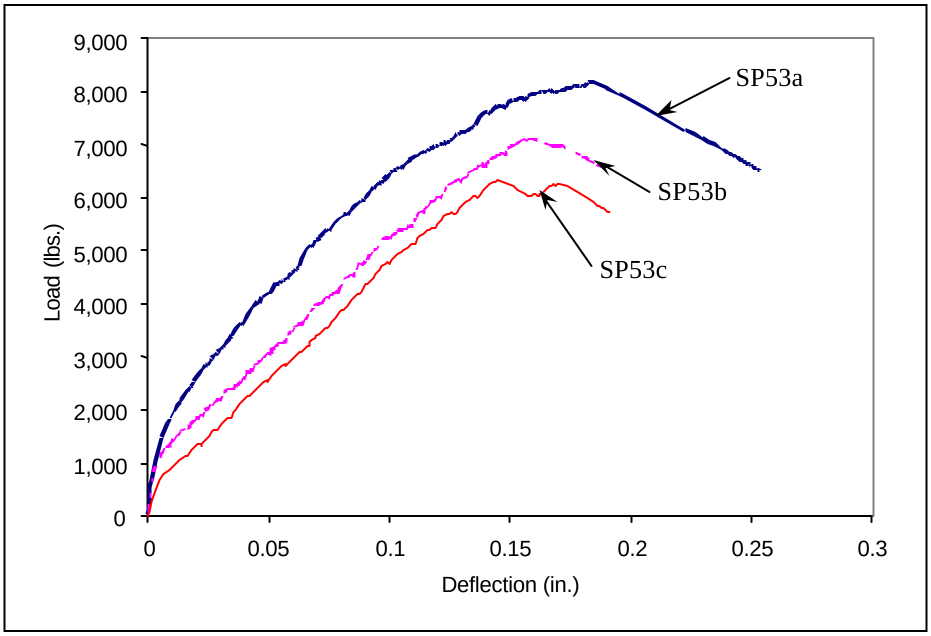

Figure 3-7 SYP Load vs. Deflection for a 1.25" Peg Repair

The stiffness of the southern yellow pine joints could not be identified. The first group of SYP joints tests conducted were constructed by students attending a timber frame workshop and a number of the joints were driven together with a mallet. The force required too overcome the frictional forces on the mortise and tenon was not determined, but undoubtedly altered the initial stiffness of the connection. The second group of SYP tests was conducted on joints constructed by professional timber framers, and the stiffness values were more consistent, but the limited number of tests prevents any relationship to be drawn. Additionally, the test setup itself can produce errors in the initial stiffness if the joint is not aligned properly in the test apparatus.

It was determined that the draw boring of timber framed joints creates a creep phenomenon that deserves more attention. Two joints were constructed with an 1/8" draw bore. Draw boring is common practice in the timber frame industry to prestress joints. The prestress helps prevent green timbers from opening at the joint after drying has occurred and is used to close gaps in joints constructed with dry material. The draw bored joints were assembled 24 hrs. prior to testing. Prior to testing, one of the joints developed a split along two lines behind one of the pegs (relish failure), while the other joint maintained its integrity. The joints were tested and showed a definite increase in initial stiffness due to the draw bore with no appreciable change in the yield or ultimate load. The joint with the relish failure prior to testing did maintain its strength due to a wedging action of the peg on the tenon material. The joint had a higher yield strength than the undamaged joint. It was decided that additional studies of the effects of draw boring on joint capacity would be left to future research. Results from these two tests can be found in the Appendix C.

3.5 Recycled Douglas Fir Results

Twelve tests were conducted on recycled coastal Douglas fir joints. The timbers were ungraded and had an average moisture content of 9.8%.

The recycled Douglas fir (RDF) joints failed most often by peg shear/bending. The joints did not allow the same minimal end and edge distances as the SYP joints due to the low tension perpendicular to grain strength of the material. Only one of the joints developed a mortise split prior to yield, but audible cracking could be heard in several joints. All of the tests with RDF were performed with 1" diameter pegs from the characteristic white oak peg population. The average strength for the monotonically loaded joints with a peg shear/bending failure was 5,494 lbs. The COV was 10.2% and the 95% exclusion value for load was 4,451 lbs. Table 3-4 shows the strengths for the 10 monotonic tests and the geometry of each connection. The average calculated shear span for the RDF joints is 0.40". It is important to note that the RDF tests were not carried out to the same relatively large displacements as the SYP tests. This was done to preserve the material in the joints for use in later dowel bearing tests. The damage caused by a mortise split virtually destroyed the specimen mention earlier and the minute checks in the RDF already hampered the collection of bearing samples. The RDF tests were carried out to a displacement of approximately 15% of the peg diameter.

Test	Peg Diameter (in)	End Dist. (l_v)	Edge Dist. (l_e)	Spacing Dist. (l_s)	Yield Disp. (in)	Yield Load (lbs)	Yield Stress (psi)	Stiffness (lbs/in)	Ultimate Disp. (in)	Ultimate Load (lbs)	Ave. Peg G	Failure Type @ Yield	Failure Type @ Ultimate
DF1	1.0	4D	2D	3D	0.12	5,880	1,960	72,600	0.16	6,510	0.66	Peg Shear/Bending	Mortise Split
DF2	1.0	4D	2D	3D				80,800	0.06	5,160	0.66		Simult. Peg & Mortise
DF3	1.0	3D	2.5D	3D	0.09	5,360	1,780	136,000	0.21	6,070	0.65	Peg Shear/Bending	Mortise Split
DF4	1.0	3D	2.5D	3D	0.12	5,360	1,800	65,100	0.18	6,270	0.60	Peg Shear/Bending	Peg Shear/Bending
DF5	1.0	2D	2.5D	3D	0.07	4,790	1,650	186,000	0.15	6,340	0.63	Peg Shear/Bending	Simult. Tenon & Mortise
DF6	1.0	2D	2.5D	3D	0.08	6,460	2,190	166,000	0.11	6,720	0.63	Peg Shear/Bending	Peg Shear/Bending
DF7	1.0	2D	2.5D	2.5D	0.09	5,610	1,840	131,000	0.17	6,530	0.65	Peg Shear/Bending	Peg Shear/Bending
DF8	1.0	2D	2.5D	2.5D	0.09	5,670	1,860	102,000	0.15	6,480	0.67	Peg Shear/Bending	Peg Shear/Bending
DF9	1.0	1.5D	2D	3D				148,000	0.03	2,950	0.66		Tenon Split
DF10	1.0	2D	2.5D	2.5D	0.12	6,480	2,140	86,700	0.23	7,110	0.77	Peg Shear/Bending	Mortise Split
					Mean=	5,700	1,900						
					Std. Dev.=	572	184						
					5% Exclusion=	4,450	1,500						
					COV=	0.100	0.097						

Table 3-4 RDF Monotonic Joint Test Results

The joint geometry for the RDF tests to assure peg failure was established. As shown in Table 3-4, the end and edge distances were 2D and 2.5D, respectively, with no additional failure modes at yield. Recommended edge distance, end distance, and spacing requirements were established at 2.5D, 2D, and 2.5D, respectively.

The stiffness values for the RDF joints were similar to the SYP joints. The RDF joints were fabricated by the researcher and while none of the joints were forcibly joined, it is safe to say that the joints were not constructed with the same consistency or skill had they been constructed by a professional joiner. Again, misalignment or sag in the test setup is thought to have affected the initial stiffness of some of the joints.

3.6 Red Oak Results

A total of 20 tests was conducted on 10 kiln dried red oak joints. Ten tests were performed monotonically with 1” diameter pegs loading, five tests used 0.75” or 1.25” pegs loaded monotonically, two joints were tested with four 1” diameter pegs in each joint and the remaining three specimens were tested cyclically. The timbers were ungraded with an average moisture content of 8.2%.

Peg shear/bending failure was the most frequent failure mode. Regardless of end and edge distance, all joints except one had this failure mode at yield. At ultimate 14 of the 20 tests displayed the same peg shear/bending failure. The remainder of the tests had a failure of the tenon or mortise at ultimate. Typically, the mortise and tenon failures occurred at large displacements, on the order of 25% of the peg diameter for the joints with 1" pegs.

Overall, the strength values for the red oak joints were consistent. The average strength for the 10 monotonically loaded joints with 1" diameter pegs was 7,331 lbs. The COV was 4.6% and the 95% exclusion value for load was 6,615 lbs. Unlike the monotonic tests on the SYP and RDF joints, the first six tests were performed on only two joints. This was done in part to save material and to help verify the assumptions made about peg shear being the failure mode of choice for the designer. Table 3-5 shows the strengths for the 10 tests and the geometry of the connections. The average calculated shear span for the 10 joints was 0.11".

The geometry for the red oak joints to assure peg failure was established. As shown in Table 3-5, the end and edge distances were reduced to 1.5D with no mortise splitting or tenon relish failures. These values were again considered to be extreme for construction practice. The recommended end and edge distance for the red oak joints was 2D with a peg spacing of 2.5D.

A second set of red oak joints was tested to verify the recommended geometry. Two joints were tested a total of five times. The two joints were tested with 0.75" round and 1.25" octagonal pegs with the recommended geometry. The 0.75" pegs were from the same peg population as the 1" diameter pegs used in the initial tests, while the 1.25" were from a different source. All of the tests had a peg shear/bending failure. Tables 3-6 and 3-7 show the results for the 5 tests.

Test	Peg Diameter (in)	End Dist. (l_v)	Edge Dist. (l_e)	Spacing Dist. (l_s)	Yield Disp. (in)	Yield Load (lbs)	Yield Stress (psi)	Stiffness (lbs/in)	Ultimate Disp. (in)	Ultimate Load (lbs)	Ave. Peg G	Failure Type @ Yield	Failure Type @ Ultimate
RO1	1.0	2.25D	2.75D	2.75D	0.16	7,150	2,360	78,900	0.30	9,220	0.75	Peg Shear/Bending	Peg Shear/Bending
RO2	1.0	2.25D	2.75D	2.75D	0.15	6,780	2,250	73,400	0.34	9,360	0.74	Peg Shear/Bending	Peg Shear/Bending
RO3	1.0	2.25D	2.75D	2.75D	0.19	7,390	2,510	65,100	0.38	10,140	0.76	Peg Shear/Bending	Peg Shear/Bending
RO4	1.0	2D	2D	2.5D	0.16	7,570	2,540	71,200	0.34	9,230	0.78	Peg Shear/Bending	Peg Shear/Bending
RO5	1.0	2D	2D	2.5D	0.20	7,420	2,480	58,100	0.36	9,050	0.79	Peg Shear/Bending	Peg Shear/Bending
RO6	1.0	2D	2D	2.5D	0.22	7,790	2,590	56,700	0.38	9,230	0.77	Peg Shear/Bending	Peg Shear/Bending
RO7	1.0	1.5D	1.5D	2.5D	0.17	6,860	2,240	63,000	0.25	7,590	0.82	Peg Shear/Bending	Mort. Split @ Check
RO8	1.0	1.5D	1.5D	2.5D	0.15	7,450	2,450	81,100	0.28	8,510	0.80	Peg Shear/Bending	Relish Failure
RO9	1.0	2D	2D	2.5D	0.14	7,730	2,510	88,500	0.30	9,860	0.80	Peg Shear/Bending	Peg Shear/Bending
RO10	1.0	2D	2D	2.5D	0.17	7,160	2,380	65,800	0.34	8,780	0.77	Peg Shear/Bending	Peg Shear/Bending
					Mean=	7,330	2,430						
					Std. Dev.=	340	120						
					5% Exclusion=	6,620	2,180						
					COV=	0.046	0.049						

Table 3-5 RO Monotonic Joint Test Results

Test	Peg Diameter (in)	End Dist. (l_v)	Edge Dist. (l_e)	Spacing Dist. (l_s)	Yield Disp. (in)	Yield Load (lbs)	Yield Stress (psi)	Stiffness (lbs/in)	Ultimate Disp. (in)	Ultimate Load (lbs)	Ave. Peg G	Failure Type @ Yield	Failure Type @ Ultimate
RO12	0.75	2D	2D	2.5D	0.16	3,480	1,990	32,200	0.25	3,980	0.66	Peg Shear/Bending	Peg Shear/Bending
RO13	0.75	2D	2D	2.5D	0.16	4,090	2,320	37,100	0.28	5,200	0.76	Peg Shear/Bending	Peg Shear/Bending
					Mean=	3,780	2,870						

Table 3-6 RO ¾” Diameter Joint Test Results

Test	Peg Diameter (in)	End Dist. (l_v)	Edge Dist. (l_e)	Spacing Dist. (l_s)	Yield Disp. (in)	Yield Load (lbs)	Yield Stress (psi)	Stiffness (lbs/in)	Ultimate Disp. (in)	Ultimate Load (lbs)	Ave. Peg G	Failure Type @ Yield	Failure Type @ Ultimate
RO15	1.25	2D	2D	2.5D	0.19	8,830	1,940	58,400	0.31	10,500	0.70	Peg Shear/Bending	Peg Shear/Bending
RO16	1.25	2D	2D	2.5D	0.20	9,150	2,010	55,500	0.28	10,300	0.69	Peg Shear/Bending	Peg Shear/Bending
RO17	1.25	2D	2D	2.5D	0.17	7,760	1,700	57,700	0.47	13,100	0.68	Peg Shear/Bending	Mortise Split
					Mean=	8,580	1,890						
					Std. Dev.=	728	163						
					5% Exclusion=	6,290	1,370						
					COV=	0.085	0.086						

Table 3-7 RO 11/4” Diameter Joint Test Results

The second set of RO joints was used to verify the desired failure mode discussed in Chapter 4. The joints were tested in the same fashion as the retrofitted joints in the SYP test. The joints were loaded to failure and the damaged pegs were replaced with new pegs. The joints behaved as expected. Unlike the SYP tests, there was no loss in initial stiffness due to the localized damage to the mortise and tenon members, and the overall strength of the joint was totally dependent on the shear capacity of the peg. The joint used with the 0.75” pegs was cyclically loaded for the first test, which was thought to amplify any possible damage to the mortise and tenon members. The cyclic load had no adverse effects on the joint and two retrofit tests following the cyclic loading were unaffected. The load verses deflection plot for one of the retrofitted joints can be seen in Figure 3-8.

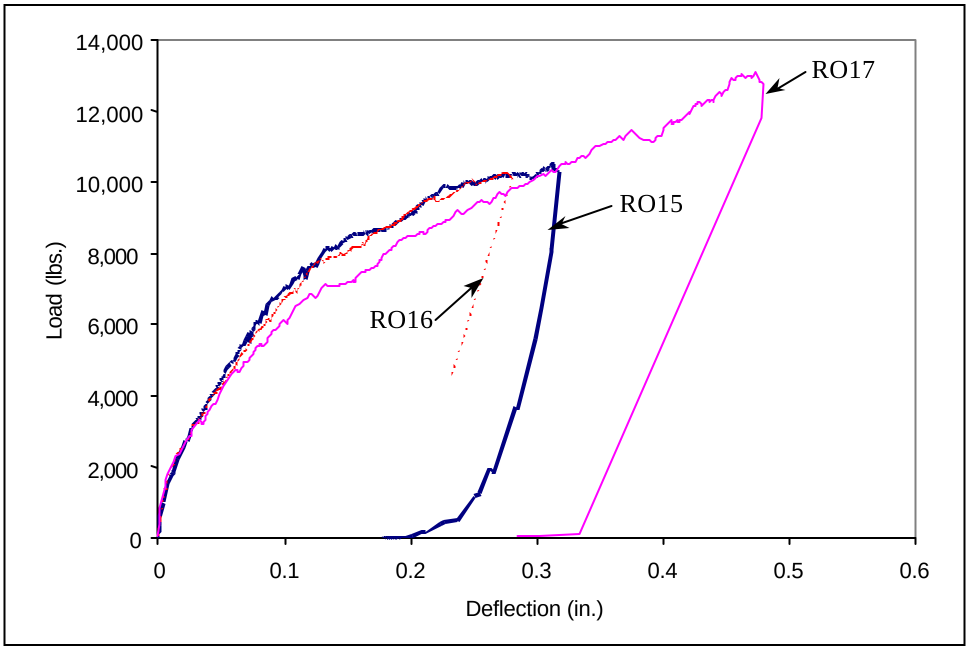

Figure 3-8 RO Load vs. Deflection for a 1.25" Peg Repair

The final monotonic tests done with the Red Oak joints were performed with four 1" diameter pegs. The joints were constructed with the same recommended spacing requirements found with the two peg tests. Figure 3-9 shows the geometry of a typical four peg test. The first of the two joints failed due to brash tensile bending on the net section of the mortised member at 8,506 lbs. This joint did contain some knots and slope of grain near the failure plane. The second test had a shear/bending failure of the pegs at a yield load of 12,975 lbs. The tests were not intended to replicate common practice, but to examine the feasibility of designing such a joint. Data for the two joints can found in the Appendix D.

The RO joints produced fairly consistent stiffness results. The RO joints were constructed by professional timber framers, and the test setup misalignment was identified during the testing of the RO joints. However, no relationship was drawn for the stiffness values of the RO joints and a method for establishing these values is recommended in section 5.3.

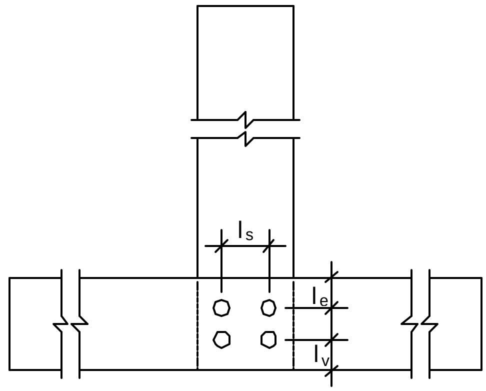

Figure 3-9 Typical 4-Peg Joint Detail

3.7 Cyclic Joint Tests

3.7.1 Method

Cyclic load tests were performed on specimens from each species group of joints. These tests were performed as a preliminary investigation to determine if timber frame joints had the ability to maintain strength under repeated loading. The joints were loaded in approximately 0.05" increments of displacement until failure. A typical test would involve loading the joint until 0.05" of displacement was reached. Then the joint would be unloaded, and upon reaching zero load the joint would be reloaded to 0.10" of displacement. This cycle would be continued until the joint lost load capacity.

As mention earlier, ductility is the primary concern with timber frame joints. Ductility is the vehicle a structure uses to develop nonlinear behavior and prevent abrupt failures. Having ductility in a system allows the structure to yield without collapse and in the case of a timber frame, allows the yielded joint to redistribute forces within the frame. Design of conventional timber structures relies on the ductility present in the steel fasteners used in a system. The NDS yield model equations are based on two important assumptions:

- Sufficient spacing of fasteners is provided to prevent the brittle tension failures of the wood members that comprise a joint.

- The fasteners that connect a joint are of a material that has an elasto-plastic behavior and allows for sufficient deformation prior to loss of load.

Wood is generally considered linearly elastic to failure. Tests of timber frame joints have shown that a definite nonlinear, ductile behavior exists.

Tests on the three different species of wood in this research has led to some promising results. All three of the test groups have demonstrated some degree of ductility prior to loss of strength. Like the monotonic tests, the cyclic tests demonstrated that the timber frame joints are capable of sustaining repeated service loads while maintaining some degree of ductility.

3.7.2 Cyclic Test Results

Two cyclic tests were performed on the SYP joints. The joints were tested as mentioned above and both had 1” diameter pegs from the white oak population. Both of the tests had a significant amount of deformation prior to loss of strength. One of the tests (SP15) had setup problems and the data file was lost, but data was recorded by hand. The results of the two tests can be seen in Table 3-8. As shown in the table, the joints had 9 and 11 cycles with an ultimate displacement of 0.55”. Both joints had a peg shear/bending failure at yield and ultimate loads well beyond what could be expected for design capacities.

Table 3-8 SYP Cyclic Test Results

Test	Peg Diameter (in.)	End Dist. (lv)	Edge Dist. (le)	Spacing Dist. (ls)	No. Cycles	Ultimate Disp. (in.)	Ultimate Load (lbs.)	Ave. Peg SG	Failure Type @ Yield	Failure Type @ Ultimate
SP15	1.0	2D	2D	3D	9	0.55	7,100	N/A	Peg Shear/Bending	Peg Shear/Bending
SP16	1.0	2D	2D	3D	11	0.55	7,850	0.66	Peg Shear/Bending	Mortise split

The load deflection plot from the SYP tests is encouraging. Figure 3-10 shows the load deflection plot from test SP16. The joint’s ultimate failure occurred on the 11th cycle. The mortise split was by prying action on the cheeks of the mortise. This failure was initiated by the deformation of the peg during previous load cycles. As the peg began to yield (Δ=0.08”, P=5000 lbs.) it deformed in the same manner shown in

Figure 3-5. As the joint was loaded repeatedly this deformation grew in magnitude, causing the mortise walls to pry outward and developing tensile stress on the inside of the mortise. Eventually a crack formed. Ultimate failure took many load cycles to develop.

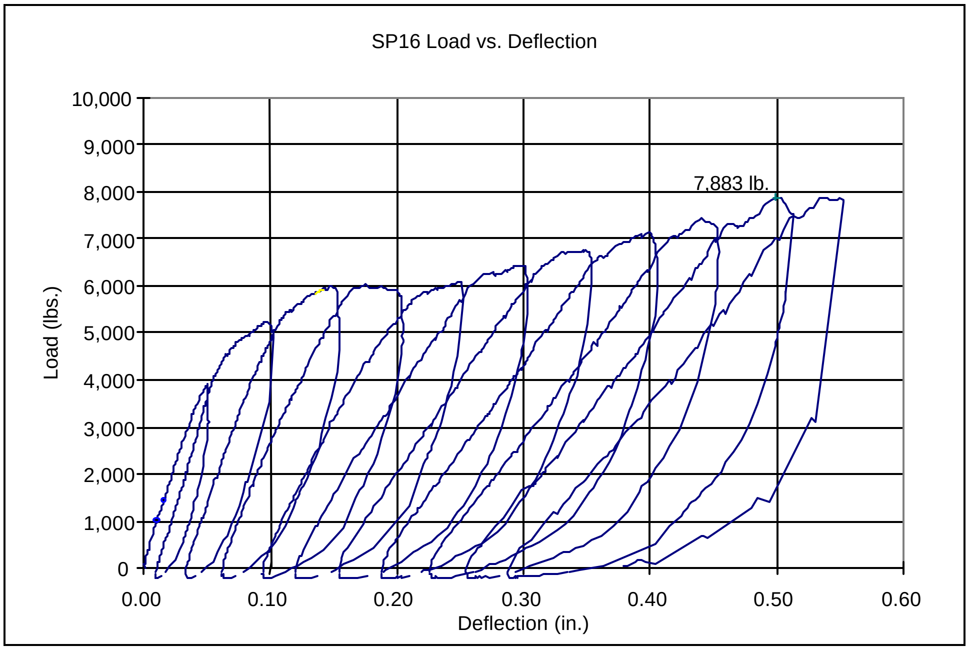

Figure 3-10 SYP Cyclic Joint Test

Two cyclic tests were conducted with the RDF joints. The joints were tested as mentioned above and both had 1” diameter pegs from the white oak population. The tests did not exhibit the same level of ductility prior to loss of strength as the SYP joints. The tensile strength perpendicular to grain of Douglas fir compared to other species commonly used in the industry is low. The RDF specimens used for the cyclic tests were not of the same quality as the joints used for the RDF monotonic tests. Specimen DF11 had a severely checked mortise, and DF12 had a single check at the center of the tenon between the two peg holes. Hence, these results should not be regarded as representative of the species.

At ultimate load, DF12 developed a tenon split behind both pegs; this failure was undoubtedly due to the original check in the tenon. As the joint was loaded, the check closed and the tenon splits formed due to the cross grain tension created at the end of the tenon. It is important to note that the end distance for test DF12 was increased in an attempt to compensate for the defective tenon, but this increase seemed to have little effect on the capacity of the joint.

Table 3-9 RDF Cyclic Test Results

Test	Peg Diameter (in)	End Dist. (l_v)	Edge Dist. (l_e)	Spacing Dist. (l_s)	No. Cycles	Ultimate Disp. (in)	Ultimate Load (lbs)	Ave. Peg G	Failure Type @ Yield	Failure Type @ Ultimate
DF11	1.0	2.5D	2D	2.5D	4	0.15	5,720	0.76	Peg Shear/Bending	Mortise split
DF12	1.0	3D	3D	3D	4	0.12	6,600	0.75	Peg Shear/Bending	Tenon split

It was more difficult to ascertain a definite cause of failure for test DF11 at ultimate. The mortise was severely checked and a mortise spilt occurred too suddenly to determine if it had originated in one of the checks. The results of the two tests can be seen in Table 3-9. As shown in the table, both joints had four cycles of 0.033” increments with an ultimate displacement of 0.15” and 0.12”. Both joints had what appeared to be a simultaneous peg shear/bending failure at ultimate. Figure 3-11 and Figure 3-12 shows the load deflection plots from both tests.

Three cyclic tests were performed with the red oak joints. The joints were tested in the same manner as the previous cyclic load tests. Two joints had 1” diameter pegs from the white oak population and the third joint had 1.25” diameter octagonal white oak pegs from another source. The tests did not demonstrate the same deformation prior to loss of strength as the SYP joints. However, the joints did exceed the ultimate displacement values from the RDF specimens.

All of the RO joints had a peg shear/bending failure at yield. Two of the three specimens had no other signs of failure. The tenon member of test RO14 had a spike knot and the pith directly behind one peg. This was definitely an influence in the relish failure of the tenon. The pith formed one fracture line of the relish failure, and is assumed to have weakened the tenon.

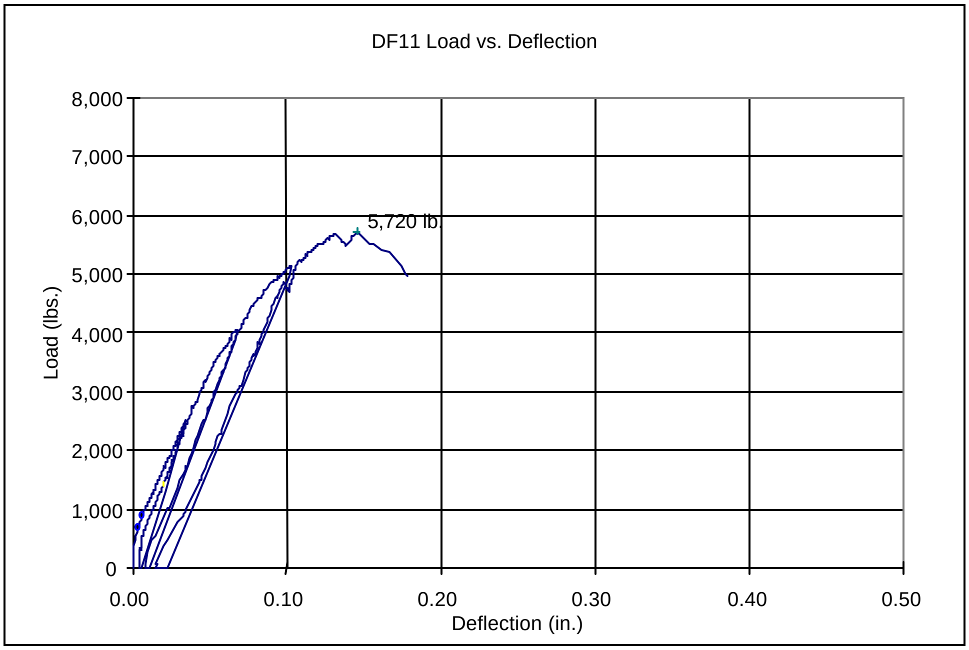

Figure 3-11 DF11 Cyclic Joint Test

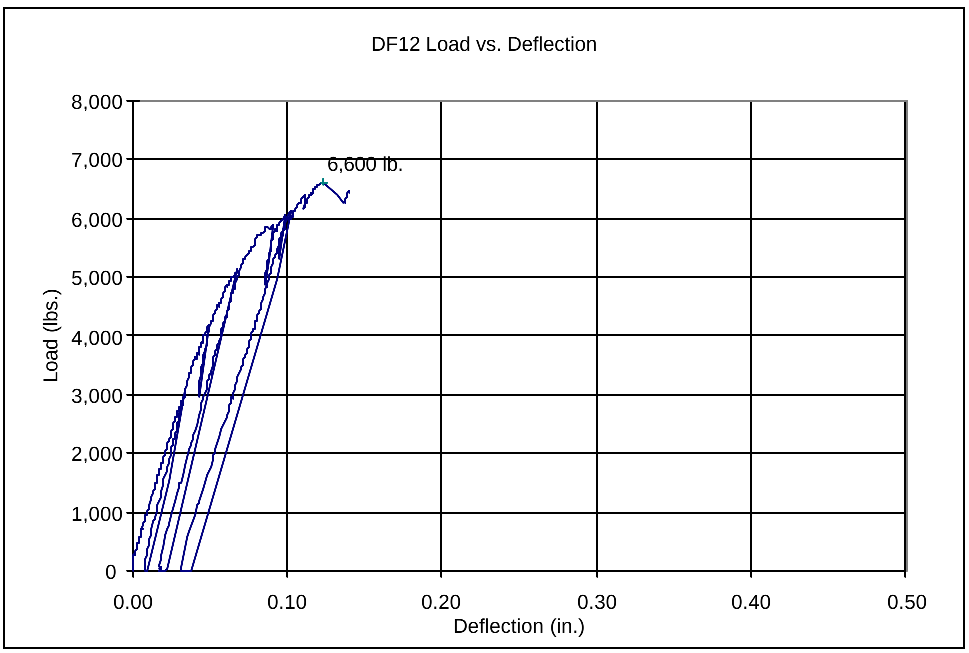

Figure 3-12 DF12 Cyclic Joint Test

The results of the three tests are shown in Table 3-10. As shown in the table, the joint with the 0.75" pegs had ten cycles with an ultimate displacement of 0.30" at a load of 5,120 lbs. Both the remaining joints had seven cycles prior to ultimate failure at displacements of 0.29" and 0.35" for the 1.0" and 1.25" diameter pegged joints, respectively.

Table 3-10 NRO Cyclic Test Results

Test	Peg Diameter (in.)	End Dist. (lv)	Edge Dist. (le)	Spacing Dist. (ls)	No. Cycles	Ultimate Disp. (in.)	Ultimate Load (lbs.)	Ave. Peg SG	Failure Type @ Yield	Failure Type @ Ultimate
RO11	0.75	2D	2D	2.5D	10	0.30	5,120	0.70	Peg Shear/Bending	Peg Shear/Bending
RO14	1.25	2D	2D	2.5D	7	0.29	10,100	0.68	Peg Shear/Bending	Relish failure
RO18	1.0	2D	2D	2.5D	7	0.35	10,500	0.76	Peg Shear/Bending	Peg Shear/Bending

The red oak joints reached approximately 40% higher loads than the SYP joints. Bulging or prying of the mortise was witnessed in the RO tests to a greater extent than previously mention in the SYP tests. However, splitting of the mortise did not occur. Figure 3-13 shows the load deflection plot for the joint with 0.75" diameter pegs.

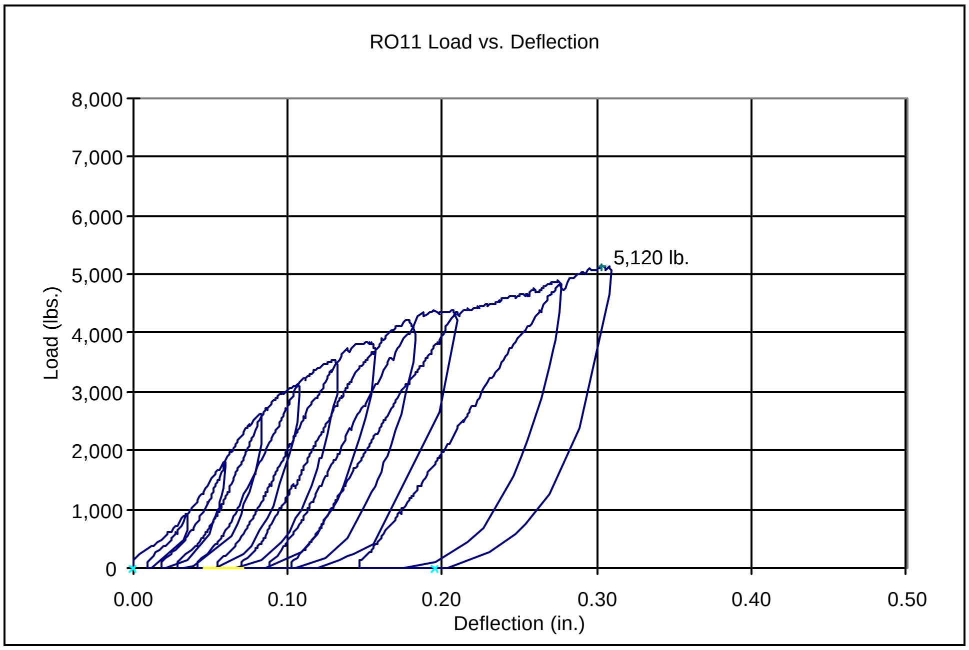

Figure 3-13 RO11 Cyclic Joint Test

4. Analysis and Results

4.1 Spring Theory

Development of dowel bearing capacities for timber framed joints is a potential difficulty in the continued effort to develop design values. Timber frame joints could be comprised of a multitude of hardwood peg and timber species. Past research in this area has involved tests with combinations of peg and base materials to obtain the mechanical properties necessary to model a timber frame connection. In the present research, an initial investigation was made to determine the feasibility of testing materials separately and then mathematically combining the results to define bearing capacities for wood-on-wood bearing combinations. If the combination of bearing test results is a viable method for establishing bearing strengths, tests of dowel bearing specimens with combinations of materials would be unnecessary. Bearing strengths of commonly used pegs and base materials could be found using the same methods used in Chapter 2, and for the base material, large amounts of data already exist from the development of timber connection capacities with steel bolts.

The concept behind the mathematical model is that the wood peg and base material bearing tests can be modeled as two springs in series. If this theory were valid, it would eliminate the need for combined testing on a large combination of peg and base materials. The bearing strengths of the materials present in a joint could be calculated using equations similar to those present in the NDS. A characteristic load-deformation curve could be developed, if in fact one has not been already, for each material and the two materials could be combined using the equation for the stiffness of two springs loaded in series.

$$\frac{1}{k_{total}} = \frac{1}{k_{peg}} + \frac{1}{k_{base}} \qquad (4\text{-}1)$$

In Eq. 4-1, k_{base} and k_{peg} represents the stiffness of a given base material and peg species, respectively. The term k_{total} represents the combined stiffness curves. The strength and stiffness of any combination of species could be found by combining the load-deformation curves for the base material and peg. The yield strength of the combination is found by applying the 5% offset method to the combined load deflection curve. Figure 4-1 shows a visual representation of the dowel bearing spring theory.

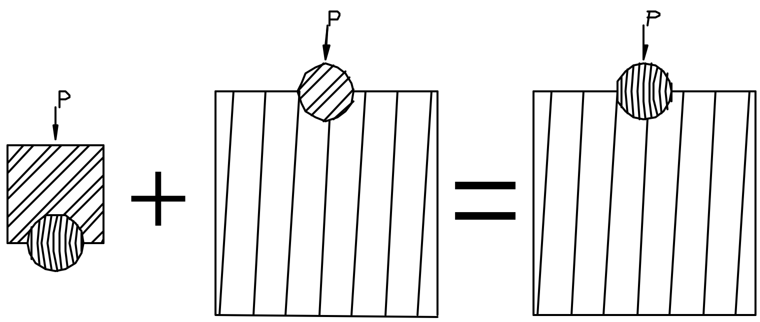

Figure 4-1 Dowel Bearing Spring Theory

Currently dowel bearing data is available for a wide variety of wood species tested with steel fasteners. The use of this existing data in combination with bearing tests of hardwood dowels would reduce the amount of testing needed to develop a standard set of properties for timber frame construction. The tests in Chapter 2 were performed under the assumption that this theory was valid. Both the white oak pegs and the base materials were tested separately with steel load applicators. Data from the tests in Chapter 2 were used with a limited number of combined tests to validate the theory.

The dowel bearing spring theory was tested using red oak base material specimens and white oak pegs. Twelve red oak dowel bearing tests were performed in combination with white oak pegs. The specimens were loaded perpendicular to grain so there was a sufficient amount of test data that was in the nonlinear region of the load deflection plots. An attempt was made to cut the red oak specimens for the tests so that four matched specimens were obtained from each red oak full size joint. Two of the specimens would be tested with the steel bar and the remaining two would be tested in combination with a white oak peg. It was not always possible to obtain four clear matched specimens from each joint. Hence, several of the spring theory comparisons are based on one base material specimen.

The combined bearing tests were compared to the previous tests of the base material and white oak pegs with steel loading fixtures. The load deflection plots from the individual bearing tests discussed in Chapter 2 were filtered into uniform increments of displacement using an interpolation technique. The peg tests from Chapter 2 were split into three groups based on specific gravity. The load deflection plots from each peg test were averaged with all of the peg tests from each group. The three resulting load deflection plots (k_{peg}) were used in combination with the individual bearing test with the 1" steel bar (k_{base}). The curves were matched according to the specific gravity of the pegs used in the combined tests. The spring theory curve was found using the following procedure:

1. The peg curve from the physical test was filtered (smoothed) to obtain a new curve with uniform increments of displacement (0.002).
2. Displacements for the filtered curve were determined for uniform increments stress (25 psi) by interpolation.
3. Steps 1 and 2 were repeated for the base material curve.
4. The displacements from the peg and base material curves were added at a common value of stress to obtain the synthesized curve for the material combination.

The 5% offset method for determining the yield point was then applied to the synthesized curve. The corresponding initial stiffness and yield points from both the combined physical tests and the synthesized curves were compared.

The synthesized curves were lower in stiffness than the actual tests. Figure 4-2 shows the plots from each material, the synthesized curve and the load deflection curve from the combined test. The plot legend is defined as:

- *982ro49s*-Actual combined test.
- *RO49Spring*-Equivalent spring theory (synthesized) curve using matched set tests and one of the three characteristic peg curves.

- *982ro07/08*-The average base material curves from the matched set.

- *Peg2*-The characteristic curve from peg group 1.

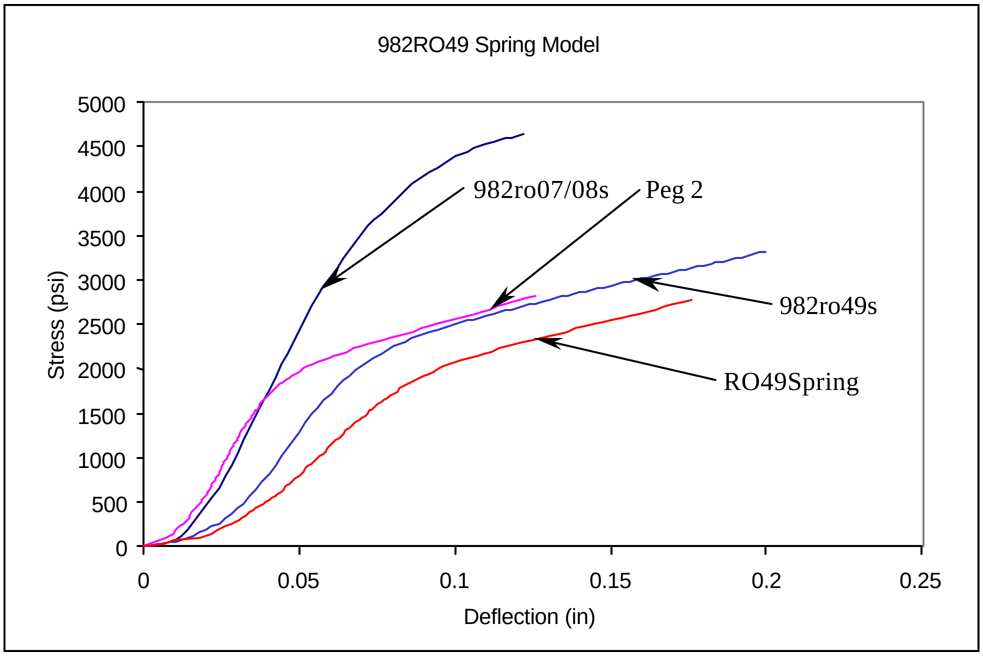

Figure 4-2 Typical Spring Theory Plot

As illustrated in the graph, the initial stiffness of the combined test and the synthesized curve appear to be relative close in value. This scenario was true for all of the comparisons. The equivalent spring yield values were essentially the same as the combined test specimens. This again was typical for all the curves. Table 4-1 shows the results from all the tests.

Combined	Initial Stiffness (lbs/in)	Yield (psi)	Spring Theory Equivalent	Initial Stiffness (lbs/in)	Yield (psi)	% Diff. Stiffness	% Diff. Yield	Peg Group
982RO40	47,900	3,470	RO40/41	39,800	3,520	16.9%	-1.4%	3
982RO41	43,700	3,190	RO40/41	39,800	3,520	8.9%	-10.3%	3
982RO42	52,500	3,810	RO42/43	38,700	3,810	26.3%	0.0%	3
982RO43	58,000	3,560	RO42/43	38,700	3,810	33.3%	-7.0%	3
982RO44	44,800	3,420	RO44/45	34,300	3,570	23.4%	-4.4%	3
982RO45	48,700	3,410	RO44/45	34,300	3,570	29.6%	-4.7%	3
982RO46	38,500	2,540	RO46/47	31,000	2,600	19.5%	-2.4%	2
982RO47	38,400	2,760	RO46/47	31,000	2,600	19.3%	5.8%	2
982RO48	40,400	2,270	RO48	31,400	2,320	22.3%	-2.2%	1
982RO49	44,100	2,820	RO49	31,400	2,610	28.8%	7.4%	2
982RO50	53,900	2,710	RO50	31,400	2,320	41.7%	14.4%	1
982RO51	47,100	2,590	RO51	31,500	2,600	33.1%	-0.4%	2
					Average=	25.3%	-0.4%	
					Maximum=	41.7%	14.4%	
					Minimum=	8.9%	-10.3%	

Table 4-1 Equivalent Spring Theory Test Results

The yield stress from the spring theory was an average of 0.4% below the actual test yield stress. The spring theory worked well for modeling the strength of a combined bearing test. The initial stiffness from the spring theory plot was always below the actual stiffness with an average difference of 21.6%. The difference in stiffness cannot be explained, but the values are usually of secondary importance to a designer.

The 5% offset values for the combined material tests and the pegs were relatively close. As illustrated in Figure 4-2, the weaker material (the peg) dominated the combined test strength. The 5% offset values for the combined tests and the 5% offset values for the pegs tested with the steel load block are surprisingly close in strength. Table 4-2 shows the strengths and the percent difference between the combined test strength and the peg strength. The average difference is -19%, and the maximum difference is 17.3%. The bearing strength of material combinations could be defined by identifying the strength of the weaker material and simply specifying that value as the dowel bearing capacity.

Table 4-2 Combined Yield Values and Peg Yield Values

Test	Combined Yield (psi)	Peg Yield (psi)	% Diff. Yield	Peg Group
982RO40	3470	3720	-6.7%	3
982RO41	3190	3720	-14.2%	3
982RO42	3810	3720	2.4%	3
982RO43	3560	3720	-4.3%	3
982RO44	3420	3720	-8.1%	3
982RO45	3410	3720	-8.3%	3
982RO46	2540	2590	-1.9%	2
982RO47	2760	2590	6.6%	2
982RO48	2270	2310	-1.7%	1
982RO49	2820	2590	8.9%	2
982RO50	2710	2310	17.3%	1
982RO51	2590	2590	0.0%	2
Average=	3050	3110	-1.9%	

4.2 Failure Modes

The European Yield Model (EYM) is used in current design practice for timber connections with steel bolts. The application of the EYM to timber frame connections has been investigated in previous research (Schmidt and MacKay 1997). The four double shear failure modes currently recognized in the NDS are shown in Figure 4-3. Modes I_m and I_s are bearing failures of the main and side member respectively. Modes III_s and IV are both dowel failures with localized crushing in the side and main members. Both modes III_s and IV rely on bending mechanisms to form in the fastener in order to produce connection yielding. Mode III_s involves two plastic hinges in the fastener and mode IV involves four plastic hinges, two under the main member and one hinge under each of the side members.

Schmidt and MacKay's work involved alternative derivations of the current NDS equations for the mentioned failure modes. The mode IV derivation showed that the hinge locations produced by the EYM equations and those witnessed in actual mortise and tenon joint tests do not correspond. The EYM equation for mode IV produced hinge spacings of approximately 3" for 1" diameter red oak pegs, while actual tests showed a mechanism at 0.26D or 0.26" (Schmidt and MacKay 1997). The mode IV failure does not seem to apply to timber frame connections.

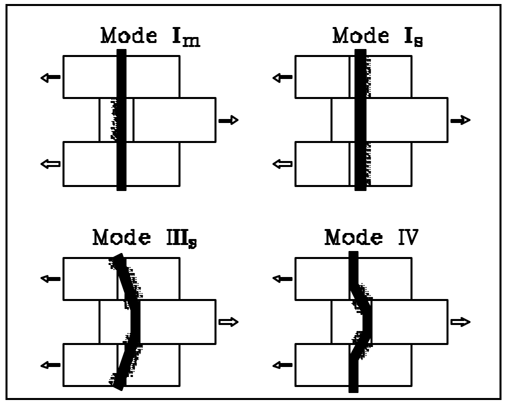

Figure 4-3 NDS Double Shear Failure Modes from Schmidt and MacKay (1997)

Mode III_s occurs in connections with thin side members, such as metal side plates that offer little or no restraint to the rotation of the fastener. This mode is unlikely in mortise and tenon joints, because the peg would have to cause a significant amount of localized crushing in the mortise member.

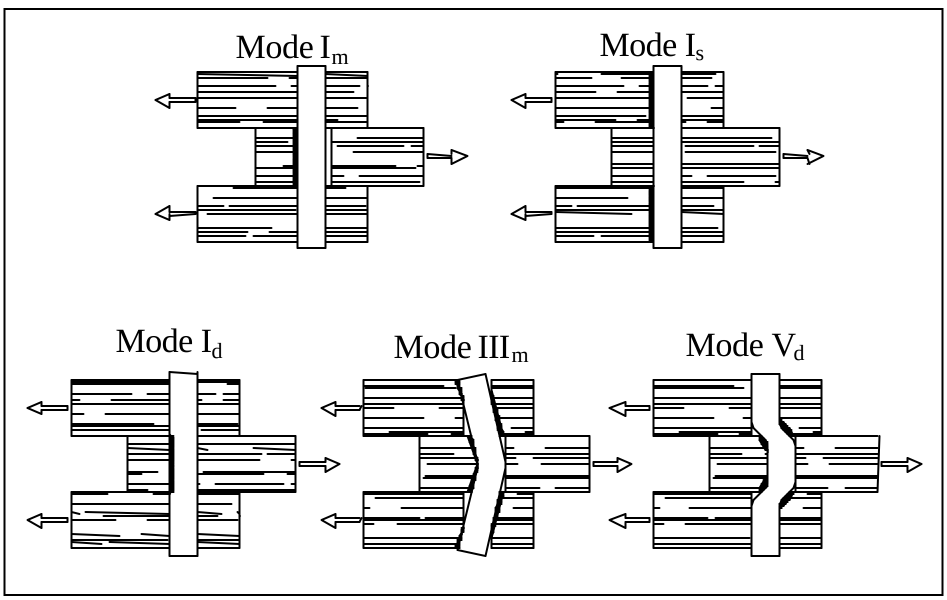

Figure 4-4 Proposed Failure Modes

The review of previous work has led to the conclusion that there are five possible failure modes for traditional timber frame construction. Figure 4-4 shows the five failure modes for timber frame joints in tension. Modes I_m and I_s are the two current NDS modes that apply to timber framed joints. Three additional failure modes that should be included are a bearing failure of the peg, peg shear/bending failure and a peg bending failure with a single flexural hinge. Bearing failure of the peg is denoted mode I_d, and the peg shear/bending failure is denoted mode $V_{d.}$ Mode V_d in a pegged connection is primarily a shear failure with fractures due to bending near ultimate loads. The third mode was reported in Schmidt and MacKay's work with joints constructed of Douglas fir 2x6 side and main members fastened with 0.75" and 1" red oak pegs (Schmidt and MacKay 1997). Three of the six tests conducted by Schmidt and MacKay involved a peg failure, two of which were the mode V_d failure and the remaining failure was denoted as III_s'. The failure was described as a single hinge at the middle of the dowel (at the center of the tenon). This failure mode occurs in connections in which the base material dowel bearing strength is low and localized crushing occurs in the peg holes of the mortise members. The crushing allows the dowel to rotate and form a flexural hinge located at the center of the tenon. This failure mode was witnessed in three of the 56 tests reported herein. The southern yellow pine tests SP53a, SP53b and SP53c had this single flexural hinge at yield and ultimate loads. This failure mode is denoted as III_m. The side member embedment length (l) to the fastener diameter (D) ratio (l/D) for the SYP tests was 1.6, while the majority of the other tests conducted had l/D ratios greater than 2. Schmidt and MacKay's joint with the mode III_m failure had a side member l/D ratio of 1.5. Modes I_m, I_s and I_d are possible due to the various combinations of wood species and mortise and tenon sizes that could comprise a joint.

4.3 Detailing Requirements

In the majority of design situations, failure of the fastener is the desired failure mode. The NDS recognizes a fastener failure as the preferred failure mode by designating minimum detailing requirements for timber construction with steel fasteners. Likewise, the tests conducted on mortise and tenon connections with wood dowels have demonstrated some degree of ductility when proper edge distance, end distance, and spacing requirements are met. The failure of the surrounding material, such as mortise splitting or a tension failure of the tenon relish is a sudden and brittle failure. In the event of such a failure, the structure becomes unserviceable and difficult to repair. In previous tests peg failure has shown some degree of ductility prior to the loss of load carrying capacity (Reid 1997, Schmidt and MacKay 1997, Kessel and Augustin 1996).

The minimum detailing requirements are a result of testing on timber connections with steel bolts (Trayer 1932). The objective of the minimum spacing requirements is to localize connection failure in or around the fastener. In this way, brittle failure of the connected wood members is avoided. The minimum spacing requirements account for a wide range of possible joint configurations relative to the bolt diameter and the breadth of the material in which it is embedded. That is to say, the aspect ratio of the fastener plays a part in the mechanics of the connection. The embedded length (l) and the diameter (D) of the fastener can be used as a guide to determine a potential mode of failure within a connection. Steel fasteners with a l/D = 2 receive load from and deliver load to the surrounding base material in a uniform bearing condition. As the l/D ratio increases the fastener bends and forms plastic hinges, therefore changing the mode of failure. Typical l/D ratios for timber frame connections are between 1.2 and 2.7 which is much lower than l/D ratios found in conventional connections with steel bolts. This information supports the conclusion that different failure modes are likely in traditional timber framed joinery, compared to conventional connections.

A summary of the minimum end distance, edge distance, and spacing requirements developed from joint tests in this research is shown in Table 4-3. The values shown in Table 4-3 are not recommended for actual practice due to the limited number of tests performed, but they do represent the minimum values necessary to develop a ductile failure of the pegs in these joints. The minimum detailing requirements can be used as a guide to determine the validity of using the equivalent steel bolt theory presented in section 4.5.

Table 4-3 Minimum Detailing Requirements

Species	**End Distance (l_e)**	**Edge Distance (l_v)**	**Spacing (l_s)**
Southern Yellow Pine	2D	2D	3D
Recycled Douglas Fir	2D	2.5D	2.5D
Red Oak	2D	2D	2.5D

4.4 Allowable Stress Values

The current design values for connections are based on the proportional limit. The original work completed by Trayer in 1932 is largely the basis for connection design in the United States. Trayer's recommendations were used directly in a table format by the National Design Specification for Wood (NDS) until 1986. The 1991 NDS adopted the European Yield Model for the design of timber connections with steel fasteners. The EYM is based on the yield strengths of both the fastener and the connected material found by the 5% offset method. The design values in the NDS are based on the EYM equations, but they have been calibrated to the proportional limit values used by the NDS prior to the 1991 edition (Wilkinson 1993). The calibration factors include factors of safety for connections secured with steel fasteners. This makes a similar calibration difficult for timber frame connections. Additionally, review of the past research of timber frame connections raises some doubt as to whether or not the use of the EYM equations or their corresponding factors of safety are applicable to connections fastened with wood dowels.

Use of the 5% offset point has led to inconsistencies with timber connections. The 5% offset line is arbitrarily established by choosing the initial straight-line portion of the load deflection plot. In the case of timber frame connections and tests with steel fasteners, the initial portion of the curve is not necessarily linear. In Theilen's research on ring shank nail connections, the subjective choice of the linear portion of the curve significantly affected the resulting 5% offset value (Theilen *et al*. 1998). Theilen proposed that a standard displacement be determined that defines the yield point for a group of connections. The corresponding load at that displacement would be defined as the yield value. The use of a standard displacement to define the yield point of timber frame connections could be accommodated, but would require that present standards, like dowel bearing tests, be reevaluated based on the new criteria.

The yield values of the joints tested in this research had reasonable levels of variation (all of the

COV values were at or below 13%). While the use of the 5% offset method is somewhat subjective, it is believed to be a more accurate and repeatable method for determining joint strength than the use of the proportional limit or ultimate strength. Consistently determining the proportional limit consistently for timber frame connections would be virtually impossible due to the nature of the load deflection plots. Localized crushing of the timber material creates subtle nonlinear response early in the load sequence and would be even more subjective than the use of the 5% offset method. The ultimate strength of the connections did have the same order of variation as the yield point, but ultimate strength is dependent on many more unknowns. The ultimate strength values were a result of any number of failure modes. The failure strength of mortises or of the relish in the tenon member has yet to be determined. Furthermore, the entire range of behavior is dependent on considerations like the quality of construction and defects such as checks, knots, and slope of grain, all of which are under the control of the builder, but not the designer.

The use of the 5% offset method to establish design values in this work has rendered a reliable rationale for joint design. Regardless of the magnitude of the safety factor applied to the 5% offset value, the connection has a known strength characteristic beyond its elastic limit. In the design of framed structures to resist extreme events (e.g. earthquakes and tornadoes), the performance of a structure depends on the ductility present in the frame, or more importantly the ductility present in the connections of the frame. The region between the proportional limit and the 5% offset value on the load deflection curve is known to perform adequately. As a connection is loaded beyond is proportional limit, the stiffness of that joint will decrease and the excessive displacement allows for dissipation of energy. For the design of structures for serviceability, the factor of safety should result in the connection remaining linear elastic.

The design strengths for timber frame connections have yet to be established. Design strengths and factors of safety must be determined for the properties of the materials that comprise a joint. Presently, two design philosophies exist for use in structural engineering, allowable stress design (ASD) and load and resistance factor design (LRFD).

Limited guidelines for the development of design standards for connections exist. ASTM standard 5457-93 is the specification for computing LRFD values for wood-based materials and connections (ASTM 1995a). However, LFRD design values are based on a soft conversion from ASD. The properties needed to develop working stress or ASD values are based on the 5% exclusion values from material tests. Figure 4-5 shows a normal distribution with the 5% exclusion value ($F_{0.05}$) where $F_{0.05} = X\text{-}K\mathbf{s}$, X is the mean value, and $\mathbf{s}$ is the standard deviation. The coefficient K depends on the number of samples, confidence level, and selected exclusion limit. The $F_{0.05}$ value, calculated using ASTM D2915, represents the point at which 95% of material strengths will exceed that value based on a chosen confidence level (ASTM 1995a). A confidence level of 75% was used for both the material and joint tests in this research.

The 5% exclusion value can be used to establish the allowable stress design strength. Table 4-3 shows the analytical procedure for determining ASD strengths and the soft conversion to LRFD strengths. The $F_{0.05}$ value is the characteristic material strength obtained by statistical analysis of physical test data (see Fig. 4-5).

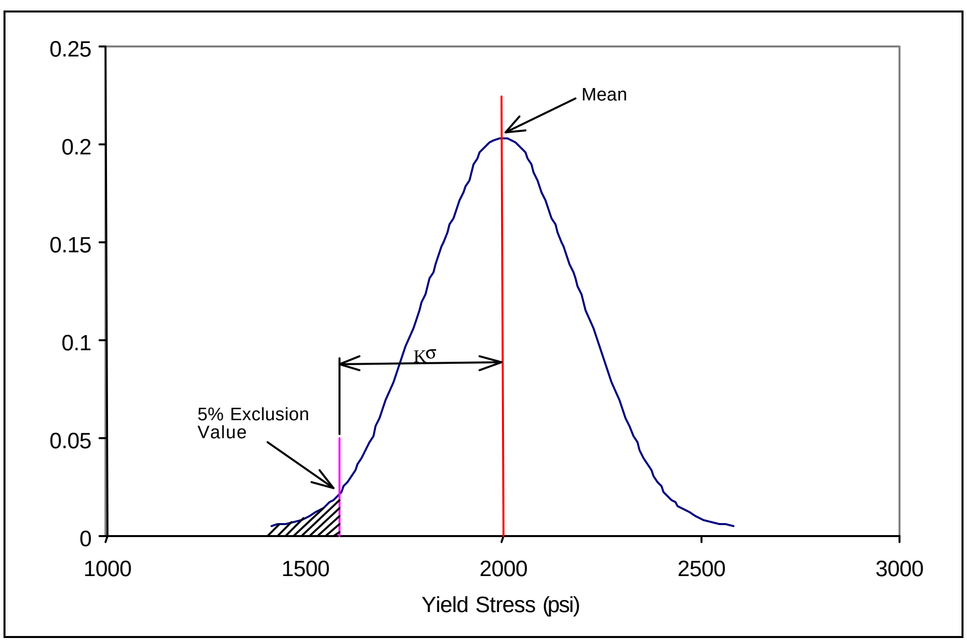

Figure 4-5 Normal Distribution

The design value for ASD is found by dividing the 5% exclusion value by a factor of safety and adjusting for duration of load effects. A divisor of 2.1 is standard for lumber properties such as flexural stress F_b and compressive stress F_c. The determination of an appropriate divisor for connections in timber frame construction has not been determined. In the United States, the design value for conventional connections (with steel fasteners) has been determined from the proportional limit of the load deflection plot, not from the 5% offset yield point.

Table 4-3 Comparison of ASD to LRFD

	ASD	LRFD
Design Value:	$R_{n(ASD)} = F_{0.05} / F.S.$	$R_{n(LRFD)} = K_F R_{n(ASD)}$
Design Inequality:	$R_{n(ASD)} \leq \Sigma Q_i$	$\phi R_{n(LRFD)} \leq \Sigma \gamma_i Q_i$

The LRFD design values are based on a soft conversion from ASD design values. The calibration factor, found in ASTM D5457, is $K_F = 2.16/\phi$. This factor relates a design using LRFD to a comparable one using ASD with a live load to dead load ratio of 3.0 (ASTM 1995a). The calibration factor accounts for the factor of safety and the difference in how load duration effects are handled between ASD and LRFD. The resistance factor f varies with the type of applied stress. The ASTM standard gives values of ϕ as 0.9 for compression, 0.85 for bending, 0.75 for shear, and 0.65 for connections. There is no method for the establishment of LRFD values directly from test data. Therefore, the establishment of LFRD design values is beyond the scope of this research.

Factors of safety for timber frame tension joints need to be determined. Kessel and Augustin (1996) recommended that the design value for a group of connections with the same geometry and properties be established as the minimum of three values.

- A factor of safety of 3.0 should be applied to the average ultimate load for the specimens in a group.
- The average value of the load corresponding to a displacement of 1.5mm (0.06”) for a series of tests divided by a factor of safety of 1.0 (in effect, this is a service load limit).
- The minimum ultimate load for a series of tests divided by a factor of safety of 2.25.

It is important to note that the procedure outlined by Kessel and Augustin was to determine design capacities based on short duration loads (e.g. wind and seismic events). Table 4-4 shows the application of the method proposed by Kessel and Augustin to the joints tested within this work. The table includes the average values from tests in which mode V_d occurred at the 5% offset point. The remaining joints were excluded because the intent of this work was to define detailing requirements that assured fastener failure. Shown in the table are the minimum values for the procedure outlined by Kessel and Augustin. The governing capacity for all the joint groups was the mean ultimate load divided by a factor of safety of 3.0.

Table 4-4 Allowable Joint Loads using Kessel’s Suggested Factors of Safety

	Joint Load (lbs)			Factor of Safety	Recommended Loads (lbs)		
	SYP	DF	RO		SYP	DF	RO
Mean Ultimate	6,720	6,500	9,100	3.0	2,240	2,170	3,030
Minimum Ultimate	5,520	6,070	7,590	2.25	2,450	2,700	3,370
Mean Load @ 1.5 mm	3,940	4,650	3,080	1.0	3,940	4,650	3,080

The allowable joint loads for the tests conducted within this work are based on Kessel and Augustin’s recommended factors of safety. Note that the displacement limit of 1.5 mm corresponds, in this work, to approximately one-half of the yield displacement. The 5% offset yield point, rather than the ultimate strength, can still be used by determining a factor of safety that will produce comparable strengths to those recommended by Kessel and Augustin. Table 4-5 shows the governing loads from Kessel’s recommendations in Table 4-4. The strength values for the three joint groups were calculated using the characteristic shear span to diameter ratio for each species and the 5% exclusion white oak peg shear equation shown in Figure 2-6. A factor of safety was calculated for each joint group so that the resulting allowable load was equal to the loads recommended by Kessel and Augustin. As shown in the table, all of the factors of safety were approximately equal. The factors were averaged to determine a common value for timber frame connections. The resulting factor of safety of 2.0 converts the 5% offset load to the recommended design value suggested by Kessel and Augustin for short duration loads. Figure 4-6 shows the allowable load plotted on the load deflection curve for a Douglas fir joint test.

The design strength of a joint for a normal duration load would require the use of the load duration factor (C_D) from the NDS. The load duration factor for wind or seismic events, which correspond to a ten minute load duration, is 1.6. This factor, which was determined from tests of flexural members, is assumed to apply to connection design as well. Hence, the design value for normal duration (10 years) loading is obtained from the lower 5% exclusion strength limit by dividing the latter by a factor of 3.2. This factor corresponds precisely with the calibration factor for design of conventional connections using the yield model approach; see Chapter 2 of the NDS (AFPA 1997).

Table 4-5 Recommended Factor of Safety

	Joint Groups		
	SYP	**RDF**	**RO**
Using Kessel's Recommended F.S. (lbs)	2240	2170	3030
5% Excl. Load based on Charact. Shear Span to Diameter Ratio (lbs)	4210	4770	5550
Factors of Safety for 5% Offset Strength	1.9	2.2	1.8

Mean Factor of Safety = 2.0

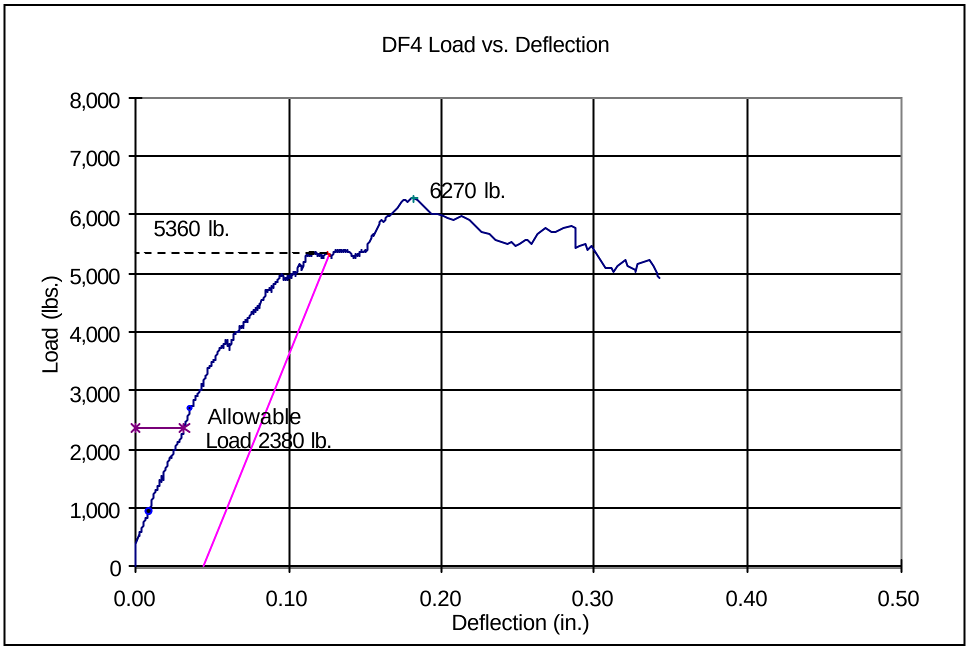

Figure 4-6 DF Allowable Load vs. Actual Test Data

4.5 Joint Design

The current NDS spacing requirements are based on the use of ASTM A307 steel fasteners. Requirements for joint detailing are based on fastener diameter. When all fasteners are A307 steel, this requirement should produce consistent results. However, required fastener diameter only indirectly corresponds to applied load. The end distance, edge distance and spacing requirements should be based on the applied load that the connection will carry. An appropriate method for establishing spacing requirements for timber frame connections with wood pegs must to be developed. The concept of an equivalent steel bolt, equal in strength to the wood peg, leads to one possible method (Schmidt and MacKay 1997).

The proposed design procedure would be as follows: A designer establishes the load capacity required in a given joint. The size and number of wood pegs required to carry this load are determined based on the five failure modes and factor of safety described earlier. The capacity of the joint based on the strength of a single peg is substituted into the four EYM equations for double shear connections with a steel bolt. The diameter of a single steel bolt required to resist this load can then be found for each of the modes. The largest diameter from the EYM equations is then used as the equivalent steel bolt for the joint design. The spacing requirements from Chapter 8 of the NDS are applied to the governing steel bolt diameter. The wood peg would be placed at the resulting distances.

Mode I_m
$$Z = \frac{D\, t_m\, F_{em}}{4K_\theta} \qquad (4\text{-}2)$$

Mode I_s
$$Z = \frac{D\, t_s\, F_{es}}{2K_\theta} \qquad (4\text{-}3)$$

Mode III_s
$$Z = \frac{k_3\, D\, t_s\, F_{em}}{1.6\, K_\theta \left(2 + R_e\right)} \qquad (4\text{-}4)$$

Mode IV
$$Z = \frac{D^2}{1.6\, K_\theta} \sqrt{\frac{2\, F_{em}\, F_{es}}{3(1 + R_e)}} \qquad (4\text{-}5)$$

The strength of a timber frame connection in double shear can be simplified to the minimum value of three equations. Based on the information in section 4.1, the various failure modes for bearing can be separated into three distinct modes based on material bearing capacities with steel load applicators. Failure modes I_m and I_d are determined using the individual dowel bearing strength for the tenon member (F_{em}) and peg (F_{ed}), respectively. Mode I_s is determined using the mortise member dowel bearing capacity (F_{es}). Mode V_d is determined using the characteristic shear span to diameter ratio for a given peg and base material and the equation given in Figure 2-6 to determine the characteristic shear stress (τ_c). Table 4-6 shows four modes of failure and their corresponding strength equations with the factor of safety for a 10 minute load duration of 2.0. The mode III_m failure discussed in section 4.4 was only witnessed in three joint tests and the corresponding capacity has yet to be developed. It is not listed in Table 4-6, but should be considered in any future work.

Table 4-6 Timber Frame Design Equations

Mode I_d

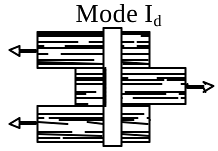

$$P_{Im} = \frac{n\,D\,t_m\,F_{ed}}{2.0} \qquad (4\text{-}6)$$

Mode I_m

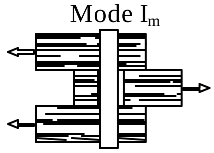

$$P_{Im} = \frac{n\,D\,t_m\,F_{em}}{2.0} \qquad (4\text{-}7)$$

Mode I_s

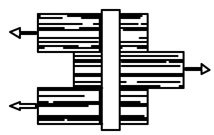

$$P_{Is} = \frac{2\,n\,D\,t_s\,F_{es}}{2.0} \qquad (4\text{-}8)$$

Mode V_d

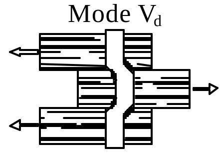

$$P_{Vd} = \frac{2\,n\,A_d\,\tau_c}{2.0} = \frac{n\,\pi\,D^2\,\tau_c}{4} \qquad (4\text{-}9)$$

n = number of fasteners
D = diameter of fastener
F_{ed} = peg dowel bearing strength
F_{em} = tenon dowel bearing strength
F_{es} = mortise dowel bearing strength
t_m = thickness of tenon,
t_s = thickness of mortise cheeks
A_d = area of the dowel
τ_c = shear capacity of the dowel

Table 4-7 shows is a comparison of end distance, edge distance, and peg spacing from experimental recommendations and values found using the equivalent steel bolt theory with a 10 minute load duration. The detailing dimensions based on the theory exceed the recommended minimum values, with the exception of peg spacing. The spacing of fasteners is thought to have a minimal effect on joint capacity, but this is based purely on test observations. The requirement for peg spacing is considered to be a constructability issue and not necessarily a strength concern. The ten minute duration values with a factor of safety of 2.0 represent the minimum experimental values reasonably well.

Recommendations for normal duration loading are not offered in this report. The applicability of the load duration factor C_D = 1.6 for timber frame connections is still under investigation.

Table 4-7 Equivalent Steel Bolt Theory, Ten Minute Load Duration

	End Distance l_e (in)	Edge Distance l_v (in)	Spacing l_v (in)
SYP Joint Theory	4.3	2.5	1.5
SYP Test	2.0	2.0	3.0
RDF Joint Theory	4.7	2.7	1.7
RDF Test	2.0	2.5	2.5
RO Joint Theory	3.7	2.9	1.8
RO Tests	2.0	2.0	2.5

A sample design of a Douglas fir joint with the same configuration as the full size joint tests used for this research is shown in Table 4-8. The equivalent steel bolt size is found with the factor of safety for a ten minute load duration (F.S. = 2.0). The factor of safety was applied to Equations 4-6, 4-7, 4-8, and 4-9. This design resulted in two 0.66 inch diameter equivalent steel bolts. The current NDS values for fastener spacing are applied to the equivalent steel bolt, which result in an end distance of 4.7 inches, an edge distance of 2.7 inches, and a peg spacing for members loaded perpendicular to grain of 1.7 inches. The end and edge distances found using this method are conservative compared to the minimum values determined from actual joint tests (see Table 4-7). The peg spacing of 1.9 inches is below what was found from tests, but a minimum value of 2.5D is recommended Douglas fir joints. Similar calculations as shown in Table 4-8 are found in the Appendices H and I for SYP and RO.

Timber Frame Joint Properties		
a/D=	0.40	
n=	2	
D=	1.0	in.
t_m=	2.0	in.
t_s=	2.0	in.
F_{ed}[1]=	2,688	
F_{em}[2]=	5,488	psi
F_{es}[2]=	2,660	psi
τ_c=	1,518	psi
P_{Id}=	5,376	
P_{Im}=	10,976	lbs.
P_{Is}=	10,640	lbs.
P_{Vd}=	2,384	lbs.
P_A=	2,384	lbs.

Equivalent Bolted Connection Properties		
F_{yb} =	45,000	psi
G_m =	0.49	
G_s =	0.49	
F_{em} =	5,488	psi
F_{es} =	2,660	psi
t_m =	2	inches
t_s =	2	inches
k_θ =	1.25	
k_3 =	1.328	
R_e =	2.063	

Equivalent Steel Bolt Calculation					
Mode	Im	Eqv. Dia.	=	0.543	in
Mode	Is	Eqv. Dia.	=	0.560	in
Mode	IIIs	Eqv. Dia.	=	0.664	in
Mode	IV	Eqv. Dia.	=	0.570	in
		Diameter	=	0.664	in

Equivalent Bolted Connection Capacitly					
Mode	Im	P/bolt	=	1,459	lb
Mode	Is	P/bolt	=	1,414	lb
Mode	IIIs	P/bolt	=	1,192	lb
Mode	IV	P/bolt	=	1,618	lb
		Total P'	=	2,384	lb

Edge Distance (in)	
Par. to Grain	**1.0**
Perp. to Grain:	
loaded edge	**2.7**
unloaded edge	**1.0**

End Distance (in)	Reduced	Full
Perp. to Grain	**1.3**	**2.7**
Par. Comp	**1.3**	**2.7**
Par. Tension:		
softwoods	**2.3**	**4.7**
hardwoods	**1.7**	**3.3**

Spacing of Rows (in)	
Par. to Grain	**1.0**
Perp. to Grain	**1.7**

[1] Peg bearing strength was taken from section 2.4.5.
[2] Material dowel bearing strengths were calculated using the NDS equations.

Table 4-8 Joint Design and Equivalent Steel Bolt Theory

5. Summary, Conclusions, and Recommendations

5.1 Materials

The objective of the material tests was to establish strength data for correlation to actual joint tests and to establish a more efficient method for determining dowel bearing strengths of timber framed connections. Peg bending, peg shear, and peg bearing tests were conducted on a single white oak peg population in an effort to accomplish the stated objectives. The peg shear tests were used to develop a characteristic equation for the white oak peg population based on shear span. Dowel bearing tests were performed on material removed from the mortise and tenon members of the full size joint tests. Several dowel bearing tests and peg bearing tests were used in a proposed spring-in-series model for determining dowel bearing capacities of timber framed connections. Experimental values for combined dowel bearing tests were obtained for verification of the model.

Testing of the mentioned materials and analytical comparisons has led to the following conclusions:

- The strength data for all of the material tests is regarded as suitable for use in design situations, but needs to be adjusted for factor of safety and duration of load.
- The peg shear test failures were similar to those in pegs removed from full size joints.
- The stiffness values from the shear tests could not be correlated to the joint tests.
- The spring theory showed that dowel bearing tests of combination of joint and peg materials can be modeled as springs in series and that the weaker material in the combination dominates the combined strength.
- The stiffness values for the spring theory model were consistently less than the combined dowel bearing test data.
- The correlation of material test bearing data to full size joints was not made due to the lack of a bearing failure in any of the joints tested.

5.2 Joints

The objective of the joint tests was to establish strength and stiffness data as well as a rational design method for joints under short duration loads. Monotonic testing, as well as a small number of cyclic tests, of joints constructed from three different wood species were used to reach the stated objectives. Several strength equations were derived based on the failure modes witnessed and those known to exist. All the joints were tested in tension and failure of the pegs was identified as the preferred failure mode. The necessary detailing requirements to insure peg failure for joints under short duration monotonic loads were found experimentally and compared to a proposed analytical procedure using the current NDS strength equations and an equivalent steel bolt theory. The strength equations and the equivalent steel bolt theory were combined to form a proposed design procedure for timber frame connections.

This experimental and analytical work allows for the following conclusions to be drawn:

- The specification of minimum end distance, edge distance, and spacing for pegs insures that a brittle failure of the connected members will not occur prior to substantial deformation of the joint after yield.
- Based on these minimum dimensions, joint design can be based on five distinct modes of failure; mode I_s, mode I_m, mode I_d, mode III_m and mode V_d.
- The equivalent steel bolt theory is a conservative and convenient method for determining end and edge distances for joint under monotonic short duration load.
- A method to describe the stiffness of timber frame connections was not established.

5.3 Recommendations for Future Work

5.3.1 Material Tests

Additional material tests are needed to define timber frame connection behavior. There is limited data on peg shear strengths and combinations of peg and base material strengths for the full range of materials used in the timber frame industry. Defining these properties is a must if the industry wants to develop design specifications. Further investigation into a weaker material dominating the strength of a combined bearing test is warranted based on the results of this work. If tests on other species and orientations behave similarly to the combined dowel bearing tests in this research, existing data could be used to define the bearing strengths of virtually any combination of materials without the need for additional testing. Below is a summary of the recommendations for future material tests to advance the development of timber frame design values:

- Dowel bearing tests to validate the spring theory model, which should include tests of various grain orientations with respect to load.
- Peg shear tests based on the simplified joint test procedure used by Reid to establish strength and stiffness data for various peg and base material combinations (Reid 1997).

5.3.2 Joint Tests

A substantial amount of work is needed to sufficiently establish a design standard for timber frame connections. The objectives of this work were to determine detailing requirements to insure peg failure and to determine the strength and stiffness of these failure modes. Two of the three objectives listed were accomplished.

The definition of stiffness properties for timber frame connections is required. A review of the work by Reid at the Michigan Technological University could be the answer to defining joint stiffness (Reid 1997). The COV values from the full size tests in this work ranged from 15% for the red oak joints to no correlation in the southern yellow pine tests. The tests performed by Reid produced consistent results and the simplified joints used by Reid are a relatively inexpensive alternative when compared to full size joint tests. The simplified joints are much easier to construct, use less material, and would allow for more quality control over the specimen.

Table 5-1 shows a comparison of the simplified maple joints tested by Reid and the average stiffness value from the 10 monotonically loaded red oak joints in this work. The comparison between the maple and red oak tests is justified because Reid reported no damage to the side or main members during testing, which is similar to what was witnessed during the red oak joint tests. The column in the table labeled *equivalent joint* contains the stiffness values from Reid's tests adjusted to reflect two pegs and a 1.5" thick tenon for comparison to the full size red oak tests. The stiffness values for both test types are essentially identical.

Table 5-1 Stiffness Comparison of Full Size Joint Tests to Simplified Joint Tests

		Stiffness (lbs/in)				Red Oak Joint
Group	Orientation	Mean	StDev	COV	Equiv. Joint	Stiffness
MT00M1	Tangential	51,900	4,850	0.090	69,200	70,200
MT00M2	Tangential	51,700	3,310	0.060	68,900	70,200

The development of stiffness values for timber frame connections should include the use of these simplified mortise and tenon connections. The simplified joints produced much less variation in stiffness. The strength values from the simplified joints could be compared to those from the full size joint tests and possibly be used to develop additional strength information.

Joint tests are needed to define the mode III_m failure. The failure mode appears to be controlled by the embedment length (l) to diameter (D) ratio of the peg and the ability of the timber to prevent rotation of the peg. The three mode III_m failures observed in this research had a l/D ratio of 1.6 and the joint tested by Schmidt and MacKay (1997) with this failure mode had an l/D ratio of 1.5. Experimental work with varying parameters such as tenon and mortise thickness and peg diameter is needed. The simplified joints used by Reid would work well for varying the mentioned parameters without using large amounts of material.

Limited tests were performed during the course of this work. In order to gain better insight into connection design more tests are needed. In particular, the effects of normal and long term load duration needs to be defined. The Douglas fir joints tested in this work were brittle compared to the other joints tested. Additional Douglas fir joints from both recycled and fresh cut timber need to be tested. The determination as to whether or not fresh cut material is as brittle as recycled, and the long term load effects on recycled material has yet to be studied. The long and short term effects of draw boring joints with seasoned and unseasoned material, and additional cyclic tests are all important to the development of connection standards. Studies on specimens made from additional commercially important species to the timber frame industry are needed for verification of the end distance, edge distance, and spacing requirements to insure peg failure. Finally, the incorporation of all the past and future work needs to be applied to the analysis and testing of timber frame assemblies. Individual joint data is valuable to the designer or builder only if it can be related to the overall structure behavior.

The recommendations for future work to define timber frame joint design capacities are listed below:

- Simplified joint tests similar to those tested by Reid for the determination of strength and stiffness properties (Reid 1997).
- Parametric studies using simplified joints to isolate the mode III_m failure mode.
- Additional full-size joint tests of commercially important species to verify the equivalent steel bolt theory.
- Tests to identify the effects of duration of load and seasoning on joint capacity.
- Frame tests to correlate individual joint behavior to overall structure response.

6.0 References

AFPA (1997). "National Design Specification for Wood Construction," American Forest & Paper Association (AFPA), Washington, DC.

ASTM, (1995a). *1995 Annual Book of ASTM Standards, 04.10 Wood*, Philadelphia, PA.

ASTM, (1995b). "Standard Method for Evaluating Dowel Bearing Strength of Wood and Wood-Base Products," Draft 10, January 1995.

Bulleit, W. M., Sandberg, L. B., O'Bryant, T. L., Weaver, D. A., and Pattison, W. E., (1996). "Analysis of Frames with Traditional Timber Connections," *Proceedings*, International Wood Engineering Conference, New Orleans, LA. 4, 232-239.

Brungraber, R. L. (1992). "Engineered Tension Joinery," *Timber Framing*. 23, 10-12.

Brungraber, R. L. (1985). "Traditional Timber Joinery: A Modern Analysis," Ph.D. Dissertation, Stanford University, Palo Alto, California.

Church, J. R. (1995). "Characterization of Factors Influencing the Bearing Strength of Wood Pegged Connections," M.S. Thesis, University of Idaho.

Church, J. R. and Tew, B. W. (1997). "Characterization of Bearing Strength Factors in Pegged Timber Connections," *Journal of Structural Engineering*, March 1997, 326-332.

Duff, S. F., Black, R. G., Mahin, S. A., and Blondet, M. (1996). "Parameter Study of an Internal Timber Tension Connections," *Journal of Structural Engineering*, 122(4), 446-452.

Kessel, M. H., Speich, M. and Hinkes, F.-J. (1988). "The Reconstruction of an Eight-Floor Timber Frame House at Hildesheim (FRG)," *Proceedings,* 1988 International Conference on Timber Engineering, Seattle, WA, 415-421.

Kessel, M. H. and Augustin, R. (1996). "Load Bearing Capacity of Timber Connections with Wood Pegs", Peavy, M. D. and Schmidt, R. J., trans. *Timber Framing, Journal of the Timber Framers Guild*. 39, March, 8-11.

McLain, T. E., and Thangjitham, S., (1983). "Bolted Wood-Joint Yield Model," *Journal of Structural Engineering*. 109(8), 1820-1835.

Patton-Mallory, M., (1988). "End Distance Effects Comparing Tensile and Compression Loads on Bolted Wood Connections," *Proceedings*, International Conference on Timber Engineering, Seattle, WA., 2, 313-319.

Reid, E. L. (1997). "Behavior of Wood Pegs in Traditional Timber Frame Connections," M.S. Thesis, Michigan Technological University.

Sandberg, L. B., Bulleit, W. M., O'Bryant, T. L., Postlewaite, J. J., and Schaffer, J. J.(1996). "Experimental Evaluation of Traditional Timber Connections," *Proceedings*, International Wood Engineering Conference, New Orleans, LA., 4, 225-231.

Schmidt , R. J. and MacKay, R. B. (1997). "Timber Frame Tension Joinery," Research Report, Department of Civil and Architectural Engineering, University of Wyoming, Laramie, WY 82071, October 1997.

Snodgrass, J. D. and Gleaves, W. W. (1960). "Effect of End Distance on Strength of Single Bolt Joints," Oregon Forest Research Center, Oregon State University.

Soltis, L. A., Hubbard, F. K. and Wilkinson, T. L. (1986). "Bearing Strength of Bolted Timber Joints," *Journal of Structural Engineering*, 112(9), 2141-2154.

Soltis, L. A., and Wilkinson, T. L. (1987). "Bolted-Connection Design." No. FPL-GTR-54, Forest Products Laboratory, U.S. Dept. of Agriculture, Washington, DC.

Theilen, R. D., Bender, D. A., Pollock, D. G., and Winistorfer, S. G. (1998), "Lateral Resistance of Ring-shank Nail Connections in Southern Pine Lumber, *Transactions of the ASAE*, 41(2):465-472.

Trayer, G. W. (1932). "The Bearing Strength of Wood Under Bolts," Technical Bulletin No. 332, Forest Products Laboratory, U.S. Dept. of Agriculture, Washington, DC.

Wilkinson, T. L. (1991). "Dowel Bearing Strength." No. FPL-RP-505, Forest Products Laboratory, U.S. Dept. of Agriculture, Washington, DC.

Wilkinson, T. L. (1993). "Bolted Connection Design Values Based on European Yield Model," *Journal of Structural Engineering*, 119(7), 2169-2186.

7.0 Appendices

Appendix A Joint Test Defects and Comments:

Southern Pine Joint Tests			
Test	**Test Comments**	**Tenon Defects**	**Mortise Defects**
SP1	joint was prestressed by overtightening nut on test apparatus		
SP2			
SP3			
SP4			
SP5			
SP6			
SP7			
SP8			
SP9			
SP10			
SP11			signs of rot below pegs, did not seem to affect test
SP12			
SP13	drawboring failed one peg hole w/ classic relish failure		
SP14			
SP15	lost data file		
SP16			
50			
51a	joint SP51 was loaded three times to test repair procedure,		
51b	there was no significant damage to the mortise or tenon		
51c	and all failures occurred in the pegs.		
52	mortise split at knot adjacent to pegs		
53a	joint SP53 was loaded three times to test repair procedure,		
53b	there was no significant damage to the mortise or tenon		
53c	and all failures occurred in the pegs.		

*Tests of joint SP53 were stopped prior to reaching the 5% offset value due to test errors.

Recycled Douglas Fir Tests			
Test	**Test Comments**	**Tenon Defects**	**Mortise Defects***
DF1	defects did not seem to affect joint strength	knot directly behind one peg	slight blow-out at one peg hole
DF2	it is likely that the mortise splitting occurred sumilt. w/peg failure but cracking was heard prior to the 5% offset point		
DF3	audible cracking heard prior to ultimate	checks throughout	checks throughout
DF4			2" dia. knot adjacent to pegs
DF5	simult. tenon relish and mortise split at ultimate		
DF6	cracking heard after yield point, but mortise seemed O.K.		
DF7			
DF8			
DF9	relish failure behind one peg, tenon damage did not seem to affect test	small peg hole blow out	
DF10			
DF11	likely that checks caused failure, but was difficult to determine		severe checks in mortise
DF12	check closed during test and the tenon formed splits behind	large check @ center	
DF13	both peg holes, increase in end distance had no effect		

*The majority of the mortise members had hair-line checks throughout. Defects were recorded for joints that had a significantly greater number of checks or large checks.

Red Oak Joint Tests*				
Test	Mortise/Tenon	Test Comments	Tenon Defects	Mortise Defects*
RO1	H/H	tests RO1, RO2, and RO3 was the same joint loaded three	bad saw cut at tenon	pith in center, honeycombing
RO2	H/H	times to test repair procedure,there was no significant damage	shoulder	and surface checks
RO3	H/H	to the mortise or tenon and all failures occurred in the pegs		
RO4	E/E	tests RO4, RO5, and RO6 was the same joint loaded three	pith with check in outer	spike knot inside one peg
RO5	E/E	times to test repair procedure,there was no significant damage	1/3	hole, pith in center and
RO6	E/E	to the mortise or tenon and all failures occurred in the pegs		honeycombing
RO7	F/F	mortise had check pass through peg holes and tenon blew out	pith in mid 1/3 and	pith on mortise face,
		at peg hole due to check, one peg hole was essentially failed	diagonal check	surface checks and large
		prior to testing, but the joint was included in the data set because		core check
		it still maintained load (impressive)		
RO8	L/L	tests RO9, and RO10 was the same joint loaded two times	diagonal check	multiple checks and pith
RO9	L/L	to test repair procedure,there was no significant damage to the		in mid 1/3
		mortise or tenon and all failures occurred in the pegs		
RO10	I/I	check passed through both mortise peg holes which had signs of	diagonal check through	large checks and large
		openning during the test but the check did not form split	peg hole	honeycombing
		(impressive) peg shear/bending was still the mode of failure		
RO11	D/D	tests RO11, RO12, and RO13 was the same joint loaded three		bark pocket at face of
RO12	D/D	times to test repair procedure,there was no significant damage to		mortise and large check
RO13	D/D	the mortise or tenon and all failures occurred in the pegs, the first		on other face
		test was a cyclic test and one set of peg holes had large check		
RO14	B/B	formed single split behind one peg at approx. 7000 lbs. on 4th	pith in outer 1/3 and knot	knot in mortise
		cycle, ultimate occurred when the same peg formed classic relish	directly behind one peg	
		failure through pith, peg failure could have occurred before first		
		tenon split, but was difficult to determine		
RO15	G/A	tests RO15, RO16, and RO17 was the same joint loaded three	pith in tenon center	bark pocket on inside face
RO16		times to test repair procedure, the mortise split at approx.		
RO17		13,200 lbs.during ultimate failure of test RO17		
RO18	A/G			

*Mortise and tenon members were labeled, and the defects were noted for use in multiple tests.

Appendix B Summary of Joint Test Plots:

Summary of SYP Joint Test Plots:

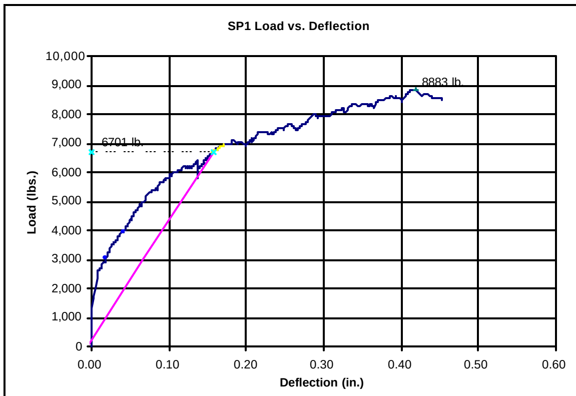

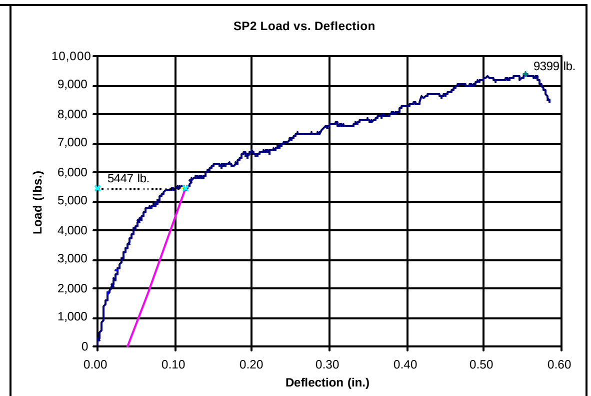

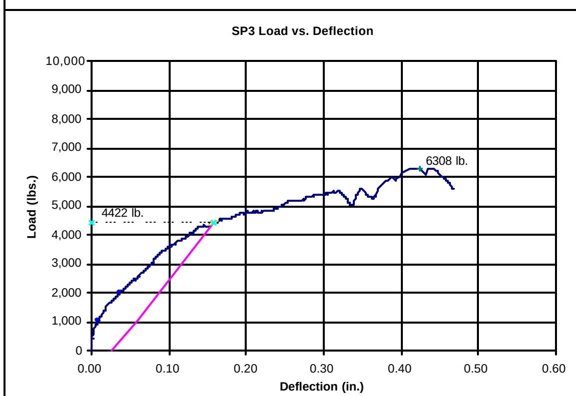

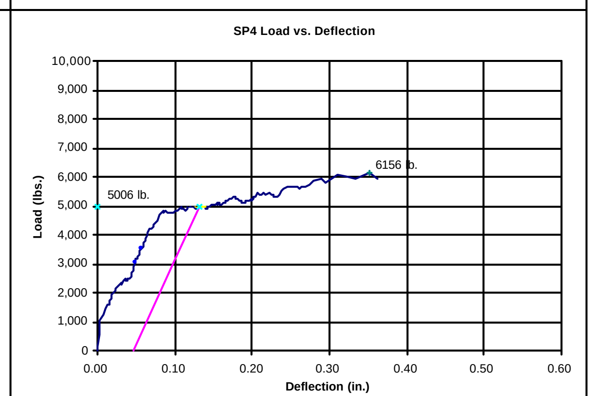

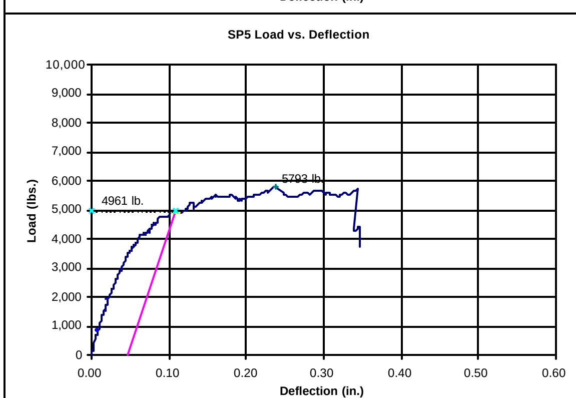

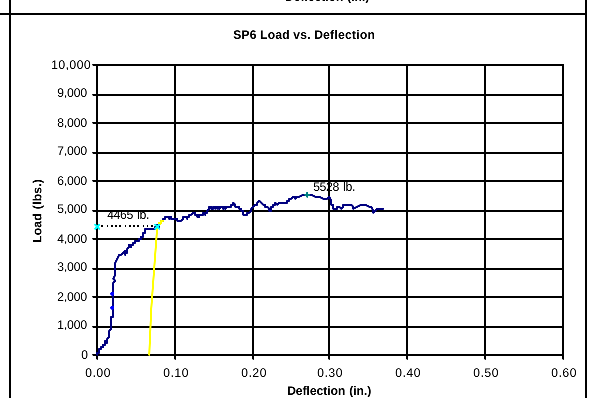

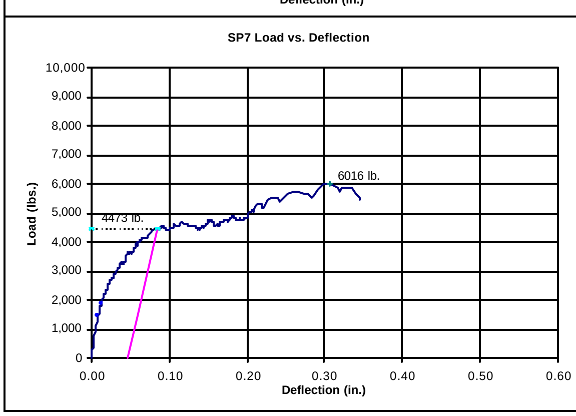

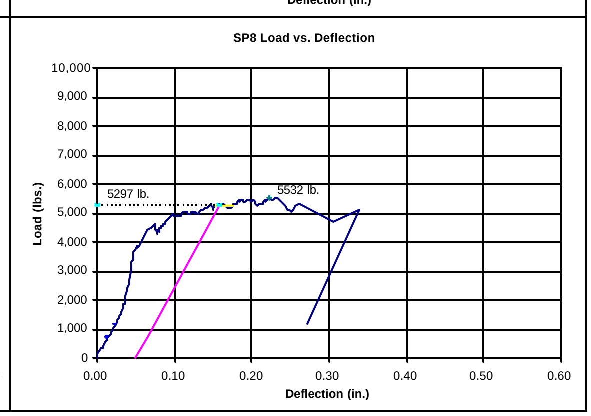

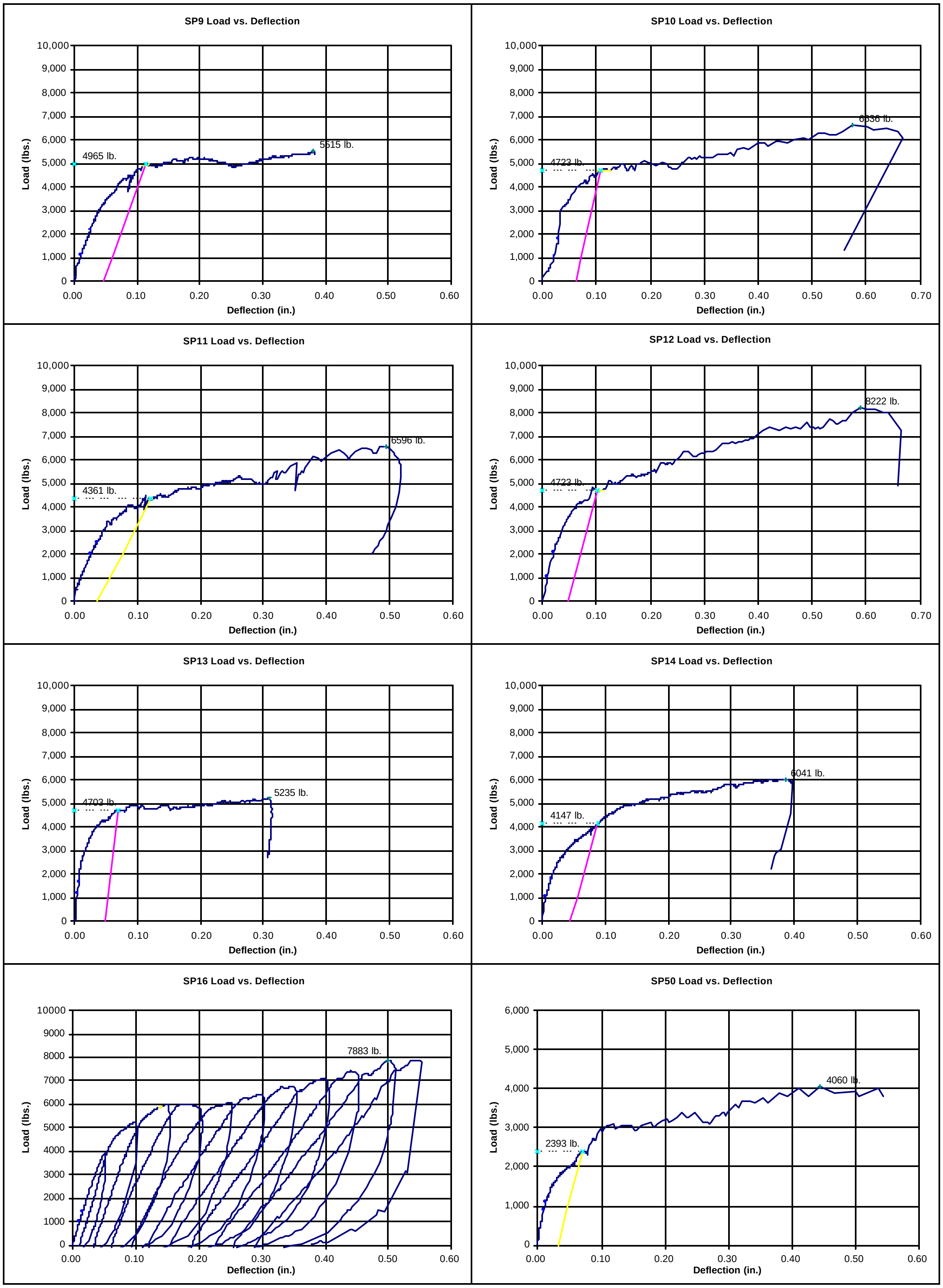

SP9 Load vs. Deflection
Load (lbs.)
Deflection (in.)
10,000
9,000
8,000
7,000
6,000
5,000
4,000
3,000
2,000
1,000
0
0.00
0.10
0.20
0.30
0.40
0.50
0.60
4965 lb.
5515 lb.
SP10 Load vs. Deflection
Load (lbs.)
Deflection (in.)
10,000
9,000
8,000
7,000
6,000
5,000
4,000
3,000
2,000
1,000
0
0.00
0.10
0.20
0.30
0.40
0.50
0.60
0.70
4723 lb.
6636 lb.
SP11 Load vs. Deflection
Load (lbs.)
Deflection (in.)
10,000
9,000
8,000
7,000
6,000
5,000
4,000
3,000
2,000
1,000
0
0.00
0.10
0.20
0.30
0.40
0.50
0.60
4361 lb.
6596 lb.
SP12 Load vs. Deflection
Load (lbs.)
Deflection (in.)
10,000
9,000
8,000
7,000
6,000
5,000
4,000
3,000
2,000
1,000
0
0.00
0.10
0.20
0.30
0.40
0.50
0.60
0.70
4723 lb.
8222 lb.
SP13 Load vs. Deflection
Load (lbs.)
Deflection (in.)
10,000
9,000
8,000
7,000
6,000
5,000
4,000
3,000
2,000
1,000
0
0.00
0.10
0.20
0.30
0.40
0.50
0.60
4703 lb.
5235 lb.
SP14 Load vs. Deflection
Load (lbs.)
Deflection (in.)
10,000
9,000
8,000
7,000
6,000
5,000
4,000
3,000
2,000
1,000
0
0.00
0.10
0.20
0.30
0.40
0.50
0.60
4147 lb.
6041 lb.
SP16 Load vs. Deflection
Load (lbs.)
Deflection (in.)
10000
9000
8000
7000
6000
5000
4000
3000
2000
1000
0
0.00
0.10
0.20
0.30
0.40
0.50
0.60
7883 lb.
SP50 Load vs. Deflection
Load (lbs.)
Deflection (in.)
6,000
5,000
4,000
3,000
2,000
1,000
0
0.00
0.10
0.20
0.30
0.40
0.50
0.60
2393 lb.
4060 lb.

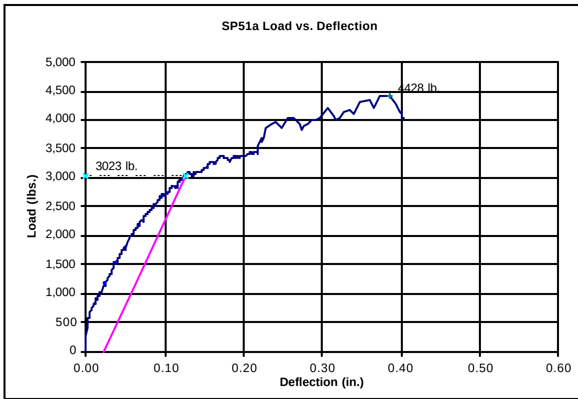
SP51a Load vs. Deflection
Load (lbs.)
Deflection (in.)
3023 lb.
4428 lb.
0
500
1,000
1,500
2,000
2,500
3,000
3,500
4,000
4,500
5,000
0.00
0.10
0.20
0.30
0.40
0.50
0.60

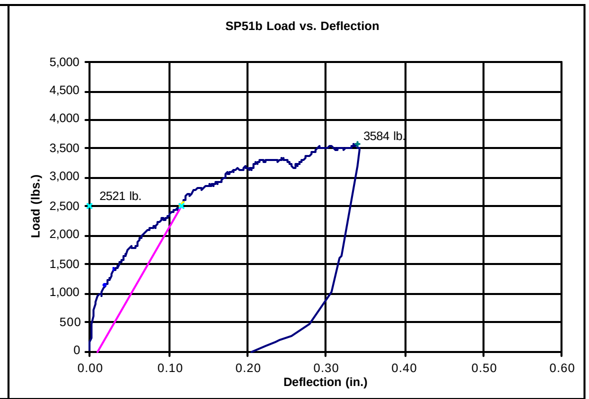
SP51b Load vs. Deflection
Load (lbs.)
Deflection (in.)
2521 lb.
3584 lb.
0
500
1,000
1,500
2,000
2,500
3,000
3,500
4,000
4,500
5,000
0.00
0.10
0.20
0.30
0.40
0.50
0.60

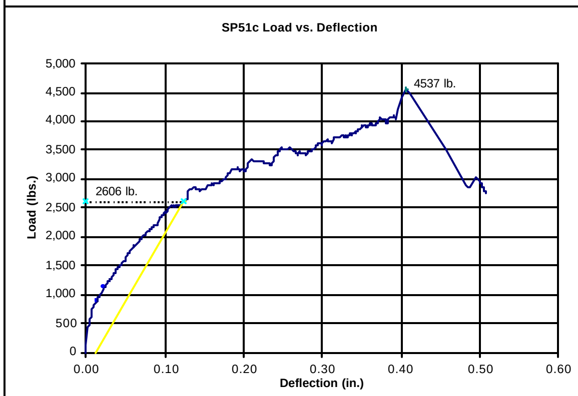
SP51c Load vs. Deflection
Load (lbs.)
Deflection (in.)
2606 lb.
4537 lb.
0
500
1,000
1,500
2,000
2,500
3,000
3,500
4,000
4,500
5,000
0.00
0.10
0.20
0.30
0.40
0.50
0.60

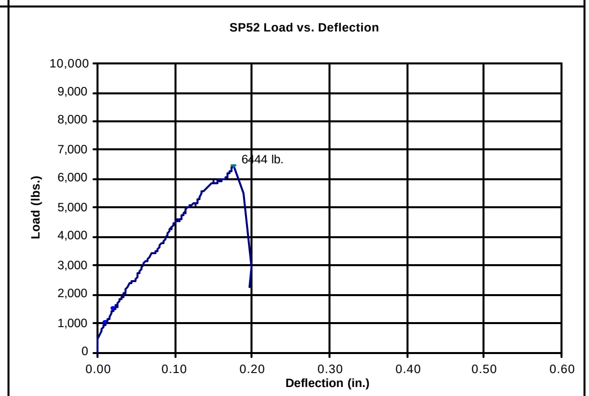
SP52 Load vs. Deflection
Load (lbs.)
Deflection (in.)
6444 lb.
0
1,000
2,000
3,000
4,000
5,000
6,000
7,000
8,000
9,000
10,000
0.00
0.10
0.20
0.30
0.40
0.50
0.60

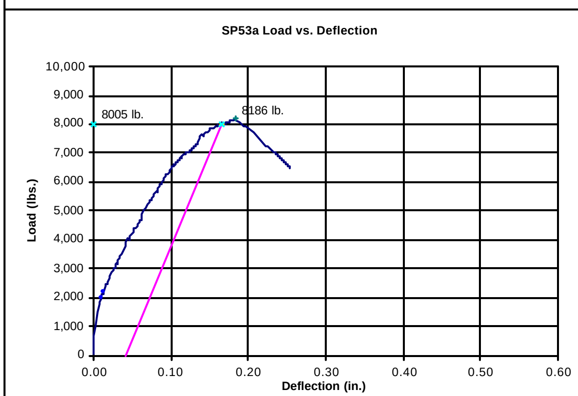
SP53a Load vs. Deflection
Load (lbs.)
Deflection (in.)
8005 lb.
8186 lb.
0
1,000
2,000
3,000
4,000
5,000
6,000
7,000
8,000
9,000
10,000
0.00
0.10
0.20
0.30
0.40
0.50
0.60

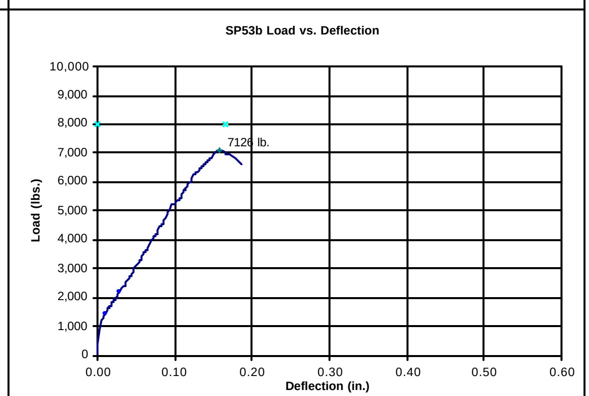
SP53b Load vs. Deflection
Load (lbs.)
Deflection (in.)
7126 lb.
0
1,000
2,000
3,000
4,000
5,000
6,000
7,000
8,000
9,000
10,000
0.00
0.10
0.20
0.30
0.40
0.50
0.60

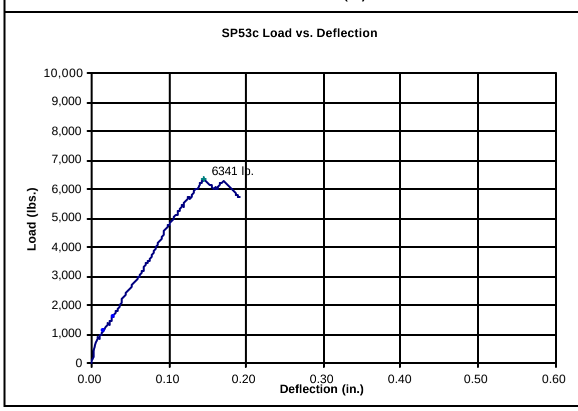
SP53c Load vs. Deflection
Load (lbs.)
Deflection (in.)
6341 lb.
0
1,000
2,000
3,000
4,000
5,000
6,000
7,000
8,000
9,000
10,000
0.00
0.10
0.20
0.30
0.40
0.50
0.60

Summary of RDF Joint Test Plots:

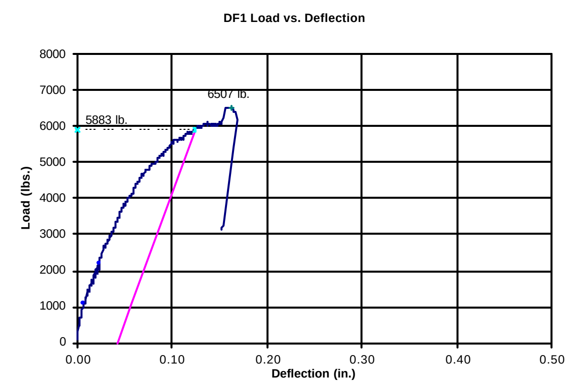

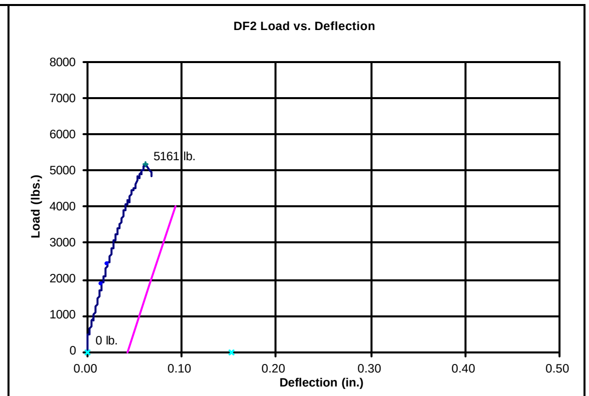

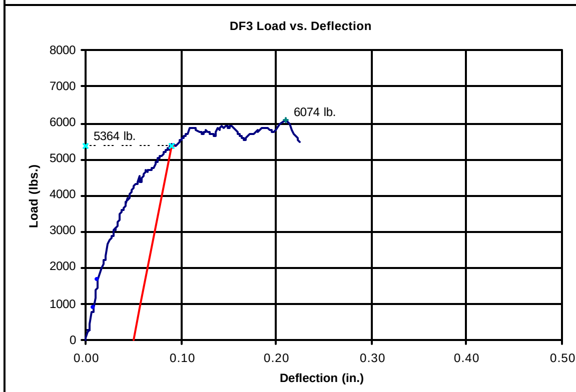

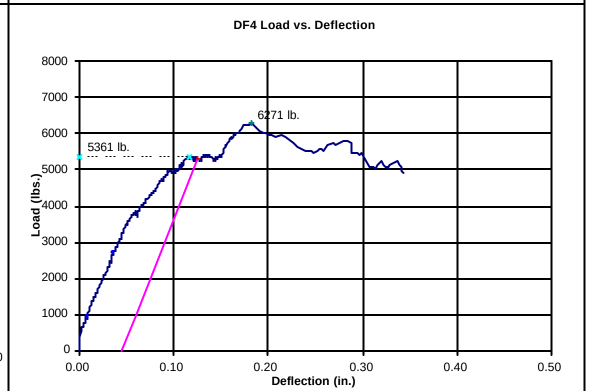

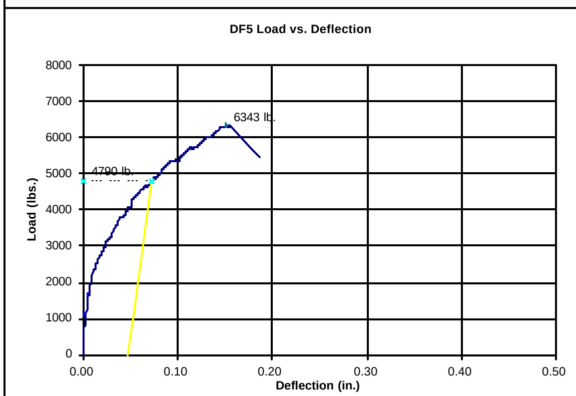

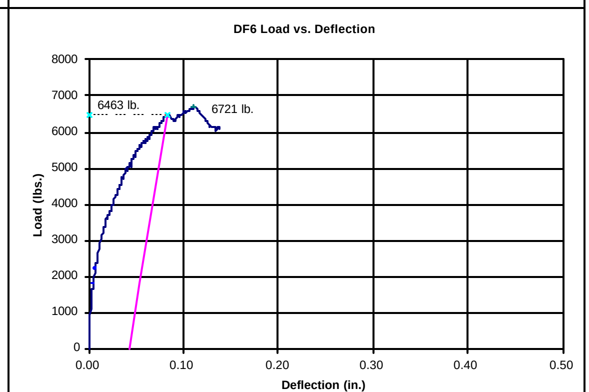

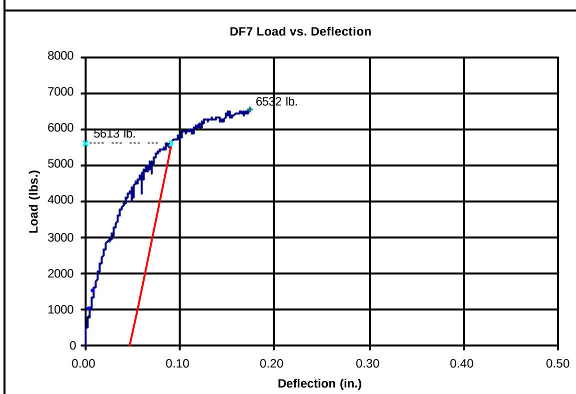

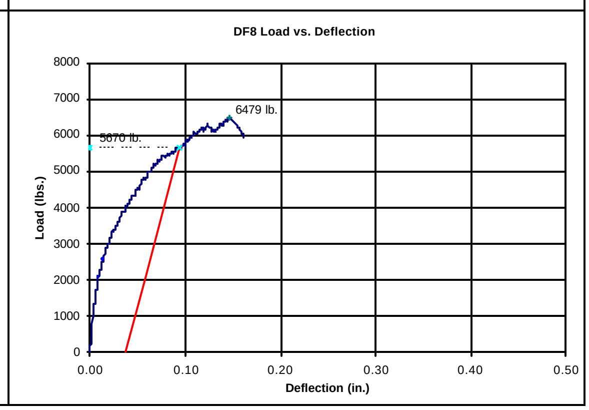

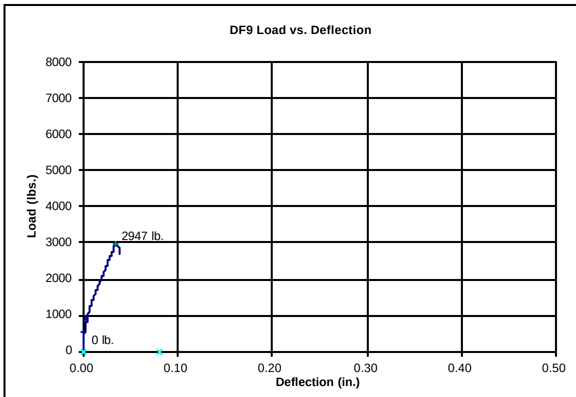
DF9 Load vs. Deflection
Load (lbs.)
Deflection (in.)
2947 lb.
0 lb.

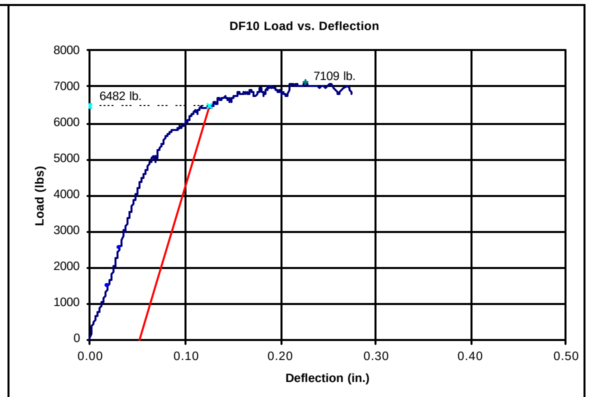
DF10 Load vs. Deflection
Load (lbs)
Deflection (in.)
7109 lb.
6482 lb.

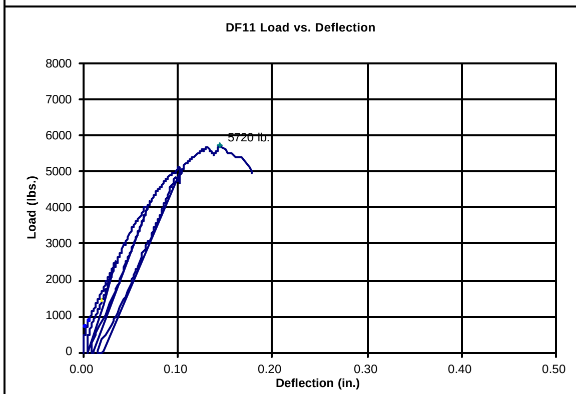
DF11 Load vs. Deflection
Load (lbs.)
Deflection (in.)
5720 lb.

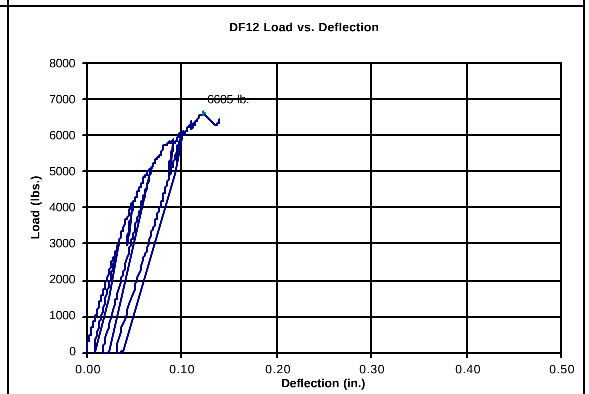
DF12 Load vs. Deflection
Load (lbs.)
Deflection (in.)
6605 lb.

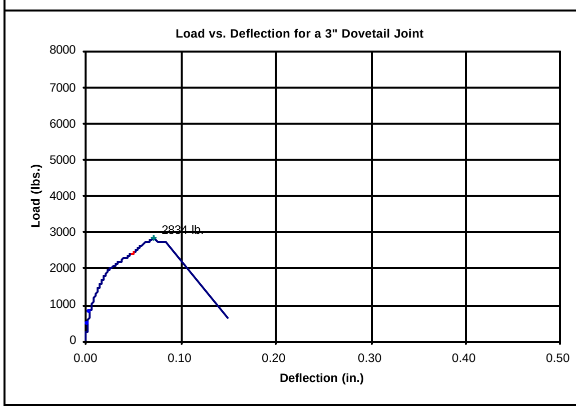
Load vs. Deflection for a 3" Dovetail Joint
Load (lbs.)
Deflection (in.)
2834 lb.

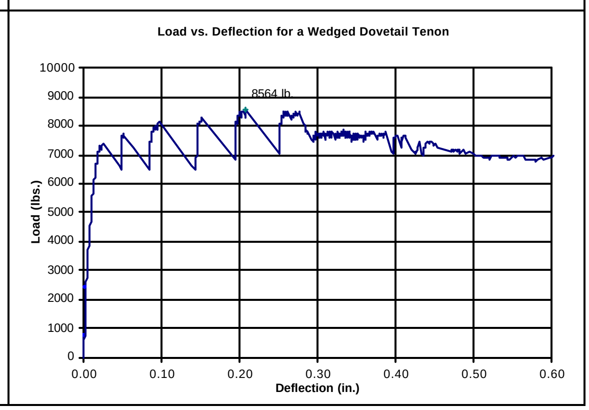
Load vs. Deflection for a Wedged Dovetail Tenon
Load (lbs.)
Deflection (in.)
8564 lb.

Summary of RO Joint Test Plots:

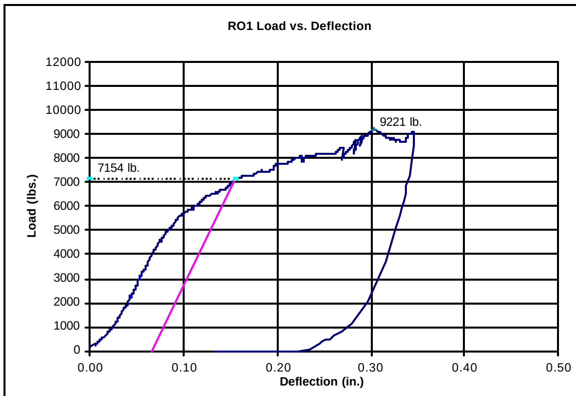

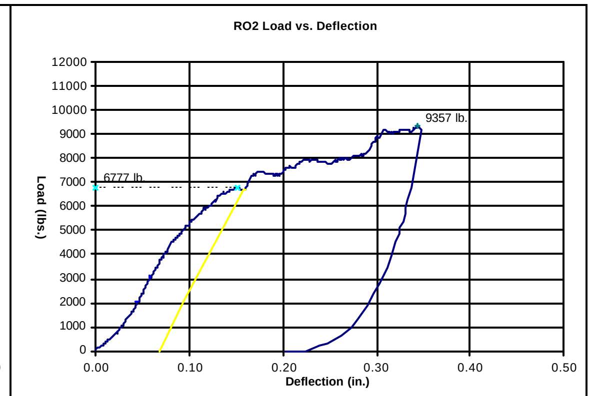

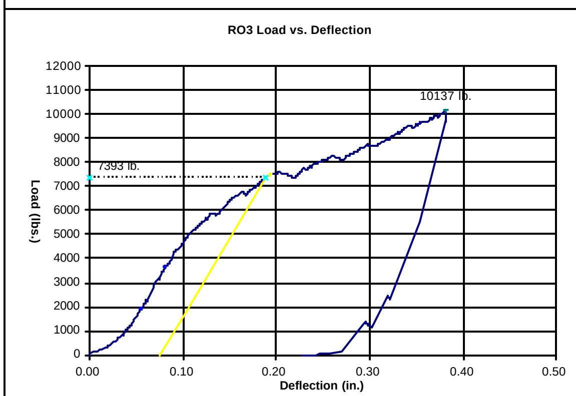

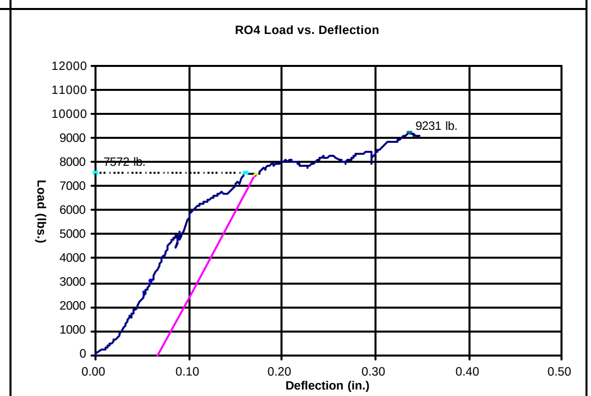

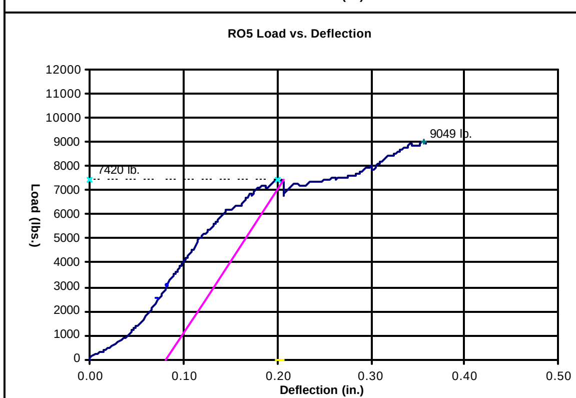

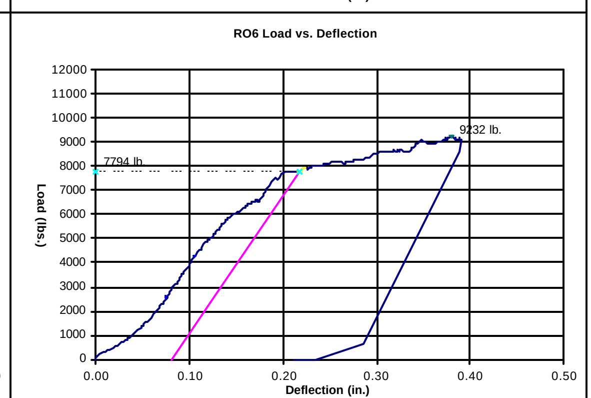

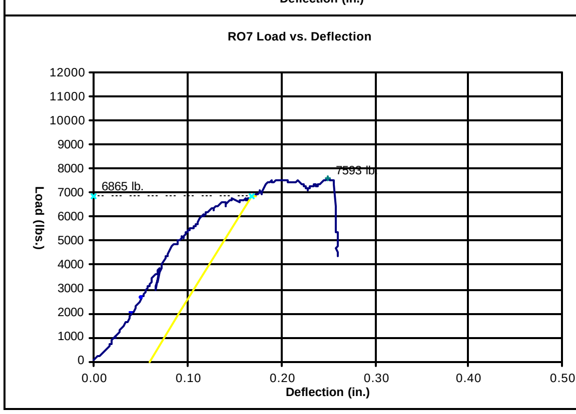

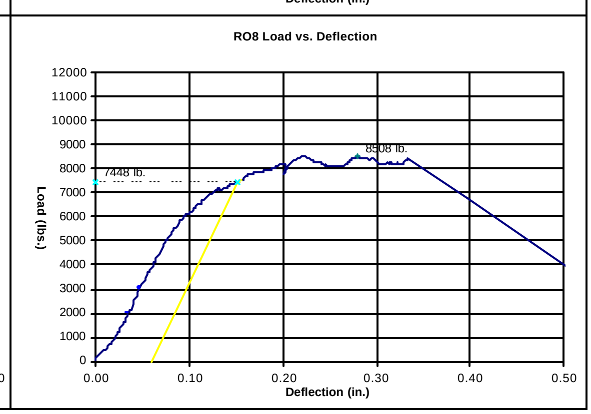

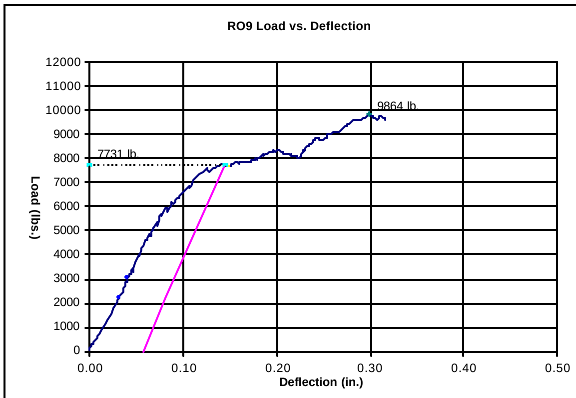
RO9 Load vs. Deflection
9864 lb.
7731 lb.
Load (lbs.)
Deflection (in.)

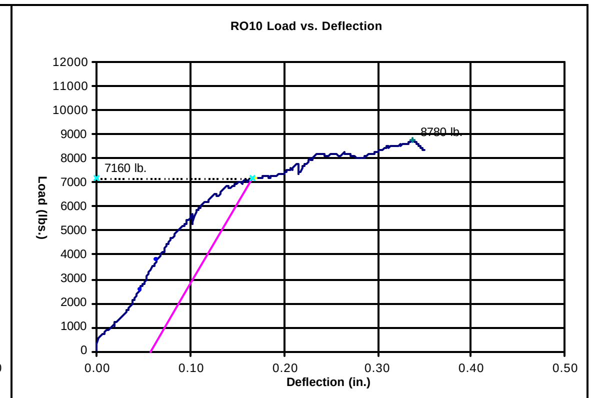
RO10 Load vs. Deflection
8780 lb.
7160 lb.
Load (lbs.)
Deflection (in.)

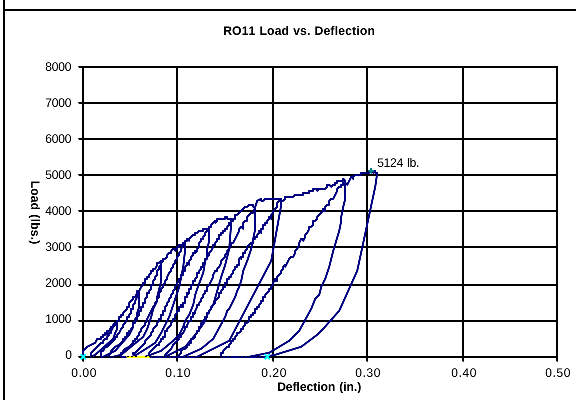
RO11 Load vs. Deflection
5124 lb.
Load (lbs.)
Deflection (in.)

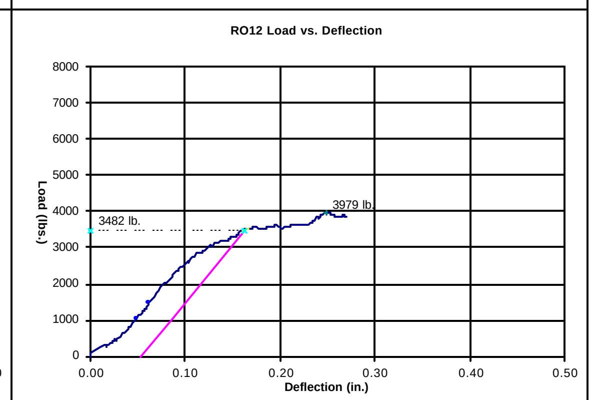
RO12 Load vs. Deflection
3979 lb.
3482 lb.
Load (lbs.)
Deflection (in.)

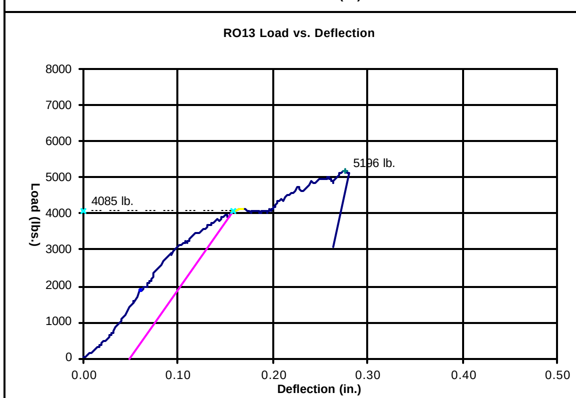
RO13 Load vs. Deflection
5196 lb.
4085 lb.
Load (lbs.)
Deflection (in.)

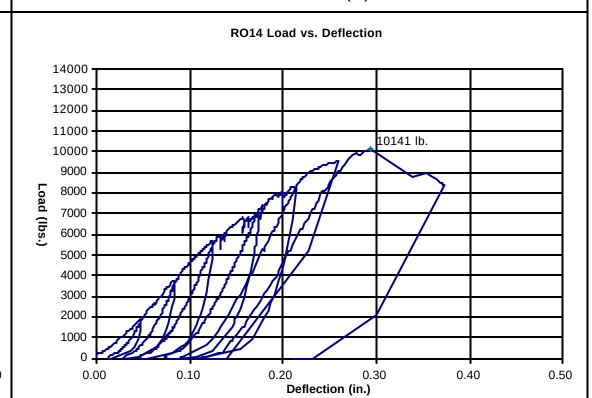
RO14 Load vs. Deflection
10141 lb.
Load (lbs.)
Deflection (in.)

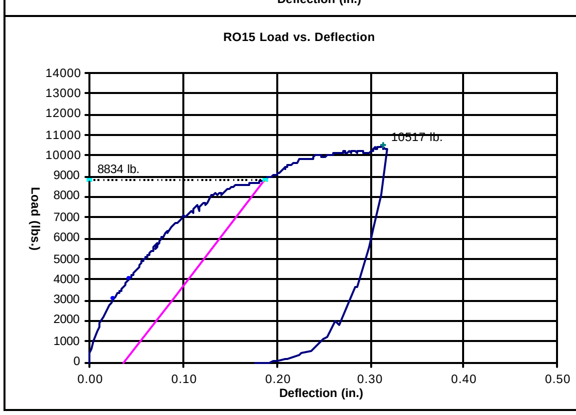
RO15 Load vs. Deflection
10517 lb.
8834 lb.
Load (lbs.)
Deflection (in.)

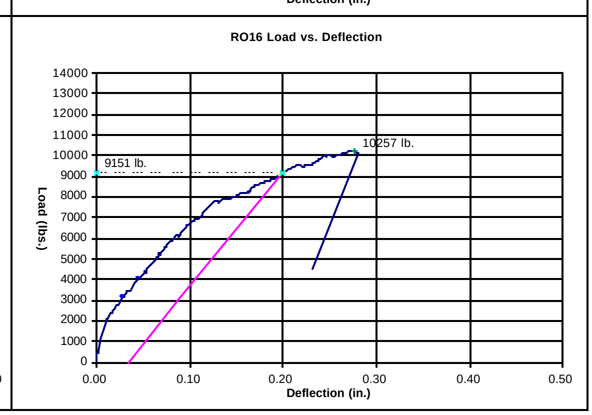
RO16 Load vs. Deflection
10257 lb.
9151 lb.
Load (lbs.)
Deflection (in.)

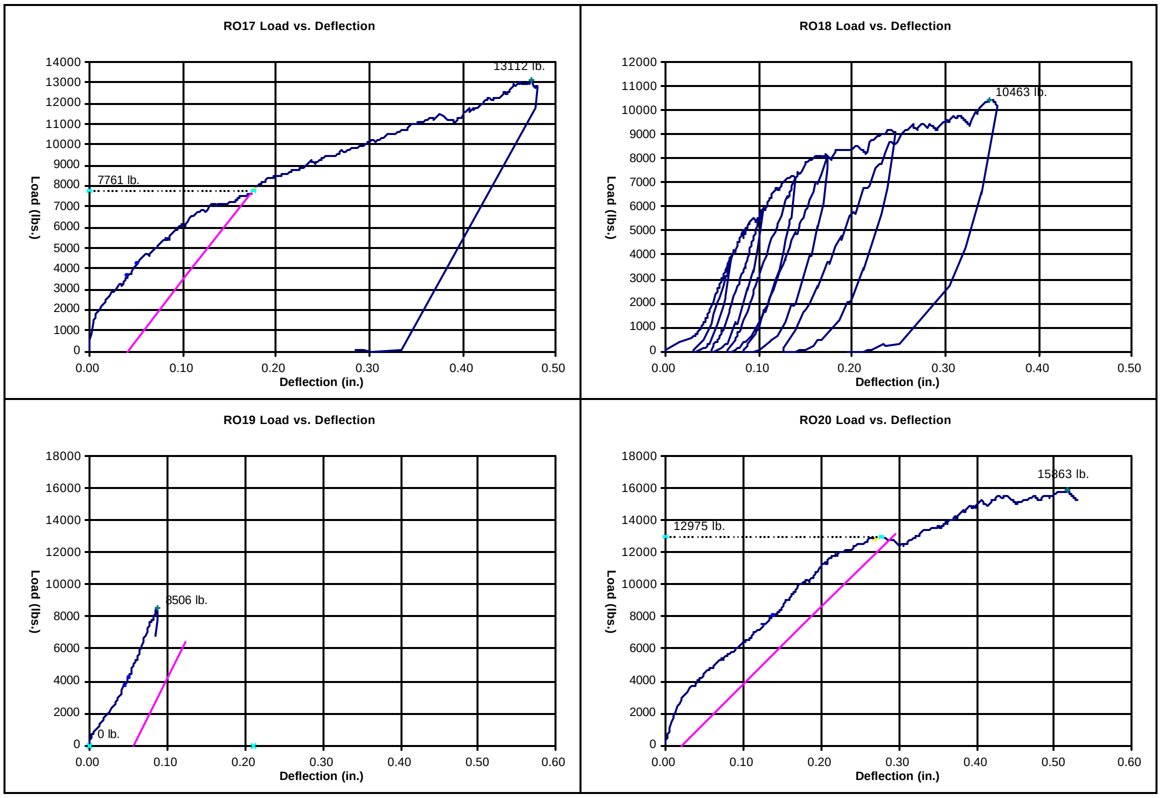

Appendix C SYP Drawbored Joint Tests:

Test	Peg Diameter (in)	End Dist. (l_v)	Edge Dist. (l_e)	Spacing Dist. (l_s)	Yield Disp. (in)	Yield Load (lbs)	Yield Stress (psi)	Stiffness (lbs/in)	Ultimate Disp. (in)	Ultimate Load (lbs)	Ave. Peg G	Failure Type @ Yield	Failure Type @ Ultimate
SP13	1.0	2D	2D	3D	0.07	4,700	1,450	246,000	0.31	5,230	0.67	Tenon Relish[1]	Peg Shear/Bending
SP14	1.0	2D	2D	3D	0.09	4,150	1,280	94,000	0.39	6,040	0.61	Peg Shear/Bending	Peg Shear/Bending

[1] Relish failure behind one peg prior to loading specimen.

Appendix D RO Four Peg Joint Tests:

Test	Peg Diameter (in)	End Dist. (l_v)	Edge Dist. (l_e)	Spacing Dist. (l_s)	Yield Disp. (in)	Yield Load (lbs)	Yield Stress (psi)	Stiffness (lbs/in)	Ultimate Disp. (in)	Ultimate Load (lbs)	Ave. Peg G	Failure Type @ Yield	Failure Type @ Ultimate
RO19	0.977	2D	2D	2.5D			95700		0.09	8510	0.76		Bending Failure of Mortise
RO20	0.984	2D	2D	2.5D	0.28	13000	48100	2140	0.52	15900	0.62	Peg Shear/Bending	Mortise splitting @ 0.51"

Appendix E Summary of Peg Bending Tests:

Summary of Dry Peg Bending Tests

Test	Species	Load Orient.	Yield Load (lb.)	Ultimate Load (lb.)	Stiffness (lb/in.)	Actual Dia (in.)	Section Modulus	Yield Stress (psi)	M.C. %	SG	SG_{12}	FAILURE TYPE
98wot033	WO	T	515	625	2,613	0.985	0.094	8,583	16.3	0.58	0.59	Brash/Simple Ten.
98wot031	WO	T	619	762	3,617	1.001	0.098	9,832	15.7	0.61	0.62	Simple Ten.
98wot042	WO	T	728	911	4,300	1.002	0.099	11,516	15.8	0.61	0.62	Brash/Cross Grain Tension
98wot035	WO	T	724	845	3,875	1.000	0.098	11,543	16.8	0.62	0.63	Brash/Simple Ten.
98wot045	WO	T	N/A	N/A	4,500	0.999	0.098	N/A	13.9	0.62	0.63	Brash/Simple Ten.
98wot037	WO	T	729	837	4,000	0.997	0.097	11,729	14.3	0.63	0.63	Brash/Simple Ten.
98wot047	WO	T	726	815	4,083	0.989	0.095	11,959	16.3	0.63	0.64	Simple Ten.
98wot044	WO	T	782	930	4,500	0.994	0.096	12,693	14.2	0.63	0.64	Simple Ten.
98wot032	WO	T	735	856	4,000	0.996	0.097	11,841	17.1	0.64	0.64	Simple Ten.
98wot043	WO	T	721	779	4,100	0.999	0.098	11,525	14.5	0.64	0.64	Simple Ten.
98wot039	WO	T	814	854	5,139	0.984	0.094	13,595	13.3	0.64	0.65	Brash/Cross Grain Tension
98wot030	WO	T	639	759	3,811	0.985	0.094	10,650	11.9	0.65	0.65	Simple Ten.
98wot049	WO	T	773	898	4,300	1.013	0.102	11,854	14.8	0.65	0.66	Cross Grain Tension
98wot034	WO	T	781	869	5,500	0.989	0.095	12,871	16.1	0.66	0.67	Simple Ten.
98wot036	WO	T	708	806	3,750	0.991	0.095	11,590	15.4	0.67	0.68	Brash/Cross Grain Tension
98wot046	WO	T	722	815	3,790	0.988	0.095	11,919	15.1	0.68	0.69	Brash/Cross Grain Tension
98wot048	WO	T	737	825	4,250	0.953	0.085	13,580	13.6	0.69	0.70	Brash/Cross Grain Tension
98wot051	WO	T	771	918	4,900	0.994	0.096	12,518	11.5	0.70	0.71	Cross Grain Tension
98wot056	WO	T	909	1,008	5,312	0.976	0.091	15,566	12.0	0.73	0.74	Brash/Cross Grain Tension
98wot059	WO	T	896	1,069	5,667	0.983	0.093	15,019	12.9	0.73	0.74	Splintering Tension
98wot060	WO	T	900	1,099	5,833	0.975	0.091	15,449	16.3	0.74	0.75	Simple Ten.
98wot054	WO	T	1,090	1,160	6,833	0.985	0.094	18,151	11.8	0.75	0.76	Cross Grain Tension
98wot053	WO	T	1,131	1,321	6,333	1.000	0.098	18,027	14.7	0.75	0.76	Cross Grain Tension
98wot055	WO	T	1,149	1,184	6,000	0.996	0.097	18,514	12.7	0.77	0.77	Cross Grain Tension
98wot052	WO	T	937	1,184	6,500	0.982	0.093	15,776	12.0	0.79	0.80	Simple Ten.
98wot057	WO	T	1,222	1,292	7,031	0.994	0.096	19,796	12.0	N/A	N/A	Brash/Cross Grain Tension
		Mean=	818	937	4,790			13,444	14.3	0.67	0.68	
		Std. Dev.=	174	180	1,129			2,879				
		5% Exclusion=	488	596	2,650			7,988				
		COV=	0.21	0.19	0.24			0.21				
		K[1]=	1.895	1.895	1.895			1.895				

[1] From ASTM D2915

Summary of Wet Peg Bending Tests

Test	Species	Load Orient.	Yield Load (lb.)	Ultimate Load (lb.)	Stiffness (lb/in.)	Actual Dia (in.)	Section Modulus	Yield Stress (psi)	M.C. %	SG	SG_{12}	Failure Type
98wot001	WO	T	658	792	5,310	1.015	0.103	10,014	34.5	0.55	0.55	Compression
98wot002	WO	T	646	718	3,785	1.013	0.102	9,887	36.4	0.62	0.62	Cross Grain Tension
98wot003	WO	T	618	742	3,996	1.004	0.099	9,738	36.3	0.65	0.65	Cross Grain Tension
98wot004	WO	T	645	741	4,787	1.015	0.103	9,811	32.9	0.57	0.57	Cross Grain Tension
98wot005	WO	T	964	1,050	5,712	1.009	0.101	14,951	28.1	0.77	0.78	Simple Tension
98wot006	WO	T	622	706	3,367	1.012	0.102	9,547	61.7	0.62	0.61	Cross Grain Tension
98wot007	WO	T	606	747	4,034	1.016	0.103	9,201	31.0	0.61	0.61	Cross Grain Tension
98wot008	WO	T	626	766	4,973	1.011	0.101	9,649	31.2	0.59	0.59	Simple Tension
98wot009	WO	T	1,065	1,200	6,349	1.020	0.104	15,978	33.1	0.74	0.73	Cross Grain Tension
98wot010	WO	T	668	799	4,170	1.019	0.104	10,047	26.8	0.66	0.67	Cross Grain Tension
98wot011	WO	T	516	644	3,158	1.026	0.106	7,609	42.7	0.57	0.57	Cross Grain Tension
		Mean=	694	809	4,513			10,585	35.9	0.63	0.63	
		Std. Dev.=	165	165	1,001			2,516				
		5% Exclusion=	352	467	2,436			5,367				
		COV=	0.24	0.20	0.22			0.24				
		K[1]=	2.074	2.074	2.074			2.074				

[1] From ASTM D2915

Appendix F Summary of Peg Shear Tests:

Shear Test Summary

Test	Shear Span	Yield Load	Stiffness	Dia	Yield Stress	MC%	SG	SG_{12}
98T1SH01	1D	2,140	27,632	0.985	1,872	9.5	0.62	0.62
98T1SH02	1D	2,211	25,000	0.981	1,951	12.7	0.62	0.62
98T1SH03	1D	2,179	30,263	0.978	1,933	13.8	0.61	0.62
98T2SH04	1D	2,344	34,706	0.984	2,054	9.6	0.65	0.66
98T2SH05	1D	2,595	24,583	0.986	2,268	8.4	0.72	0.73
98T2SH06	1D	2,330	26,579	0.980	2,059	9.5	0.70	0.71
98T3SH07	1D	2,468	65,000	0.980	2,183	8.1	0.79	0.80
98T3SH08	1D	2,479	53,500	0.966	2,256	12.4	0.79	0.80
98T3SH09	1D	2,473	42,000	0.999	2,102	14.2	0.75	0.76
				Mean=	2,075	10.91	0.69	0.70
				Std. Dev.=	141			
				5% Exclusion=	1,773			
				COV=	0.07			
				K[1]=	2.142			
98T1SH10	1/2D	2,532	60,357	0.987	2,207	13.1	0.64	0.65
98T1SH11	1/2D	2,844	40,250	0.996	2,435	14.0	0.63	0.64
98T1SH12	1/2D	2,489	58,929	0.975	2,222	14.7	0.63	0.64
98T2SH13	1/2D	2,874	54,583	0.998	2,448	12.1	0.65	0.66
98T2SH14	1/2D	3,124	41,250	0.976	2,785	13.3	0.71	0.71
98T2SH15	1/2D	2,612	48,125	0.983	2,295	11.0	0.64	0.65
98T3SH16	1/2D	3,085	70,000	0.982	2,717	13.7	0.82	0.83
98T3SH17	1/2D	2,855	56,944	0.985	2,498	12.2	0.70	0.70
98T3SH18	1/2D	3,315	56,000	0.992	2,859	14.1	0.76	0.76
				Mean=	2,496	13.14	0.69	0.69
				Std. Dev.=	242			
				5% Exclusion=	1,978			
				COV=	0.10			
				K[1]=	2.142			
98T1SH19	1/4D	2,733	66,429	0.968	2,477	12.9	0.64	0.65
98T1SH20	1/4D	2,718	66,000	0.971	2,446	13.8	0.63	0.64
98T1SH21	1/4D	3,210	70,000	0.978	2,851	13.0	0.64	0.65
98T2SH22	1/4D	3,278	120,000	0.988	2,852	15.1	0.72	0.72
98T2SH23	1/4D	2,960	110,000	0.983	2,602	11.4	0.69	0.69
98T2SH24	1/4D	3,374	111,667	0.985	2,950	12.2	0.70	0.70
98T3SH25	1/4D	3,602	85,000	0.973	3,231	13.0	0.76	0.77
98T3SH26	1/4D	3,405	120,833	0.984	2,985	13.4	0.80	0.81
98T3SH27	1/4D	3,608	99,375	0.997	3,079	13.3	0.79	0.80
				Mean=	2,830	13.12	0.71	0.72
				Std. Dev.=	271			
				5% Exclusion=	2,250			
				COV=	0.10			
				K[1]=	2.142			
98T1SH28	1/8D	2,916	86,917	0.966	2,655	12.0	0.63	0.64
98T1SH29	1/8D	3,246	112,848	0.972	2,917	10.5	0.63	0.63
98T1SH30	1/8D	3,030	85,409	0.983	2,663	13.7	0.59	0.59
98T1SH31	1/8D	2,916	76,466	0.979	2,584	16.7	0.60	0.61
98T3SH32	1/8D	3,890	106,314	0.980	3,438	12.1	0.78	0.79
98T3SH33	1/8D	3,885	113,593	0.989	3,373	13.5	0.76	0.77
98T3SH34	1/8D	3,923	108,750	0.967	3,559	13.4	0.78	0.79
98T3SH35	1/8D	4,013	100,000	0.976	3,580	13.0	0.75	0.76
98T3SH36	1/8D	3,836	117,619	0.974	3,431	13.2	0.78	0.79
				Mean=	3,133	13.11	0.70	0.71
				Std. Dev.=	421			
				5% Exclusion=	2,231			
				COV=	0.13			
				K[1]=	2.142			

[1] From ASTM D2915

Appendix G Summary of Peg Bearing Tests:

Summary of Dry Peg Bearing Tests

Test	Species	Load Orient.	Failure Type	Yield Load (lb.)	Stiffness (lb/in.)	Actual Dia. (in.)	Yield Stress (psi)	M.C. %	SG	SG_{12}
98DBT201	WO	T	Bearing	3,449	110,952	0.988	2,327	11.9	0.63	0.63
98DBT202	WO	T	Bearing	3,496	112,500	0.989	2,357	13.7	0.63	0.63
98DBT203	WO	T	Bearing	3,346	90,596	0.986	2,263	14.8	0.60	0.61
98DBT204	WO	T	Bearing	3,765	127,983	0.973	2,580	13.8	0.67	0.68
98DBT205	WO	T	Bearing	3,228	96,812	0.981	2,194	13.0	0.61	0.61
98DBT206	WO	T	Bearing	2,838	71,541	0.985	1,921	13.7	0.69	0.69
98DBT207	WO	T	Bearing	3,078	97,127	0.992	2,069	15.0	0.60	0.60
98DBT208	WO	T	Bearing	3,275	118,561	0.993	2,200	13.7	0.63	0.63
98DBT209	WO	T	Bearing	3,360	85,882	1.002	2,237	13.9	0.63	0.64
98DBT210	WO	T	Bearing	3,657	73,571	0.988	2,469	13.2	0.64	0.64
98DBT211	WO	T	Bearing	4,169	81,494	1.001	2,777	11.9	0.69	0.70
98DBT212	WO	T	Bearing	3,469	97,500	0.991	2,335	12.7	0.68	0.68
98DBT213	WO	T	Bearing	3,691	79,341	1.001	2,458	13.0	0.68	0.69
98DBT214	WO	T	Bearing	3,676	86,798	0.974	2,518	13.7	0.66	0.67
98DBT215	WO	T	Bearing	3,369	103,897	0.991	2,268	13.0	0.71	0.71
98DBT216	WO	T	Bearing	3,359	106,507	0.990	2,263	14.1	0.67	0.68
98DBT217	WO	T	Bearing	3,653	99,030	0.983	2,478	15.1	0.66	0.66
98DBT218	WO	T	Bearing	4,145	98,437	0.990	2,793	13.4	0.68	0.69
98DBT219	WO	T	Bearing	4,119	94,420	0.990	2,775	12.9	0.69	0.70
98DBT220	WO	T	Bearing	4,383	95,597	0.983	2,974	12.2	0.70	0.71
98DBT221	WO	T	Bearing	N/A	128,824	0.977	N/A	13.9	0.78	0.79
98DBT222	WO	T	Bearing	N/A	109,091	0.994	N/A	10.7	0.77	0.78
98DBT223	WO	T	Bearing	5,451	146,808	0.990	3,673	15.3	0.73	0.74
98DBT224	WO	T	Bearing	5,637	141,706	0.974	3,860	15.3	0.77	0.78
98DBT225	WO	T	Bearing	5,530	166,310	0.998	3,696	14.4	0.79	0.80
98DBT226	WO	T	Bearing	5,719	153,507	0.988	3,859	14.9	0.79	0.80
98DBT227	WO	T	Bearing	4,714	116,713	0.993	3,165	13.0	0.77	0.78
98DBT228	WO	T	Bearing	5,686	127,775	0.992	3,821	16.0	0.78	0.79
98DBT229	WO	T	Bearing	4,850	139,531	0.990	3,266	14.7	0.76	0.77
98DBT230	WO	T	Bearing	5,147	149,093	0.988	3,475	13.6	0.79	0.80
				Mean=	110,263		2,688	13.7	0.69	0.70
				Std. Dev.=	25,084		580			
				5% Exclusion=	63,382		1,604			
				COV=	0.23		0.22			
				K[1]=	1.869		1.869			

[1] From ASTM D2915

Summary of Wet Peg Dowel Bearing Tests									
Test	**Species**	**Load Orient.**	**Failure Type**	**Yield Load (lb.)**	**Stiffness (lb/in.)**	**Actual Dia. (in.)**	**Yield Stress (psi)**	**M.C. %**	**SG**
98DBT01	WO	T	Bearing	2,643	51,457	1.031	1,709	33.8	0.61
98DBT02	WO	T	Bearing	2,880	72,772	1.000	1,921	25.6	0.69
98DBT03	WO	T	Bearing	2,544	72,326	1.001	1,694	33.3	0.60
98DBT04	WO	T	Bearing	3,357	86,788	0.996	2,248	35.7	0.70
98DBT05	WO	T	Bearing	2,262	46,045	0.999	1,510	31.4	0.61
98DBT06	WO	T	Bearing	2,822	73,246	0.999	1,883	31.7	0.58
98DBT07	WO	T	Bearing	2,706	83,343	0.991	1,820	40.0	0.61
98DBT08	WO	T	Bearing	2,424	73,159	0.990	1,633	33.8	0.61
98DBT09	WO	T	Bearing	2,589	82,962	0.998	1,730	31.0	0.64
98DBT10	WO	T	Bearing	2,512	62,528	0.991	1,690	30.9	0.59
98DBT11	WO	T	Bearing	2,477	47,773	1.000	1,651	27.3	0.62
98DBT12	WO	T	Bearing	2,550	52,752	0.996	1,707	39.4	0.62
98DBT13	WO	T	Bearing	2,672	82,665	0.996	1,790	25.0	N/A
98DBT14	WO	T	Bearing	2,475	63,504	0.993	1,662	34.9	0.62
98DBT15	WO	T	Bearing	2,301	64,673	1.000	1,534	36.6	0.53
98DBT16	WO	T	Bearing	2,011	67,187	0.995	1,347	24.4	0.61
98DBT17	WO	T	Bearing	1,996	67,977	0.994	1,339	31.8	0.62
98DBT18	WO	T	Bearing	2,546	81,858	1.000	1,697	28.9	0.62
98DBT19	WO	T	Bearing	3,014	61,090	1.002	2,005	22.9	0.69
98DBT20	WO	T	Bearing	2,796	57,713	0.987	1,890	22.8	0.63
				Mean=	67,591		1,723	31.1	0.62
				Std. Dev.=	12,406		212		
				5% Exclusion=	43,622		1,314		
				COV=	0.18		0.12		
				K[1]=	1.932		1.932		

[1] From ASTM D2915

Appendix H Summary of Dowel Bearing Tests:

Summary of Southern Pine Dowel Bearing Tests

Joint	Test	Species	Load Orient.	Trough Length (in.)	Yield Load (lb.)	Yield Stress (psi)	M.C. %	SG	SG_{12}	Stiffness (lb/in.)	Defects
SP6	982SP1	S-Y-P	Perp.	1.965	2,039	1,038	16.5	0.48	0.49	25,304	small crack along grain
SP6	982SP2B	S-Y-P	Perp.	2.042	2,412	1,181	16.7	0.49	0.49	30,260	damage at bottom due to check
SP2	982SP3	S-Y-P	Perp.	1.896	2,575	1,359	17.7	0.63	0.63	31,894	
SP2	982SP4	S-Y-P	Perp.	2.046	2,847	1,392	17.2	0.66	0.67	37,684	check thru trough
SP10	982SP5	S-Y-P	Perp.	1.951	2,549	1,307	17.7	0.48	0.48	22,112	
SP10	982SP6	S-Y-P	Perp.	1.950	3,046	1,562	17.9	0.67	0.67	51,254	
SP1	982SP7	S-Y-P	Perp.	1.399	1,720	1,230	17.3	0.54	0.54	25,279	poor hole
SP1	982SP8	S-Y-P	Perp.	1.501	2,292	1,527	15.0	0.40	0.40	34,058	pith below trough
SP4	982SP9	S-Y-P	Perp.	1.505	3,089	2,052	19.1	0.45	0.45	53,217	
SP4	982SP10	S-Y-P	Perp.	1.496	2,910	1,946	16.7	0.50	0.51	44,190	
SP14	982SP11	S-Y-P	Perp.	1.514	2,777	1,834	15.8	0.54	0.55	49,459	
SP14	982SP12	S-Y-P	Perp.	1.543	2,659	1,723	19.7	0.53	0.53	43,405	
SP7	982SP13	S-Y-P	Perp.	1.496	2,750	1,839	16.0	0.45	0.45	39,350	rot at mid-hgt of sample
SP7	982SP14	S-Y-P	Perp.	1.468	2,753	1,876	15.5	0.50	0.51	36,959	rot at mid-hgt of sample
SP11	982SP15	S-Y-P	Perp.	1.496	3,783	2,530	15.7	0.58	0.58	50,158	small checks
SP11	982SP16	S-Y-P	Perp.	1.530	3,588	2,346	17.5	0.55	0.55	47,912	small checks
SP3	982SP17	S-Y-P	Perp.	1.515	2,760	1,822	16.0	0.46	0.46	40,702	
SP3	982SP18	S-Y-P	Perp.	1.531	3,340	2,181	15.8	0.51	0.51	46,023	
SP5	982SP19	S-Y-P	Perp.	1.518	3,321	2,188	16.7	0.45	0.45	50,966	
SP5	982SP20	S-Y-P	Perp.	1.517	3,284	2,165	13.0	0.48	0.48	40,449	
SP8	982SP21	S-Y-P	Perp.	1.529	3,140	2,054	16.4	0.45	0.45	42,306	small check at mid-hgt of sample
SP8	982SP22	S-Y-P	Perp.	1.515	3,125	2,064	15.5	0.49	0.49	39,788	small check at mid-hgt of sample
SP9	982SP23	S-Y-P	Perp.	1.411	2,696	1,911	16.1	0.43	0.43	37,980	
SP9	982SP24	S-Y-P	Perp.	1.538	3,493	2,272	17.2	0.43	0.43	54,007	small check below trough
SP12	982SP25	S-Y-P	Perp.	1.506	3,704	2,460	17.3	0.57	0.58	65,482	
SP12	982SP26	S-Y-P	Perp.	1.516	3,387	2,234	15.9	0.56	0.56	47,546	
SP13	982SP27	S-Y-P	Perp.	1.523	3,394	2,229	14.7	0.54	0.54	44,553	
SP13	982SP28	S-Y-P	Perp.	1.486	2,990	2,013	15.5	0.54	0.55	49,255	
					Mean=	1,869	16.5		0.52	42,198	
					Std. Dev.=	407				9,793	
					5% Exclusion=	1,104				38,571	
					COV=	0.218				0.23	
					K[1]=	1.879					

Joint	Test	Species	Load Orient.	Trough Length (in.)	Yield Load (lb.)	Yield Stress (psi)	M.C. %	SG	SG_{12}	Stiffness (lb/in.)	Defects
SP6	981SP01	S-Y-P	Parallel	ERROR NO DATA!							
SP6	981SP02	S-Y-P	Parallel	1.965	2,039	1,038	16.5	0.48	0.49	25,304	check 1" from trough
SP10	981SP03	S-Y-P	Parallel	1.945	4,510	2,319	14.8	0.44	0.44	185,897	check 3/8" from trough
SP2	981SP04	S-Y-P	Parallel	1.908	5,911	3,098	15.5	0.62	0.62	178,372	check 1" from trough
SP10	981SP05	S-Y-P	Parallel	2.010	4,510	2,244	18.6	0.44	0.44	193,815	small checks at trough
SP1	981SP06	S-Y-P	Parallel	1.452	4,314	2,971	14.4	0.53	0.53	147,249	
SP1	981SP07	S-Y-P	Parallel	ERROR NO DATA!							

[1] From ASTM D2915

Summary of Douglas Fir Dowel Bearing Tests

Joint	Test	Load Orient.	Yield Load (lb.)	Trough Length (in.)	Yield Stress (psi)	MC%	SG	SG_{12}	Stiffness (lb/in.)	Defects
DF1T	981DF01	Parallel	7,507	1.504	4,991	11.8	0.42	0.42	262,800	
DF1T	981DF02	Parallel	7,596	1.504	5,051	12.4	0.41	0.41	324,093	
DF9T	981DF03	Parallel	7,821	1.532	5,105	9.1	0.40	0.40	305,197	
DF9T	981DF04	Parallel	7,722	1.528	5,054	11.7	0.40	0.40	253,593	
DF10T	981DF05	Parallel	10,226	1.546	6,617	6.3	0.51	0.51	272,525	
DF10T	981DF06	Parallel	10,204	1.548	6,592	9.2	0.50	0.50	358,187	
DF3T	981DF07	Parallel	12,552	1.495	8,399	7.5	0.56	0.56	530,680	tested twice error during first test
DF3T	981DF08	Parallel	12,615	1.494	8,447	9.0	0.57	0.57	463,112	
DF6T	981DF09	Parallel	9,560	1.545	6,188	10.1	0.43	0.44	327,278	
DF6T	981DF10	Parallel	9,524	1.497	6,364	7.9	0.43	0.43	311,618	
DF2T	981DF11	Parallel	11,221	1.469	7,639	7.6	0.46	0.46	369,328	
DF2T	981DF12	Parallel	10,903	1.476	7,387	9.3	0.51	0.52	383,078	
DF7T	981DF13	Parallel	11,417	1.493	7,647	7.8	0.50	0.51	360,041	
DF7T	981DF14	Parallel	11,101	1.509	7,357	7.2	0.51	0.51	339,758	
DF4T	981DF15	Parallel	8,036	1.482	5,422	14.4	0.43	0.43	231,415	
DF4T	981DF16	Parallel	8,558	1.499	5,709	14.2	0.42	0.42	284,858	
DF5T	981DF17	Parallel	8,862	1.503	5,898	12.4	0.46	0.46	304,615	
DF5T	981DF18	Parallel	8,971	1.508	5,951	12.1	0.46	0.46	337,129	
DF8T	981DF19	Parallel	10,531	1.534	6,865	6.8	0.48	0.48	331,135	
DF8T	981DF20	Parallel	11,224	1.531	7,331	6.6	0.48	0.48	324,163	
DF12T	981DF21	Parallel	11,330	1.547	7,324	6.3	0.43	0.43	304,056	
DF12T	981DF22	Parallel	10,391	1.407	7,385	6.7	0.43	0.43	307,214	
DF11T	981DF23	Parallel	9,230	1.530	6,035	8.6	0.42	0.42	247,882	
DF11T	981DF24	Parallel	10,152	1.533	6,622	6.1	0.45	0.46	247,731	
				Mean=	6,557	9.2	0.46	0.46	324,229	
				Std. Dev.=	1,042					
				5% Exclusion=	4,577					
				COV=	0.16					
				K[1]=	1.90					

Joint	Test	Load Orient.	Yield Load (lb.)	Trough Length (in.)	Yield Stress (psi)	MC%	SG	SG_{12}	Stiffness (lb/in.)	Defects
DF8M	982DF01	Perp.	3,115	1.542	2,021	7.9	0.60	0.61	58,579	
DF8M	982DF02	Perp.	3,850	1.534	2,511	7.7	0.57	0.57	73,247	
DF7M	982DF03	Perp.	3,162	1.514	2,089	15.1	0.46	0.47	54,007	
DF7M	982DF04	Perp.	3,231	1.505	2,148	15.5	0.50	0.51	36,953	
DF3M	982DF05	Perp.	2,860	1.501	1,906	6.4	0.51	0.52	35,652	
DF3M	982DF06	Perp.	2,665	1.497	1,780	9.2	0.51	0.52	35,811	
DF11M	982DF07	Perp.	N/A	1.486	N/A	12.3	0.50	0.50	29,066	
DF11M	982DF08	Perp.	N/A	1.488	N/A	13.3	0.50	0.50	25,523	check at mid-hgt
DF4M	982DF09	Perp.	3,098	1.527	2,029	13.2	0.49	0.50	45,383	not orient. w/joint test
DF4M	982DF10	Perp.	N/A	1.528	N/A	11.2	0.43	0.43	33,822	not orient. w/joint test
DF6M	982DF11	Perp.	4,093	1.514	2,703	9.2	0.59	0.60	68,819	
DF6M	982DF12	Perp.	4,017	1.523	2,638	7.2	0.58	0.59	62,650	
DF1M	982DF13	Perp.	3,225	1.479	2,181	8.6	0.47	0.47	40,942	nail hole thru sample and trough damage
DF1M	982DF14	Perp.	3,200	1.497	2,138	10.4	0.44	0.45	39,830	nail holes
DF9M	982DF15	Perp.	2,605	1.511	1,724	15.1	0.41	0.42	28,591	large check at base
DF9M	982DF16	Perp.	2,829	1.507	1,877	12.3	0.47	0.47	36,385	
DF5M	982DF17	Perp.	2,831	1.485	1,906	13.1	0.43	0.43	35,279	
DF5M	982DF18	Perp.	3,331	1.484	2,245	12.4	0.44	0.45	47,643	
DF10M	982DF19	Perp.	3,576	1.533	2,333	6.7	0.64	0.65	54,621	
DF10M	982DF20	Perp.	3,538	1.522	2,325	7.5	0.57	0.58	67,846	
DF12M	982DF21	Perp.	3,530	1.524	2,317	9.4	0.45	0.46	59,376	
DF12M	982DF22	Perp.	3,760	1.518	2,478	8.5	0.45	0.45	70,043	
DF2M	982DF23	Perp.	2,697	1.526	1,768	8.2	0.50	0.51	37,398	
DF2M	982DF24	Perp.	2,367	1.519	1,559	7.3	0.50	0.51	28,050	
				Mean=	2,126	10.3	0.50	0.51	46,063	
				Std. Dev.=	335					
				5% Exclusion=	1,481					
				COV=	0.16					
				K[1]=	1.924					

[1] From ASTM D2915

Summary of Red Oak Dowel Bearing Tests

Joint	Test	Load Orient.	Yield Load (lb.)	Trough Length (in.)	Yield Stress (psi)	MC%	SG	SG$_{12}$	Stiffness (lb/in.)	Defects
C	981RO01	Perp.	16,617	1.526	10,889	7.0	0.62	0.63	405,797	
C	981RO02	Perp.	16,410	1.517	10,818	6.8	0.60	0.61	433,400	
D	981RO03	Perp.	16,796	1.522	11,039	8.9	0.64	0.64	450,411	
D	981RO04	Perp.	17,067	1.535	11,118	8.2	0.66	0.67	349,429	sample 3" in hgt.
J	981RO05	Perp.	16,465	1.490	11,054	7.5	0.66	0.66	526,520	2 checks, one in trough
J	981RO06	Perp.	15,139	1.452	10,426	8.1	0.68	0.69	411,340	2 knots & 2 checks away from trough
I	981RO07	Perp.	18,136	1.579	11,486	8.9	0.66	0.66	507,903	
I	981RO08	Perp.	18,660	1.572	11,870	6.9	0.65	0.66	503,885	
G	981RO09	Perp.	21,491	1.601	13,428	6.9	0.78	0.79	423,077	
G	981RO10	Perp.	21,267	1.607	13,238	7.8	0.69	0.70	468,015	
F	981RO11	Perp.	17,953	1.633	10,994	7.7	0.62	0.63	423,393	small checks throughout
F	981RO12	Perp.	18,647	1.640	11,374	6.8	0.64	0.65	278,296	
A	981RO13	Perp.	18,089	1.597	11,327	5.6	0.65	0.65	523,789	
A	981RO14	Perp.	17,511	1.577	11,108	6.9	0.64	0.65	485,000	
L	981RO15	Perp.	21,826	1.525	14,312	6.1	0.72	0.74	540,835	
L	981RO16	Perp.	22,458	1.550	14,489	3.9	0.74	0.75	549,302	
E	981RO17	Perp.	11,717	1.563	7,496	11.3	0.59	0.59	356,776	
E	981RO18	Perp.	10,940	1.558	7,024	13.4	0.60	0.60	337,237	check in trough
B	981RO19	Perp.	19,303	1.471	13,127	2.7	0.77	0.78	393,634	check in trough
B	981RO20	Perp.	20,126	1.493	13,480	3.7	0.76	0.77	417,917	
H	981RO21	Perp.	15,058	1.456	10,345	9.3	0.67	0.68	426,429	
H	981RO22	Perp.	14,992	1.466	10,227	8.7	0.67	0.68	419,022	
				Mean=	11,394	7.4	0.67	0.68	437,791	
				Std. Dev.=	1,852					
				5% Exclusion=	7,845					
				COV=	0.16					
				K[1]=	1.916					

Joint	Test	Load Orient.	Yield Load (lb.)	Trough Length (in.)	Yield Stress (psi)	MC%	SG	SG$_{12}$	Stiffness (lb/in.)	Defects
G	982RO01	Parallel	N/A	1.636	N/A	6.8	0.68	0.69	101,522	2 checks
G	982RO02	Parallel	7,668	1.607	4,771	5.9	0.68	0.69	111,794	2 checks
F	982RO03	Parallel	7,754	1.447	5,359	10.3	0.64	0.65	101,803	small checks throughout
F	982RO04	Parallel	6,670	1.425	4,680	5.6	0.66	0.67	90,086	one interior check
H	982RO05	Parallel	5,933	1.502	3,951	10.9	0.66	0.66	59,737	bad specimen excluded test
H	982RO06	Parallel	6,719	1.491	4,506	9.9	0.67	0.68	109,446	small checks throughout
E	982RO07	Parallel	7,038	1.534	4,588	9.4	0.59	0.60	100,176	
E	982RO08	Parallel	7,751	1.522	5,093	7.0	0.66	0.67	123,530	
A[2]	982RO09	Parallel	6,931	1.549	4,475	5.8	0.63	0.64	113,277	one interior check in trough
A[2]	982RO10	Parallel	8,207	1.554	5,283	6.8	0.66	0.67	129,028	one interior check in trough
B	982RO11	Parallel	8,430	1.455	5,794	4.4	0.62	0.63	150,671	check at bottom of specimen
B	982RO12	Parallel	8,922	1.506	5,924	5.9	0.64	0.65	134,299	check at bottom of specimen
C	982RO13	Parallel	7,287	1.508	4,832	10.2	0.63	0.64	99,979	check at mid-hgt.
C	982RO14	Parallel	6,597	1.450	4,550	12.4	0.48	0.48	111,561	
D	982RO15	Parallel	7,593	1.466	5,179	11.5	0.62	0.63	105,636	
D	982RO16	Parallel	7,404	1.487	4,981	11.0	0.64	0.65	114,219	sample 3" in hgt.
I	982RO17	Parallel	6,949	1.498	4,639	9.6	0.65	0.65	101,092	
I	982RO18	Parallel	6,630	1.490	4,450	10.6	0.64	0.65	120,220	
L	982RO19	Parallel	6,583	1.430	4,605	12.0	0.76	0.77	113,428	
L	982RO20	Parallel	6,636	1.430	4,640	13.0	0.77	0.78	110,867	
				Mean=	4,908	9.0	0.65	0.66	110,119	
				Std. Dev.=	446					
				5% Exclusion=	4,043					
				COV=	0.09					
				K[1]=	1.942					

[1] From ASTM D2915

[2] Specimen not oriented the same as joint test

Summary of RO Dowel Bearing w/ White Oak Peg Tests:

Summary of Combined Red Oak Dowel Bearing w/ White Oak Peg Tests														
Joint	Test	Load Orient.	Yield Load (lb.)	Trough Length (in.)	Yield Stress (psi)	Base M.C. %	Base SG	Base SG_{12}	Stiffness (lb/in.)	Peg Dia. (in.)	Peg M.C. %	Peg SG	Peg SG_{12}	Base Defects
A[2]	982RO40	Parallel	5,268	1.565	3,413	8.11	0.65	0.66	80,775	0.987	11.6	0.79	0.80	internal check in trough
A[2]	982RO41	Parallel	4,763	1.534	3,192	7.14	0.66	0.67	65,297	0.973	12.6	0.80	0.81	internal check below trough
B	982RO42	Parallel	5,450	1.431	3,859	8.00	0.63	0.63	70,138	0.987	9.5	0.80	0.82	check at bottom of specimen
B	982RO43	Parallel	5,056	1.482	3,511	6.75	0.62	0.63	89,216	0.972	12.5	0.77	0.78	check at bottom of specimen
C	982RO44	Parallel	5,036	1.490	3,449	12.28	0.67	0.68	62,940	0.980	12.8	0.79	0.80	check at mid-hgt.
C	982RO45	Parallel	4,997	1.496	3,396	12.18	0.66	0.67	73,642	0.984	13.6	0.79	0.80	check at mid-hgt.
D	982RO46	Parallel	3,488	1.431	2,525	11.08	0.68	0.69	55,037	0.966	13.5	0.67	0.67	interior check below trough
D	982RO47	Parallel	3,867	1.472	2,728	11.91	0.66	0.67	58,300	0.963	12.7	0.66	0.67	1/4" dia. knot
E	982RO48	Parallel	3,339	1.510	2,279	8.85	0.60	0.60	57,572	0.971	12.4	0.65	0.65	check at mid-hgt.
E	982RO49	Parallel	4,131	1.530	2,795	9.74	0.59	0.60	68,189	0.966	9.6	0.67	0.68	
I	982RO50	Parallel	3,932	1.499	2,709	9.54	0.65	0.66	80,104	0.969	14.5	0.65	0.66	
I	982RO51	Parallel	3,712	1.481	2,589	10.76	0.64	0.65	67,818	0.968	11.8	0.65	0.66	
				Mean=	3,037									
				Std. Dev.=	492									
				5% Exclusion=	2,029									
				COV=	0.16									
				K[1]=	2.048									

[1] From ASTM D2915

[2] Specimen not oriented the same as joint test

Appendix I SYP Example Joint Design:

Timber Frame Joint Properties			Equivalent Bolted Connection Properties			Equivalent Steel Bolt Calculation				
a/D=	1.14		F_{yb} =	45,000	psi	Mode	Im	Eqv. Dia. =	0.480	in
n=	2					Mode	Is	Eqv. Dia. =	0.475	in
D=	1.0	in.	G_m =	0.52		Mode	IIIs	Eqv. Dia. =	0.612	in
t_m=	2.0	in.	G_s =	0.52		Mode	IV	Eqv. Dia. =	0.532	in
t_s=	2.0	in.	F_{em} =	5,488	psi					
F_{ed}[1]=	2,688		F_{es} =	2,770	psi			Diameter =	0.613	in
F_{em}[2]=	5,488	psi								
F_{es}[2]=	2,770	psi	t_m =	2	inches	**Equivalent Bolted**				
τ_c=	1,341	psi	t_s =	2	inches	**Connection Capacitly**				
P_{Id}=	5,376		K_θ =	1.25		Mode	Im	P/bolt =	1,345	lb
P_{Im}=	10,976	lbs.	k_3 =	1.248		Mode	Is	P/bolt =	1,358	lb
P_{Is}=	11,081	lbs.	R_e =	1.981		Mode	IIIs	P/bolt =	1,054	lb
P_{Vd}=	2,107	lbs.				Mode	IV	P/bolt =	1,394	lb
P_A=	2,107	lbs.						Total P' =	2,107	lb

Edge Distance (in)		End Distance (in)	Reduced	Full	Spacing of Rows (in)	
Par. to Grain	**0.9**				Par. to Grain	**0.9**
Perp. to Grain:		Perp. to Grain	**1.2**	**2.5**	Perp. to Grain	**1.5**
loaded edge	**2.5**	Par. Comp	**1.2**	**2.5**		
unloaded edge	**0.9**	Par. Tension:				
		softwoods	**2.1**	**4.3**		
		hardwoods	**1.5**	**3.1**		

[1] Peg bearing strength was taken from section 2.4.5.

[2] Material dowel bearing strengths were calculated using the NDS equations.

Appendix J RO Example Joint Design:

Timber Frame Joint Properties			Equivalent Bolted Connection Properties			Equivalent Steel Bolt Calculation				
$a/D=$	0.11		F_{yb} =	45,000	psi	Mode	Im	Eqv. Dia. =	0.632	in
$n=$	2					Mode	Is	Eqv. Dia. =	0.684	in
$D=$	1.0	in.	G_m =	0.67		Mode	IIIs	Eqv. Dia. =	0.730	in
$t_m=$	2.0	in.	G_s =	0.67		Mode	IV	Eqv. Dia. =	0.620	in
$t_s=$	2.0	in.	F_{em} =	5,488	psi					
$F_{ed}{}^{1}=$	2,688		F_{es} =	2,537	psi			Diameter =	0.730	in
$F_{em}{}^{2}=$	5,488	psi								
$F_{es}{}^{2}=$	2,537	psi	t_m =	2	inches	**Equivalent Bolted**				
$\tau_c=$	1,767	psi	t_s =	2	inches	**Connection Capacitly**				
$P_{Id}=$	5,376		k_θ =	1.25		Mode	Im	P/bolt =	1,604	lb
$P_{Im}=$	10,976	lbs.	k_3 =	1.441		Mode	Is	P/bolt =	1,483	lb
$P_{Is}=$	10,148	lbs.	R_e =	2.163		Mode	IIIs	P/bolt =	1,388	lb
$P_{Vd}=$	2,776	lbs.				Mode	IV	P/bolt =	1,925	lb
$P_A=$	2,776	lbs.						Total P' =	2,776	lb

Edge Distance (in)		**End Distance (in)**			**Spacing of Rows (in)**	
Par. to Grain	**1.1**		Reduced	Full	Par. to Grain	**1.1**
Perp. to Grain:		Perp. to Grain	**1.5**	**2.9**	Perp. to Grain	**1.8**
loaded edge	**2.9**	Par. Comp	**1.5**	**2.9**		
unloaded edge	**1.1**	Par. Tension:				
		softwoods	**2.6**	**5.1**		
		hardwoods	**1.8**	**3.7**		

[1] Peg bearing strength was taken from section 2.4.5.

[2] Material dowel bearing strengths were calculated using the NDS equations.

Appendix K Instron Model 1332 Test Set-up:

1. Turn on the Instron inside the panel door at the rear of the machine.
2. Assemble the necessary test fixtures.
3. Start pump.
4. Set the controller to stroke control and set the loading function to ramp.
5. Turn on actuator and cycle piston several times manually.
6. Turn on computer and open the data acquisition program.
7. Set the load range to an appropriate value for the test being conducted.
8. Zero the stroke by adjusted the controller knob manually, and reading the digital display on the Instron machine, or use the data acquisition system to monitor the voltage readings.
9. Zero the load by adjusted the fine and coarse screws on top of the load controller module. (Note: Do not adjust the calibration screw.)
10. Set the displacement rate with the knob on the function generator. (Note: Recommend using a dial gauge to determine what numbers on the dial correspond to a given rate.)
11. Place a specimen in Instron.
12. Check to make sure the machine is set to stroke control (green light should be lit on stroke control module), and the interlock is set to an appropriate value on the load control module.
13. Lower the machine cross-head using the valves below the test platform until the test fixture is lightly resting on the specimen. Check the Instron output readings for zero.
14. Start the data acquisition system and the Instron machine simultaneously (push the start bottom on the function generator).
15. Push the reset button on the function generator at the end of the test (the Instron should return to the zero position), and record the pertinent data.
16. Stop the data acquisition system.
17. Remove the tested specimen from the machine.
18. If more tests are to be done repeat steps 13-17.
19. Turn of actuator, pump, and the Instron power.
20. Clean-up

Appendix L Joint Test Set-up:

1. Assemble test frame. (no instructions needed)
2. Find the appropriate hardware. (the most difficult task in the procedure)
   - hydraulic jack
   - hydraulic hoses and manifold
   - hand pump
   - pressure transducer
   - power supply
   - 2 linear potentiometers
   - hot glue gun (glue sticks)
3. Assemble the above items in an appropriate fashion.
4. Attach the load plates the tenon member of the joint with lag bolts.
5. Record the MC% of both the mortise and tenon members.
6. Label the pegs with the test number and the peg number.
7. Record the weight, orientation (i.e. annual rings tangent or radial to the load), defects and the diameters of the pegs that are to secure the joint.
8. Record the mortise and tenon dimensions and defects.
9. Assemble the joint with the pegs in the proper orientation.
10. Place the joint in the test frame using the threaded rod and the steel pipe load spreader.
11. Align the joint so it is concentrically loaded top to bottom and side to side.
12. Finger tighten bolt on threaded rod and be careful not to prestress the joint.
13. Attach the linear pots to the tenon member, and hot glue an aluminum de-mag point to the mortise member under each pot.
14. Turn on the data acquisition program and run the trouble shooting file to check the readings of all the instruments.
15. Open the loaddefl2 file and input the data file name and the deflection rate. (check the constants associated with the linear pots and pressure transducer to make sure the program matches the hardware)
16. Record the time and start the test.
17. The pump should follow the deflection rate plot at the left-hand side of the screen.
18. At failure record the pertinent information and stop the data acquisition software.
19. Release the pump valve and remove the joint from the test frame.
20. Back-up the data file.